

291  
1-5-98  
7-79 d  
plus UK, Germany  
+ Special on DF (Instr.)

Sh. 1723

ORNL/TM-6152  
(ENDF-257)

**MASTER**

## Evaluation of the $^{238}\text{U}$ Neutron Cross Sections for Incident Neutron Energies up to 4 keV

G. de Saussure  
D. K. Olsen  
R. B. Perez  
F. C. Difilippo

cb

**OAK RIDGE NATIONAL LABORATORY**  
OPERATED BY UNION CARBIDE CORPORATION · FOR THE DEPARTMENT OF ENERGY

DISTRIBUTION OF THIS DOCUMENT IS UNLIMITED

## DISCLAIMER

**This report was prepared as an account of work sponsored by an agency of the United States Government. Neither the United States Government nor any agency Thereof, nor any of their employees, makes any warranty, express or implied, or assumes any legal liability or responsibility for the accuracy, completeness, or usefulness of any information, apparatus, product, or process disclosed, or represents that its use would not infringe privately owned rights. Reference herein to any specific commercial product, process, or service by trade name, trademark, manufacturer, or otherwise does not necessarily constitute or imply its endorsement, recommendation, or favoring by the United States Government or any agency thereof. The views and opinions of authors expressed herein do not necessarily state or reflect those of the United States Government or any agency thereof.**

## **DISCLAIMER**

**Portions of this document may be illegible in electronic image products. Images are produced from the best available original document.**

Printed in the United States of America. Available from  
National Technical Information Service  
U.S. Department of Commerce  
5285 Port Royal Road, Springfield, Virginia 22161  
Price: Printed Copy ~~\$6.50~~; Microfiche \$3.00

6.00

This report was prepared as an account of work sponsored by an agency of the United States Government. Neither the United States Government nor any agency thereof, nor any of their employees, contractors, subcontractors, or their employees, makes any warranty, express or implied, nor assumes any legal liability or responsibility for any third party's use or the results of such use of any information, apparatus, product or process disclosed in this report, nor represents that its use by such third party would not infringe privately owned rights.

ORNL/TM-6152  
(ENDF-257)  
Dist. Category UC-79d

Contract No. W-7405-eng-26

Neutron Physics Division

EVALUATION OF THE  $^{238}\text{U}$  NEUTRON CROSS SECTIONS FOR  
INCIDENT NEUTRON ENERGIES UP TO 4 keV

G. de Saussure, D. K. Olsen, R. B. Perez, and F. C. Difilippo\*

\*On assignment from Comisión Nacional de Energía Atómica, Argentina.

Date Published: January 1978

**NOTICE** This document contains information of a preliminary nature.  
It is subject to revision or correction and therefore does not represent a  
final report.

Prepared by the  
OAK RIDGE NATIONAL LABORATORY  
Oak Ridge, Tennessee 37830  
operated by  
UNION CARBIDE CORPORATION  
for the  
DEPARTMENT OF ENERGY

**NOTICE**  
This report was prepared as an account of work sponsored by the United States Government. Neither the United States nor the United States Department of Energy, nor any of their employees, nor any of their contractors, subcontractors, or their employees, makes any warranty, express or implied, or assumes any legal liability or responsibility for the accuracy, completeness or usefulness of any information, apparatus, product or process disclosed, or represents that its use would not infringe privately owned rights.

DISTRIBUTION OF THIS DOCUMENT IS UNLIMITED  
*See*

THIS PAGE  
WAS INTENTIONALLY  
LEFT BLANK

## TABLE OF CONTENTS

	<u>Page No.</u>
Abstract	vii
1. Introduction	1
2. Recent Measurements and Analyses of $^{238}\text{U}$ Cross Sections	2
3. Evaluation of the Resonance Parameters for the Levels with Energies Between 1 and 4000 eV	3
A. General Considerations	3
B. Determination of the Level Energies	10
C. Neutron Widths	14
D. Capture Widths	17
E. Fission Widths	19
F. Angular Momentum Assignment	23
G. Parameters of the Low Energy Resonances	24
H. Resonance Formalism and Scattering Radius	31
4. Evaluation of the Smooth Backgrounds (File 3)	33
5. Fine Adjustments to the Parameters and Smooth Backgrounds	44
6. Capture Cross Sections	45
7. Distribution of the Resonance Parameters	52
A. s-Wave Levels	52
B. p-Wave Levels	60
8. Estimated Uncertainties	68
9. Conclusions	80
References	85

THIS PAGE  
WAS INTENTIONALLY  
LEFT BLANK

## ACKNOWLEDGMENT

The authors wish to acknowledge many helpful discussions with the participants of the Seminar on  $^{238}\text{U}$  Resonance Capture and are particularly indebted to F. Poortmans, G. Rohr, and H. Weigmann of the BCMN, Geel, Belgium; to R. C. Block and K. Kobayashi of RPI; to R. E. Chrien and H. I. Liou of BNL and D. Finch of SRL for communication of the results of their work prior to publication.

The authors would also like to thank R. Q. Wright for considerable help, especially in putting this evaluation in the ENDF/B format.

Very helpful comments were provided by R. L. Macklin, R. W. Peelle, and C. R. Weisbin who reviewed the report.

Finally the authors would like to extend special thanks to Erma Howe who typed and organized this report.

THIS PAGE  
WAS INTENTIONALLY  
LEFT BLANK

## ABSTRACT

This report describes an evaluation of the  $^{238}\text{U}$  cross sections below 4 keV. Recent measurements and reanalyses of older data are discussed. Evaluated resonance parameters are obtained for 164 s-wave and 280 p-wave levels. The capture widths of the first three s-wave levels are significantly lower than in the ENDF/B-IV evaluation. The s-wave strength function above 1.5 keV is systematically larger than in ENDF/B-IV. Statistical and systematic uncertainties are evaluated for the resonance parameters and for the smooth backgrounds. The statistical distributions of the resonance parameters are compared with theoretically expected distributions.

## 1. INTRODUCTION

In this report we discuss an evaluation of the  $^{238}\text{U}$  cross sections below 4 keV, intended for inclusion in ENDF/B-V.

These cross sections were evaluated for ENDF/B-IV by F. J. McCrosson<sup>C1</sup> in September 1973. Since that time a number of important new measurements of the low energy  $^{238}\text{U}$  cross sections have been reported,<sup>B21-B33</sup> and some older measurements have been carefully reexamined.<sup>A7</sup>

The  $^{238}\text{U}$  resonance parameters are particularly important to the calculation of the Doppler effect in fast reactors and of the conversion ratio in thermal reactors. Much of the recent interest in the reevaluation of these parameters has arisen from the apparent inability of the ENDF/B data to predict the  $^{238}\text{U}$  capture rate in thermal critical lattices. New precise measurements and new analyses of older measurements have been greatly stimulated by a "Specialists Meeting on Resonance Parameters of Fertile Nuclei and  $^{239}\text{Pu}$ " held in Saclay on May 20-22, 1974<sup>A5</sup> and by a "Seminar on  $^{238}\text{U}$  Resonance Capture" held in Brookhaven National Laboratory on March 18-20, 1975.<sup>A7</sup> The proceedings of these meetings contain considerable information on the experimental differential measurements and on the utilization of the data for the analysis of integral experiments.

In the next section of this report we briefly review measurements and analyses of the  $^{238}\text{U}$  cross sections below 4 keV, performed since 1974. Earlier experiments have been reviewed by Moxon.<sup>C5</sup> In the third section we discuss the evaluation of the resonance parameters. Smooth backgrounds (File 3) are discussed in Section 4. The distribution of the evaluated parameters is examined in Section 5 and a discussion of the errors is presented in Section 6.

## 2. RECENT MEASUREMENTS AND ANALYSES OF $^{238}\text{U}$ CROSS SECTIONS

Measurements of the  $^{238}\text{U}$  resonance parameters done before 1974 have been reviewed and discussed by M. C. Moxon.<sup>C5</sup> Since then extensive series of measurements have been reported by Nakajima et al.,<sup>B26</sup> Olsen et al.,<sup>B31</sup> and Poortmans et al.<sup>B32</sup> These three series of measurements extend to energies well above 4 keV, but the analysis of the Geel measurements is not yet completed. Liou and Chrien<sup>B30</sup> have performed transmission, self-indication and gamma-ray spectra measurements for epithermal neutron energies and have obtained resonance parameters for the s-wave levels up to 116.85 eV. Corvi, Rohr, and Weigmann<sup>B25</sup> were able to make many p-wave assignments in the neutron energy range from 10 to 1600 eV by measuring the fraction of capture gamma rays above 4.3 MeV. Subthreshold fission in  $^{238}\text{U}$  below 4 keV has recently been investigated by Block et al.,<sup>B27</sup> Blons, Mazur, and Paya,<sup>B28</sup> Wartena, Weigmann, and Migneco,<sup>B24</sup> Difilippo et al.,<sup>B33</sup> and Slovacek et al.<sup>B29</sup> Finally a series of self-indication measurements was recently completed at RPI.<sup>B34</sup> The analyses of these measurements by Block et al. and by Finch<sup>D1</sup> are still preliminary. Some experimental details of the recent measurements are summarized in Table I.

Some of the older measurements have recently been reexamined. The very high accuracy of the resonance parameters of the 6.67-eV level reported by Jackson and Lynn<sup>B8</sup> has been questioned by a group of experimentalists at the "Seminar on  $^{238}\text{U}$  Resonance Capture." In their view "this high accuracy is not supported by any details reported in the paper and is judged to be unrealistic."<sup>A7</sup> Liou and

Table I. Experimental Details of Recent Measurements  
(For experiments prior to 1974 see Moxon's review, Ref. C5)

Author, Year, Laboratory	Ref.	Energy Range (eV)	Type of Measurements	Detectors	Samples	Type of Analysis	Comments
Corvi, Rohr, Weigmann (75) Euratom, Geel, Belgium	B25	10-1600	Capture and $\sigma(E, E_\gamma)$ Linac, 50 m	NaI(Tl)	13.9 g/cm <sup>2</sup> and 4.64 g/cm <sup>2</sup>	Area	P-wave assignments
Nakajima et al. (75) JAERI, Japan	B25	20-4700	Transmission, Linac, 190 m	1.25 cm thick <sup>6</sup> Li glass	.00725 } .014 } atom/b .0236 } N.U.	Atta Harvey Area	One sample at 77°K
Liou and Chrien (76) BNL	B30	<120	Transmission, Self-indication, capture fast chopper	NaI + <sup>10</sup> B and Ge Li	from 8.6.10 <sup>-5</sup> to .09 atom/b	Area & multi-level shape fits	---
Olsen et al. (77) ORNL	B31	1-4000	Transmission, Linac 40 and 150 m	1 mm and 2.5 cm thick <sup>6</sup> Li glass	from 1.85.10 <sup>-4</sup> to 3.62 atom/b	SI08: Multilevel shape analysis	---
Poortmans et al. (77) Euratom, Geel, Belgium	B32	1-4270	Transmission, capture, scattering, Linac 30 and 60 m	C <sub>6</sub> F <sub>6</sub> liquid scint. for capture <sup>3</sup> He gas scint. for scattering and transmission	from 10 <sup>-5</sup> to .03 atom/b	Atta Harvey shape and area; & SI08 multilevel shape	Some samples at 77°K. Data Preliminary
Block et al. (77) RPI	B34		Self-indication Linac 25 m	Large liquid scint.	.08 to 1.3 cm thick	multilevel fits	Analysis incomplete
Block et al. (73) RPI	B21	>600	Subthreshold fission Linac, 10 m	Ionization fission chambers	---	Area	---
Wartana, Weigmann, Migneco (75) Euratom, Geel, Belgium	B24	>600	Subthreshold fission Linac 30 m	Liquid-scint. (to detect prompt fission gammas)	250g <sup>238</sup> U sample	Area	
Blons, Mazur, Paya (75) Saclay, France	B28	>600	Subthreshold fission Linac 22.4 & 52 m	gas-scint.	---		---
Slovacek et al. (77) RPI	B29	>1	Subthreshold fission slowing down spect.	Ionization fission chamber	---	Area	Includes estimate of thermal fission cross sec.
Difilippo et al. (77) ORNL	B33	>1	Subthreshold fission Linac 20 & 40 m	Ionization fission chamber	4.7g <sup>238</sup> U in chamber	Area	Relatively good resolution

3

Chrien<sup>B30</sup> have carefully reviewed the work of Jackson and Lynn and have noted that these authors failed to account for the increase in resonance parameter error required by the uncertainty in the vibrational parameter. Liou and Chrien estimate that the uncertainty in the width of the 6.67-eV level from the measurement of Jackson and Lynn should be more than three times as large as that given by those authors.

Derrien<sup>D2,D3</sup> and Ribon<sup>D2</sup> have reanalyzed some of the transmission measurements of Rahn et al.<sup>B20</sup> and of Carraro and Kolar<sup>B17</sup> using least-square shape analysis. The neutron widths obtained by their shape analysis are considerably different than those obtained by area analysis. Between 1450 and 1760 eV the neutron widths obtained by Derrien and Ribon from the data of Carraro and Kolar are 16% smaller than those given by Carraro and Kolar. Between 2.5 and 2.8 keV Derrien's values of  $\Gamma_n$  obtained from the analysis of the transmission measurements of Rahn et al. are 14% higher than those given by Rahn et al. Derrien attributes these differences to errors in the transmission backgrounds in the measurements. The shape analysis technique can "fit" a residual transmission background and hence should be more reliable.

The comparison between shape analysis and area analysis results is illustrated in Tables II and III (taken from the paper of Derrien). It is noteworthy that some values of  $\Gamma_n$  obtained from the same data, by the two methods of analysis, differ by an amount larger than their quoted uncertainties.

Table II.  $^{238}\text{U}$  Neutron Widths for Large Resonances Between 1450 eV and 1760 eV

Energy eV	Shape analysis of Geel data (2 thicknesses) $\Gamma_n$ , meV	Shape analysis of Columbia data (3 thicknesses) $\Gamma_n$ , meV	Geel published values B17 $\Gamma_n$ , meV	Columbia published values B20 $\Gamma_n$ , meV
1473.4	114 $\pm$ 2	108 $\pm$ 2	125 $\pm$ 8	125 $\pm$ 10
1522.3	215 $\pm$ 4	236 $\pm$ 3	260 $\pm$ 15	240 $\pm$ 15
1597.5	309 $\pm$ 6	352 $\pm$ 4	351 $\pm$ 40	355 $\pm$ 25
1622.3	97 $\pm$ 2	88 $\pm$ 2	116 $\pm$ 15	68 $\pm$ 14
1637.4	50 $\pm$ 1	46 $\pm$ 2	60 $\pm$ 5	50 $\pm$ 8
1662.0	201 $\pm$ 4	214 $\pm$ 4	241 $\pm$ 20	171 $\pm$ 20
1687.3	98 $\pm$ 2	97 $\pm$ 2	104 $\pm$ 9	92 $\pm$ 10
1709.0	81 $\pm$ 2	77 $\pm$ 2	94 $\pm$ 7	86 $\pm$ 8
1755.2	121 $\pm$ 3	116 $\pm$ 3	135 $\pm$ 10	105 $\pm$ 10
$\Sigma \Gamma_n$	1286	1334	1486	1292

(This Table, including the comments, is reproduced from the paper of H. Derrien, Ref. D3)

In the shape analysis of Geel data the adjusted background parameters  $a$  were negligible ( $< 10^{-3}$ ).

In the shape analysis of Columbia the adjusted background parameters  $a$  were equal to:

0.0011 for 0.084 at/b sample;  
 -0.010 for 0.0348 at/b sample;  
 0.027 for 0.0084 at/b sample.

For the signification of the parameter  $a$  see comments on Table III.

Table III.  $\Gamma_n$  Values for Large Resonances Between 2.5 keV and 2.8 keV

Energy eV	Shape analysis on Geel transmissions	CARRARO et al. results (Helsinki)	Shape analysis on Columbia transmissions	RAHN et al. results
2547.2	716 $\pm$ 30	706 $\pm$ 36	675 $\pm$ 27	550 $\pm$ 55
2558.5	282 $\pm$ 12	234 $\pm$ 10	271 $\pm$ 27	230 $\pm$ 30
2579.9	439 $\pm$ 22	394 $\pm$ 20	436 $\pm$ 27	340 $\pm$ 39
2599.0	760 $\pm$ 38	790 $\pm$ 50	795 $\pm$ 42	740 $\pm$ 45
2671.3	281 $\pm$ 14	280 $\pm$ 10	265 $\pm$ 24	270 $\pm$ 20
2716.5	171 $\pm$ 8	170 $\pm$ 10	155 $\pm$ 18	145 $\pm$ 14
$\Sigma \Gamma_n$	2649	2574	2596	2275

(This Table, including the comments, is reproduced from the paper of Derrien, Ref. D3)

#### COMMENTS ON TABLE III

The Geel shape analysis has been done on the 0.011 at/b sample; no background correction is needed; but the normalization coefficient is equal to 0.975. The Columbia shape analysis has been done on the 0.084 at/b and 0.035 at/b samples; the background corrections are respectively equal to 0.007 and 0.013, at 2600 eV neutron energy.

The theoretical formulation of the transmission used in the shape analysis is the following:

$$T_r = a + c \left( e^{-n\sigma_\Delta} \right) * R$$

$\sigma_\Delta$  is the usual Breit-Wigner one level formulation of the total cross section, broadened by the Doppler effects, plus one term taking into account the level-level interference in the neutron channel; R is the resolution function, a the background parameter and c the normalization coefficient.

Recently Olsen et al.,<sup>B31</sup> Liou and Chrien<sup>B30</sup> and Finch<sup>D1</sup> have stressed the importance of multilevel effects in obtaining resonance parameters from transmission data and in describing neutron transmission through thick  $^{238}\text{U}$  samples. For instance, Olsen et al. have shown that a shape analysis of their transmission data converges towards the values of  $\Gamma_n = 1.39$  mV,  $\Gamma_\gamma = 25.1$  mV for the level at 6.67 eV, when multilevel effects are ignored. When multilevel effects are taken into account, the analysis of the same data converges toward the values  $\Gamma_n = 1.48$  mV and  $\Gamma_\gamma = 23.0$  mV.

### 3. EVALUATION OF THE RESONANCE PARAMETERS FOR THE LEVELS WITH ENERGIES BETWEEN 1 AND 4000 eV

#### A. General Considerations

Since 1955, between 30 and 35 independent determinations of the  $^{238}\text{U}$  resonance parameters have been reported.<sup>B1-B34</sup> Most of the earlier experiments<sup>B1-B10</sup> cover only the low energy resonances, up to 1 keV. Among the more recent experiments six sets of measurements extend to 4 keV and above.<sup>B11,B17,B20,B26,B31,B32</sup> The comparison of the resonance parameters from the different experiments often shows discrepancies considerably larger than the estimated uncertainties and sometimes systematic. The reasons for these discrepancies are often not understood.

The evaluation of resonance parameters can be done in several ways, including the selection of the values from one single measurement estimated to be the most accurate, or, at the other extreme, averaging the results of all available measurements, weighting each by the inverse square of the reported error. The latter approach was followed by Moxon in his 1974 evaluation<sup>C5</sup> and the former approach was used by McCrosson<sup>C1</sup> for evaluating neutron widths. We believe that the best estimate of the value of the resonance parameters can be obtained by averaging results from a number of independent measurements. Before averaging we have attempted to correct individual measurements for suspected systematic errors and have tried to weight the measurements in a consistent way.

Pitterle et al.<sup>C1</sup> have observed the existence of systematic differences among resonance parameters reported by different measurers and have tried to "correct" the experimental data for the systematic effects by a regression analysis technique. We have used a very similar approach here.

Unfortunately there is no uniform method of estimating and reporting the uncertainty in a resonance parameter derived from a set of measurements. In the most recent experiments statistical uncertainties have become relatively unimportant due to the high intensity of presently available neutron sources. Hence the uncertainties are mostly systematic and often due to poorly known causes: undetected backgrounds, method of analysis, and so on. Some authors report only statistical errors, others combine them with estimated systematic errors; many authors report errors as generated by a resonance analysis computer code, on the basis of some goodness of fit criterion that has more to do with the model used to analyze the data than with the systematic errors in the measurements.

Since there are inconsistencies in the methods used by different authors to estimate and report their errors, it does not seem justified to weight each determination of a parameter by the inverse square of the reported error. We have attempted to weight the different experiments consistently by giving more weight to those experiments for which the parameters, corrected for systematic effects, agree well with the average of the other experiments.

Above 200 eV we have considered only data reported since 1967,<sup>B14-B34</sup> except for the data reported in 1964 by Garg et al.<sup>B11</sup> which cover an extensive energy range (6 to 3900 eV). We think that the inclusion of older data in our evaluation would not have improved the precision because these earlier results are likely to have large systematic errors which are difficult to assess because statistical errors are also large and because many of the measurements cover only a restricted energy range.

Most transmission, self-indication, capture or scattering measurements yield strongly correlated values of  $\Gamma_\gamma$  and  $\Gamma_n$  for a given resonance; in fact, many measurements yield only a relation between those two widths.<sup>D4</sup> Nevertheless we observed no significant external correlation between the values of  $\Gamma_\gamma$  and  $\Gamma_n$  reported by different authors. The absence of such external correlations is partly due to the fact that each value is based on a number of experiments that have different internal correlations between the widths, and partly due to the fact that the capture widths have relatively large uncertainties obscuring any possible correlation. Since no important external correlations were observed between the capture and neutron widths, these two widths were evaluated independently.

#### B. Determination of the Level Energies

The energy scales of the various measurements were aligned on the energy scale of the 150-m time-of-flight measurement of

Olsen et al.<sup>B31</sup> This energy scale was selected as a standard because it is well documented and has been extensively compared with other energy scales.<sup>D5</sup> In Table IV a comparison is shown of the energies of some typical resonances as obtained by Olsen et al. and by other laboratories. The position of most levels, as given by Olsen et al. is intermediate between those given by Rahn et al.<sup>B20</sup> and by Poortmans et al.<sup>B23</sup>

The following procedure is used to align the energy scale of the  $k^{\text{th}}$  experiment to that of Olsen et al. The energy of  $j^{\text{th}}$  level reported by the  $k^{\text{th}}$  experimenter,  $E_{kj}$ , is assumed to be related to the energy reported by Olsen et al. for that level,  $E_j^*$  by the relation:

$$E_j^* = E_{kj} (\alpha_k + \beta_k E_{kj}^{1/2}) \text{ where } j = 1, \dots, N_k \quad (1)$$

$N_k$  is the number of level energies reported by the  $k^{\text{th}}$  experimenter. The structure of equation (1) is justified by analysis of the sources of uncertainties in the time-of-flight technique.<sup>D6</sup>

The values of  $\alpha_k$  and  $\beta_k$  were obtained by minimizing

$$\sum_{j=1}^{N_k} w_j [E_j^* - E_{kj} (\alpha_k + \beta_k E_{kj}^{1/2})]^2 \quad (2)$$

where the sum is carried over a number of large levels which are easily identified. The weights  $w_j$  were taken inversely proportional to the square of the uncertainties reported by the  $k^{\text{th}}$  experimenter. Rohr et al.<sup>B16</sup> and Poortmans et al.<sup>B32</sup> do not report uncertainties associated with the resonance

Table IV. Comparison of the Energies of Selected Resonances

(All energies in eV)

Olsen et al.	Corvi et al. (a,b)	Rahn et al.	James et al. (b)
145.63 $\pm$ .03	145.68 $\pm$ .10	145.57 $\pm$ .15	145.603 $\pm$ .021
463.14 $\pm$ .14	463.62 $\pm$ .4	462.8 $\pm$ .4	463.12 $\pm$ .14
619.95 $\pm$ .19	620.18 $\pm$ .2	619.75 $\pm$ .35	
708.27 $\pm$ .22	708.59 $\pm$ .25	707.9 $\pm$ .4	708.18 $\pm$ .45
905.03 $\pm$ .19	905.47 $\pm$ .30	904.5 $\pm$ .3	
1419.76 $\pm$ .29	1420.7 $\pm$ .3	1419.2 $\pm$ .3	1419.88 $\pm$ .46
1473.82 $\pm$ .31	1474.6 $\pm$ .3	1473.4 $\pm$ .4	
1638.07 $\pm$ .34	1639.1 $\pm$ .3	1637.4 $\pm$ .5	
2030.49 $\pm$ .43	2031.9 $\pm$ .3	2029.8 $\pm$ .6	
2145.56 $\pm$ .45	2146.7 $\pm$ .3	2144.6 $\pm$ .6	
2489.18 $\pm$ .43	2490.8 $\pm$ .4	2488.4 $\pm$ .7	2489.50 $\pm$ .71
2672.22 $\pm$ .56	2674.0 $\pm$ .8	2671.3 $\pm$ .9	
2865.39 $\pm$ .60	2867.5 $\pm$ .8	2864.1 $\pm$ .9	
3205.81 $\pm$ .67	3208.1 $\pm$ 1.0	3204.9 $\pm$ 1.1	
3458.14 $\pm$ .73	3461.0 $\pm$ 1.2	3456.3 $\pm$ 1.3	
3574.04 $\pm$ .75	3576.6 $\pm$ 1.2	3572.3 $\pm$ 1.3	

a) Private communication from F. Corvi to G. D. James (1977).

b) Private communication from G. D. James (1977).

Table V. Parameters for Energy Scales Alignment

All energy scales are aligned on the scale of Olsen et al.<sup>B31</sup> by the relation:

$$E^* = E_k (\alpha_k + \beta_k E_k^{1/2})$$

the values of  $\alpha_k$  and  $\beta_k$  are tabulated below:

Experiment and Year	Ref.	$\alpha_k$	$10^4 \times \beta_k$ (eV <sup>-1/2</sup> )	$\alpha_k + \beta_k (4000)^{1/2}$
Garg et al. (64)	B11	.999658	.08653	1.000205
Glass et al. (68)	B14	.999658	.08653	1.000205
Rohr et al. (70)	B16	.998714	.18726	.999898
Carraro & Kolar (70)	B17	1.000312	-.20615	.999008
Maletski et al. (72)	B19	1.000625	-.83687	.995332
Rahn et al. (72)	B20	1.000340	.00290	1.000358
Corvi et al. (75)	B25	.999428	.07633	.999911
Nakajima et al. (75)	B26	1.000340	.00290	1.000358
Liou and Chrien (77)	B30	1.	0.	1.
Olsen et al. (77)	B31	1.	0.	1. (standard)
Poortmans et al. (77)	B32	.999428	.07633	.999911

(The number of levels given in Ref. B30 is not sufficient for determining  $\alpha_k$  and  $\beta_k$ .)

energies. For these two measurements the energy uncertainties were assumed to be the same as those given by Carraro and Kolar.<sup>B17</sup> In Table V the values of  $\alpha_k$  and  $\beta_k$  for a number of measurements are listed. Note that all corrections are much smaller than 1%. The values of the level energies were obtained by averaging the various independent determinations after realignment of the energy scales.

### C. Neutron Widths

We have obtained  $\langle \Gamma_{nj} \rangle$ , the average value of the neutron width of the  $j^{\text{th}}$  level, as:

$$\langle \Gamma_{nj} \rangle = \frac{\sum_k \frac{\Gamma_{njk}^*}{\delta_{jk}^{*2}}}{\sum_k \frac{1}{\delta_{jk}^{*2}}} \quad (3)$$

where:

$$\Gamma_{njk}^* = \Gamma_{njk} (a_k + b_k E_{jk}) \quad (4)$$

$$\delta_{jk}^* = C_k \delta_{jk} \quad (5)$$

and where  $\Gamma_{njk} \pm \delta_{jk}$  is the  $k^{\text{th}}$  experimenter's determination of the neutron width of the  $j^{\text{th}}$  level, with its reported standard deviation, and  $E_{jk}$  is the energy of the level, after alignment of the energy scale.

The parameters  $a_k$  and  $b_k$  are intended to correct the results of the  $k^{\text{th}}$  experiment for possible systematic effects and were obtained by minimizing with respect to  $a_k$  and  $b_k$  the quantity

$$S_k = \sum_{j=1}^{N_k} \frac{[\langle \Gamma_{nj} \rangle - \frac{\Gamma_{njk} (a_k + b_k E_{jk})}{C_k^2 \delta_{jk}^2}]^2}{C_k^2 \delta_{jk}^2} \quad (6)$$

The parameters  $C_k$  are intended to give consistent weights to the various experiments and were obtained from the relation:

$$\frac{1}{N_k - 1} \sum_{j=1}^{N_k} \frac{[\langle \Gamma_{nj} \rangle - \frac{\Gamma_{njk} (a_k + b_k E_{jk})}{C_k^2 \delta_{jk}^2}]^2}{C_k^2 \delta_{jk}^2} = 1 \quad (7)$$

The sums in (6) and (7) were carried over the s-wave levels. The equations (3) to (7) are coupled and were solved by successive iterations. The values of  $N_k$ ,  $a_k$ ,  $b_k$ , and  $C_k$  for the eleven measurements considered are listed in Table VI. For the experiments of Glass et al.<sup>B14</sup>, Corvi et al.<sup>B25</sup>, and Liou and Chrien<sup>B30</sup> the values of  $a_k$ ,  $b_k$ , and  $C_k$  could not be determined by the method just discussed, because these experiments did not report values of  $\Gamma_n$  for a sufficient number of large levels. The values of  $a_k$ ,  $b_k$ , and  $C_k$  for these measurements were assigned somewhat arbitrarily and are shown in Table VI.

The systematic trends in the values of  $\Gamma_n$  reported by different experimenters are illustrated in Fig. 1. The left

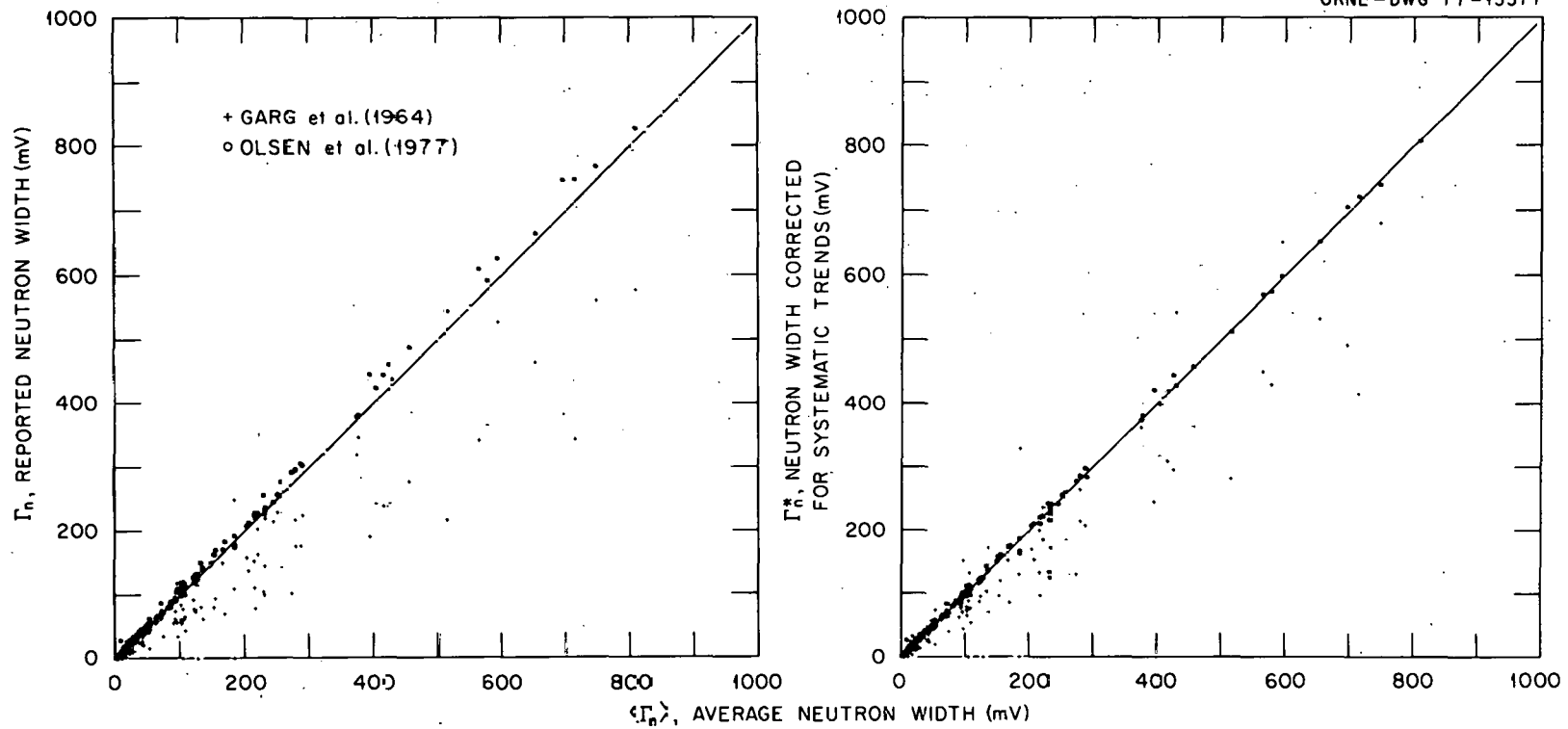


Fig. 1. Systematic trends in the measured values of  $\Gamma_n$ . The left part of the figure shows the values of  $\Gamma_n$  reported by Garg et al.<sup>B11</sup> and by Olsen et al.<sup>B31</sup> against corresponding values obtained by averaging eleven measurements. The values of Garg et al. tend to be lower than average whereas those of Olsen et al. tend to be higher than average, with the difference increasing with increasing  $\Gamma_n$ . In the right part of the figure, the corresponding values of  $\Gamma_n^*$ , i.e.,  $\Gamma_n$  corrected for systematic trends are plotted against the average value of  $\Gamma_n$ .

part of the figure shows the values of  $\Gamma_n$  reported by Garg et al.<sup>B11</sup> and by Olsen et al.<sup>B31</sup> against corresponding values obtained by averaging eleven measurements as just discussed. The values of Garg et al. tend to be lower than average whereas those of Olsen et al. tend to be higher than average, with the difference increasing with increasing  $\Gamma_n$ . In the right part of the figure, the corresponding values of  $\Gamma_n^*$ , i.e.,  $\Gamma_n$  corrected for systematic trends, are plotted against the average values of  $\Gamma_n$ .

In the averages defined by equation (3) each experiment is given a weight inversely proportional to  $C_k^2$ . The method used to determine  $C_k$ , equation (7) corresponds to a requirement that  $\chi^2$  per degree of freedom be approximately equal to unity for the levels selected for the adjustment, after correction for systematic trends. As may be seen in Table VI the older experiment of Garg et al.<sup>B11</sup> is downweighted by a factor of 21, the experiment of Nakajima et al.<sup>B26</sup> is upweighted by a factor of 1.34, presumably because those authors overestimated their errors.

#### D. Capture Widths

In most experiments the capture widths have been determined only for selected levels at low energies. Above 1 keV, resolution and Doppler broadening prevent the reliable determination of resonance widths by shape analysis, and capture widths have been obtained only for a few levels with relatively large neutron

Table VI. Parameters for Correction of Systematic Trends in  $\Gamma_n$ 

Corrected values $\Gamma_{njk}^* = \Gamma_{njk} (a_k + b_k E_{jk})$ (see equation 4)					
$\delta_{jk}^* = C_k \delta_{jk}$ (see equation 5)					
Experiment	Ref.	$a_k$	$10^3 b_k$ ( $eV^{-1/2}$ )	$C_k$	$a_k + b_k * 4000^{(1)}$
Garg et al. (64)	B11	.99755	.08252	4.64	1.3276
Glass et al. (68)	B14	1.	0.	2.	
Rohr et al. (70)	B16	.98039	.08432	.87	
Carraro & Kolar (70)	B17	.97853	.00255	.75	.98873
Maletski et al. (72)	B19	1.0074	.17217	1.31	
Rahn et al. (72)	B20	1.0085	.05600	1.26	1.2325
Corvi et al. (75)	B25	1.	0.	2.	
Nakajima et al. (75)	B26	.97176	.03171	.86	1.0986
Liou & Chrien (77)	B30	1.	0.	1.	
Olsen et al. (77)	B31	1.0195	-.02192	1.47	.9318
Poortmans et al. (77)	B32	.99313	-.00689	1.06	.9656

(The coefficients for Ref. B14, B25, and B30 could not be obtained from the reduced number of parameters given and were assigned arbitrarily, see text.)  
 (1) Given only for the experiments reporting data up to 4 keV.

widths; and for these, the uncertainties are large (10% or more). For this reason the statistical tests which were performed on the neutron widths could not be applied to the capture widths.

The capture widths were obtained from the values reported by Rohr, Weigmann, and Winter,<sup>B16</sup> Maletski et al.,<sup>B19</sup> Rahn et al.,<sup>B20</sup> Liou and Chrien,<sup>B30</sup> Poortmans et al.,<sup>B32</sup> and Olsen et al.<sup>B31</sup> For those levels for which more than one determination of the width existed, the evaluated value was obtained by averaging, weighting by the inverse square of the reported error. For the many levels for which no value was reported, a value of 23.5 mV was assumed. This is the value that had been assumed by the ENDF/B-III and ENDF/B-IV evaluators;<sup>C1</sup> it is consistent with the average value 23.55 mV recently evaluated by Rahn and Havens<sup>D7</sup> and with the value  $23.43 \text{ mV} \pm .11 \text{ mV}$  (stat)  $\pm .70 \text{ mV}$  (syst) obtained by Poortmans et al.<sup>B32</sup>

#### E. Fission Widths

For the levels at 6.67 eV, 20.9 eV and 36.7 eV, the consistent subthreshold widths obtained by Slovacek et al.<sup>B29</sup> and by Difilippo et al.<sup>B33</sup> were averaged. For the other levels the widths obtained by Difilippo et al.<sup>B33</sup> were used. The measurements of Difilippo et al. have appreciably better energy resolution than previous experiments, which permits a resolution of all the "clusters" below 4 keV into their Class 1 level components. The two main subthreshold clusters below 4 keV are illustrated in Figs. 2, 3, and 4.

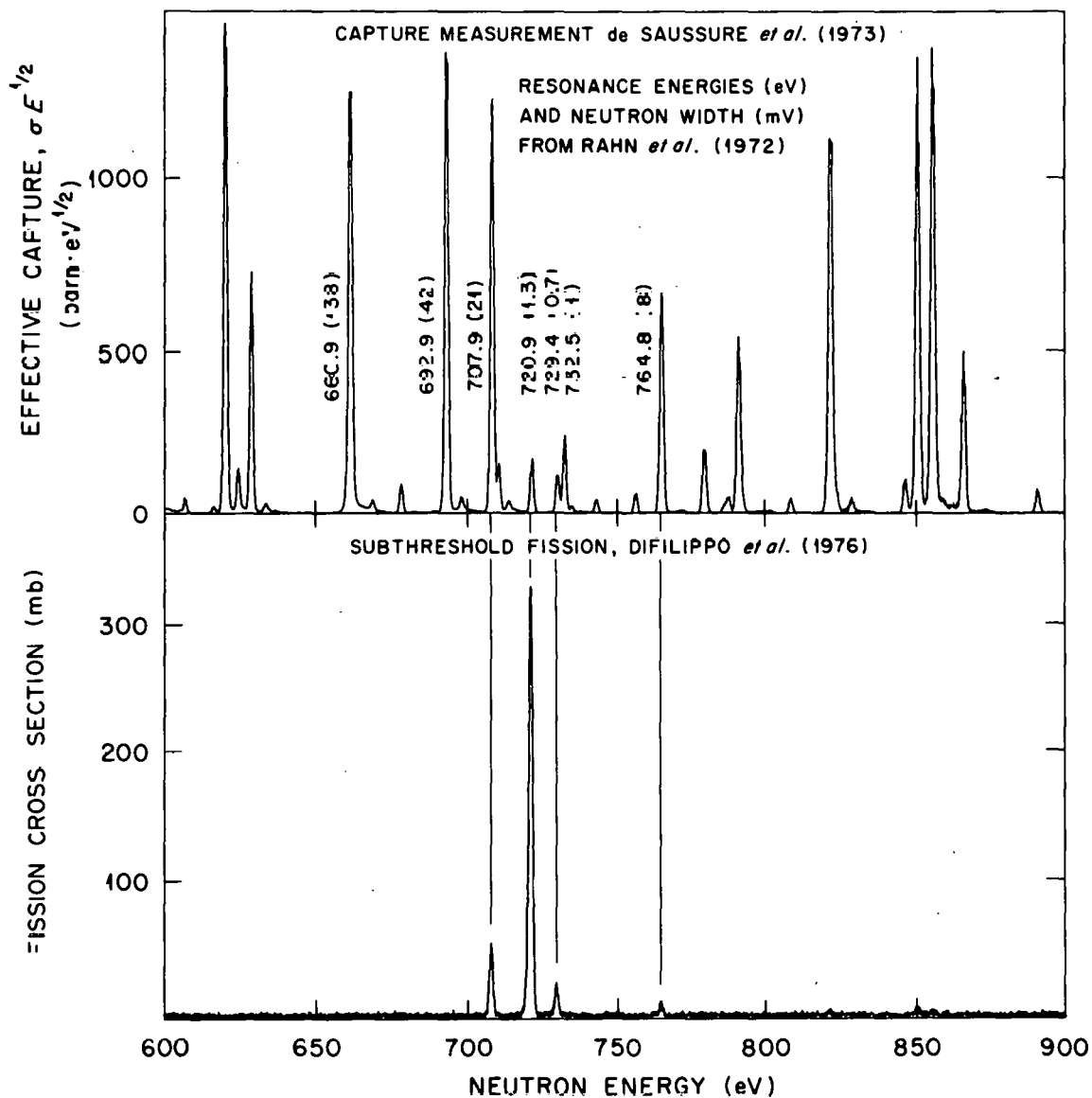


Fig. 2. High resolution  $^{238}\text{U}$  capture and fission cross sections in the neighborhood of the subthreshold fission cluster near 720 eV. The lower part of the figure shows the fission cross section, the upper part, the effective capture cross section (multiplied by  $E^{1/2}$ ) on the same energy scale. The levels at 720.9 eV, 729.4 eV, and 764.8 eV are taken to be s-wave levels because they are part of the same subthreshold fission cluster as the known s-wave level at 707.9 eV.

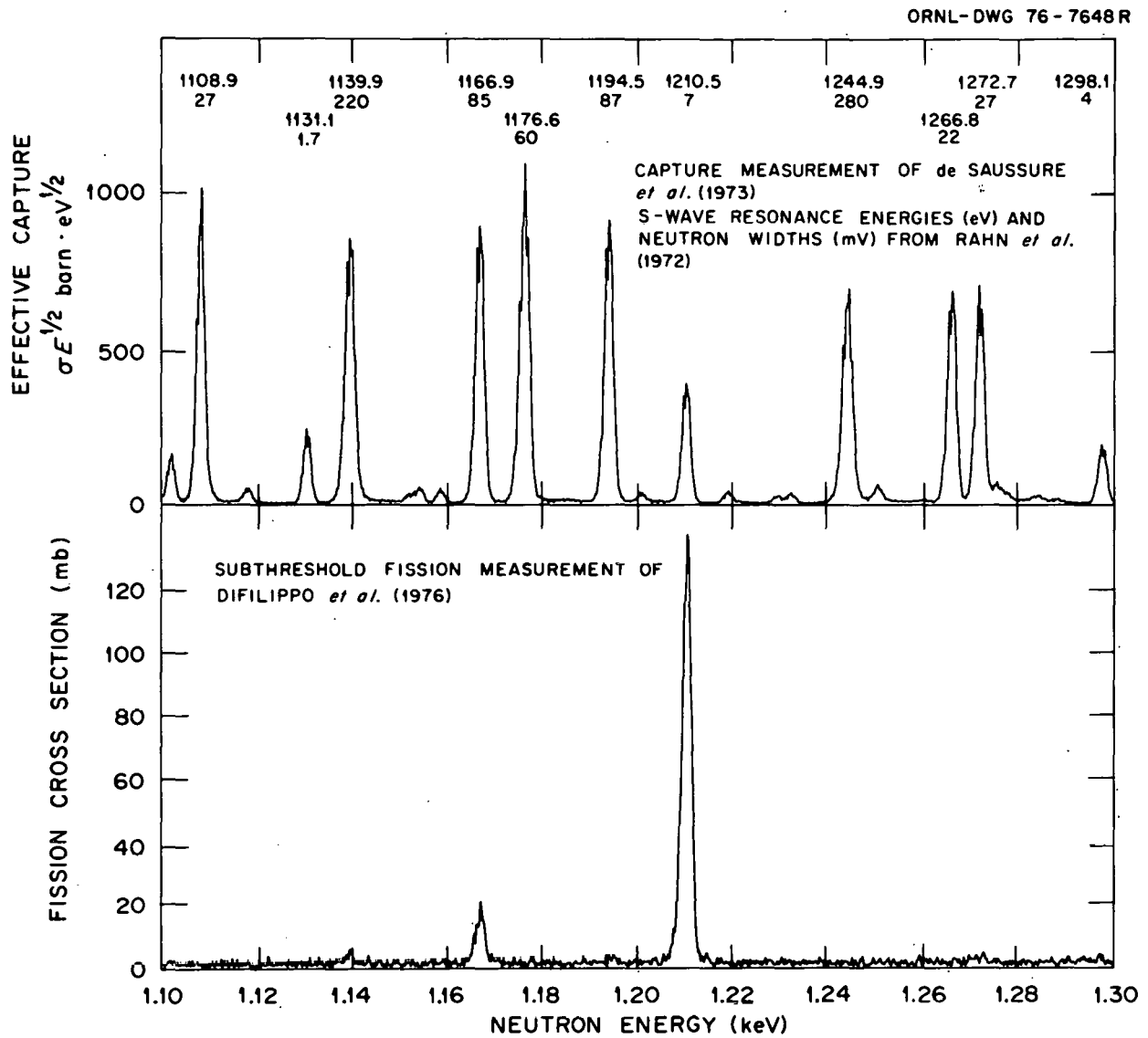


Fig. 3. High resolution  $^{238}\text{U}$  capture and fission cross sections in the neighborhood of the subthreshold fission cluster near 1200 eV. The lower part of the figure shows the fission cross sections, the upper part the effective capture cross section (multiplied by  $E^{1/2}$ ) on the same energy scale.

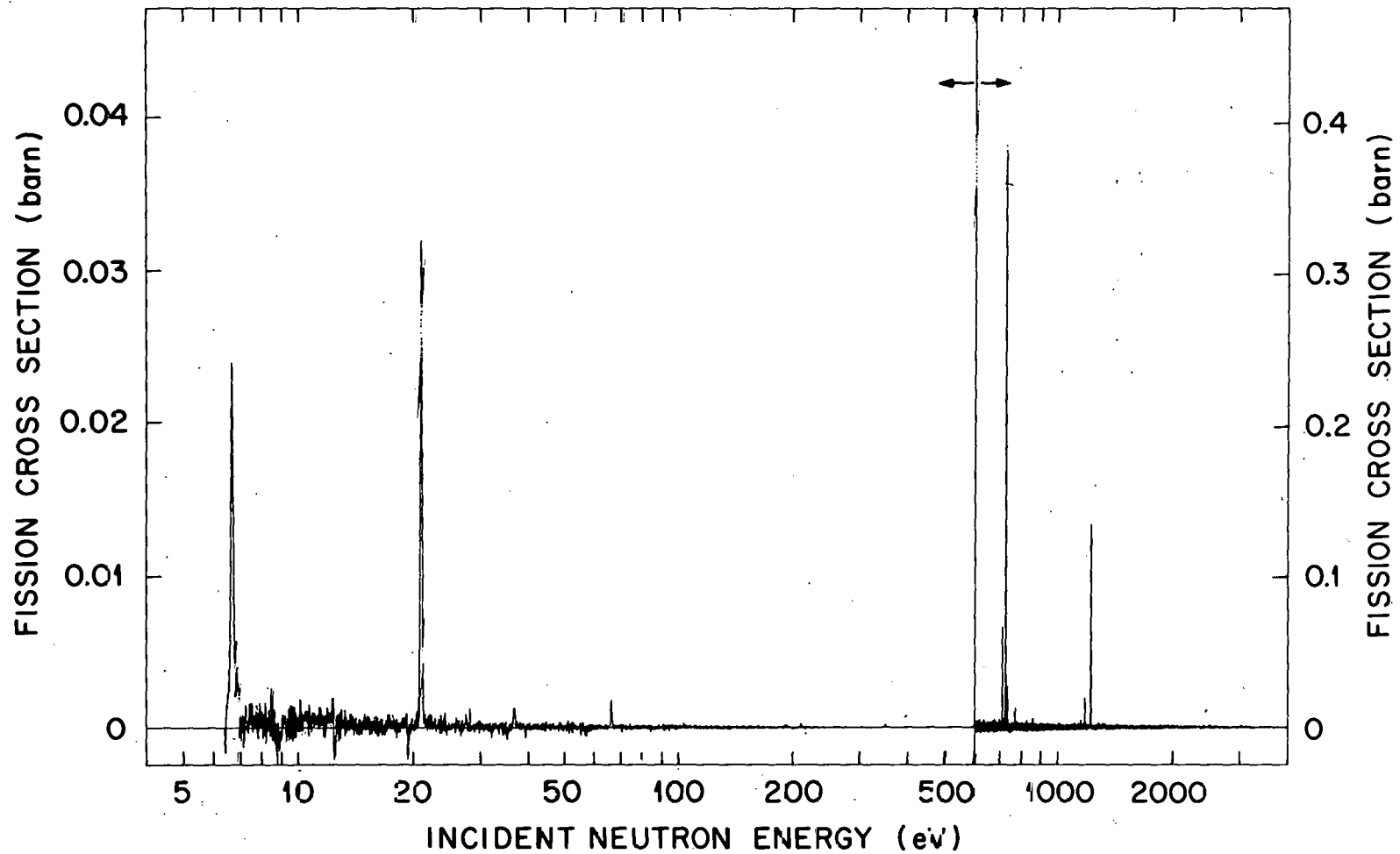


Fig. 4. Fission cross section below 4 keV. Note that there is a factor 10 change in the ordinate scale at 600 eV. A small background due to  $^{235}\text{U}$  contaminant was subtracted from the data, hence there are large statistical fluctuations near 8.8, 12.4 and 19.3 eV where  $^{235}\text{U}$  has large fission resonances.

## F. Angular Momentum Assignment

Those levels which have large neutron widths (a few mV) can be identified as s- or p-wave levels from the depth of the interference minimum between the resonance and potential scattering. For many levels with smaller neutron width such an identification is not possible. Corvi, Rohr, and Weigmann<sup>B25</sup> were able to identify 57 levels below 1600 eV as p-waves by measuring the fraction of capture gamma rays above 4.3 MeV. It is reasonable to assume that all levels which belong to a subthreshold fission cluster have the same parity and angular momentum; since in the two clusters below 4 keV at least one level can be identified as an s-wave, all the levels with an observable subthreshold fission component were taken to be s-waves.

For many small levels no unambiguous angular momentum assignment could be given. The angular momentum of those levels was then evaluated according to the following criteria: (1) All observed levels below 4 keV were assumed to be either s-wave or p-wave levels. This is reasonable, since the height of the penetration barriers below 4 keV make the neutron widths excited by neutrons of higher angular momenta exceedingly small. (2) The Bayes's conditional probability that a resonance be excited by p-wave neutrons,  $P(p, g\Gamma_n)$ , was computed for all the levels, following the method described by Bollinger and Thomas.<sup>B15</sup> All the levels with  $P(p, g\Gamma_n) < .5$  were assumed to be excited by

s-wave neutrons. (3) In order to satisfy the  $\Delta_3$  statistic<sup>D8</sup> for the s-wave levels in the interval 0-4 keV, a few levels with  $P(p, g\Gamma_n) > .5$  had to be taken as s-wave levels. Those levels were chosen to minimize the product of their probabilities to be excited by p-wave neutrons. The energy, neutron width and value of  $P(p, g\Gamma_n)$  of the s-wave levels with  $P(p, g\Gamma_n) > .5$  are given in Table VII. It should be clear that the division of levels with small neutron widths into s- and p-wave levels is not unique and is based on rather weak probability criteria.

#### G. Parameters of the Low Energy Resonances

The neutron and capture widths of the first six large s-wave levels and of the p-wave level at 10.24 eV have been evaluated in more detail. These parameters are particularly important for the calculation of thermal reactor performance.<sup>A7, D9</sup> A comparison of the reported parameters of these seven levels illustrates the difficulties in evaluating best values. Measurements of these parameters have been reported for more than 20 years. Most of the experimental values as well as a few evaluations are given in Tables VIII and IX.

There are very large discrepancies between some of the values reported for the capture widths. For the important level at 6.67 eV there are at least five standard deviations between the value of Jackson and Lynn,<sup>B8</sup>  $27.2 \pm 0.4$  mV, and that of Liou and Chrien,<sup>B30</sup>  $21.8 \pm 1.0$  mV. Similar discrepancies exist for the other levels.

Table VII. s-Wave Levels with Small Neutron Widths

Energy (eV)	Neutron Width (mV)	$P(p, g\Gamma_n)$	Comment
2787.4	13.29	.62	
1565.4	5.50	.69	
3492.6	14.34	.72	
1298.6	3.59	.77	
3169.8	10.89	.78	
2806.4	9.28	.78	
721.59	1.64	.78	Subthreshold Fission
3831.6	11.66	.82	
3219.7	9.19	.82	
1550.6	3.40	.85	
1953.8	3.94	.87	
730.15	1.13	.89	Subthreshold Fission
1913.3	1.71	.93	
1867.6	.88	.95	

$P(p, g\Gamma_n)$  is the Bayes's conditional probability that the resonance is excited by p-wave neutrons (see text and reference B15). The levels listed above have all  $P(p, g\Gamma_n) > .5$ ; they were nevertheless taken as s-wave levels either because they were observed in subthreshold fission groups, or to satisfy the  $\Delta_3$  statistics for level spacings.

Table VIII. Comparison of Measured and Evaluated Neutron Widths  
(Widths are given in mV)

Year	Ref.	$E_0$ (eV)	6.67	20.9	36.7	66.0	80.7	102.5	10.2
Harvey et al.	55	B1		8.5 $\pm$ .4	32.5 $\pm$ 1.9	25 $\pm$ 2			
Levin	56	B2	1.54 $\pm$ .10	8.3 $\pm$ .7	30 $\pm$ 4				
Lynn	56	B3	1.4 $\pm$ .1	8.7 $\pm$ .3	28.6 $\pm$ 1.5	22.6 $\pm$ 1.5	1.8 $\pm$ .6	57.5 $\pm$ 3	
Fluharty	56	B4		10.3 $\pm$ .2	32.6 $\pm$ .9	25.4 $\pm$ .7	2.34 $\pm$ .80	69 $\pm$ 20	
Bollinger	57	B5	1.45 $\pm$ .12	9.9 $\pm$ .4	34 $\pm$ 2.3	23.5 $\pm$ 1.5	2.1 $\pm$ .2	74 $\pm$ 5	.0014
Radkevich	57	B6	1.15 $\pm$ .04	6.35 $\pm$ .59	22 $\pm$ 3.5	19.1 $\pm$ 4.5	2.7 $\pm$ 1.1		
Jackson	62	38	1.52 $\pm$ .01						
Moxon	62	39			34.5 $\pm$ 3	23.5 $\pm$ 1.5	1.8 $\pm$ .3	69 $\pm$ 3	
Firk	63	B10			31 $\pm$ .9	25.1 $\pm$ 1.2		65.9 $\pm$ 2	
Garg	64	B11	1.52 $\pm$ .01	8.7 $\pm$ .3	31 $\pm$ .9	25 $\pm$ 1	2.06 $\pm$ .17	65.9 $\pm$ 2	
Ashgar	66	B13	1.578 $\pm$ .1	9.34 $\pm$ .5	30.95 $\pm$ 1.17	22.74 $\pm$ .77	1.85 $\pm$ .15	58.64 $\pm$ 2	.0014
Rohr	68	B16				24.8 $\pm$ 1.5		72.6 $\pm$ .5	
Carraro	71	B17				25.3 $\pm$ 1	2 $\pm$ 1.5	69.5 $\pm$ 7	
Maletski	72	B19				24.0 $\pm$ 1.5	2.2 $\pm$ .2	70 $\pm$ 3	
Rahn	72	B20	1.52 $\pm$ .05	8.5 $\pm$ .78	38 $\pm$ 2	26 $\pm$ 2	1.71 $\pm$ .18	70 $\pm$ 4	.00177 $\pm$ .0004
Nakajima	75	B26		10.1 $\pm$ 1.0	33.4 $\pm$ 1.7	25.5 $\pm$ 1.3	2.25 $\pm$ .18	71.3 $\pm$ 4.3	
Liou	77	B30	1.50 $\pm$ .03	9.86 $\pm$ .50	33.3 $\pm$ 1.2	25.6 $\pm$ 1.8	2.16 $\pm$ .18	68 $\pm$ 5	.00165 $\pm$ .00015
Olsen	77	B31	1.480 $\pm$ .032	10.16 $\pm$ .21	33.76 $\pm$ .70	24.37 $\pm$ .53	1.823 $\pm$ .046	70.9 $\pm$ 1.6	.00169 $\pm$ .00005
Poortmans	77	B32		10.2 $\pm$ .1	34.1 $\pm$ .5	23.9 $\pm$ .8	1.81 $\pm$ .08	70 $\pm$ 2	.00167 $\pm$ .00004
BNL-325	65	C2	1.52 $\pm$ .02	8.5 $\pm$ .5	31 $\pm$ .9	25 $\pm$ 1.2	2 $\pm$ .2	68 $\pm$ 3	.0014
	73	C2	1.52 $\pm$ .02	8.7 $\pm$ .5	32 $\pm$ 1	26 $\pm$ 1.5	2 $\pm$ .2	70 $\pm$ 3	.00156 $\pm$ .00001
Moxon	74	C5	1.51 $\pm$ .009	8.97 $\pm$ .175	31.6 $\pm$ .5	24 $\pm$ .4	1.96 $\pm$ .07	70.8 $\pm$ .4	.00156 $\pm$ .00001
ENDF/B-IV	75	C1	1.50	8.8	31.1	25.3	2	71	.00156
This Evaluation *	77		1.510 $\pm$ .015	10.12 $\pm$ .10	33.9 $\pm$ .4	24.6 $\pm$ .4	1.91 $\pm$ .04	71.6 $\pm$ .4	.00167 $\pm$ .00004

\*Error given here is statistical (uncorrelated) standard deviation also given in Table XXII and XXIII.

Table IX. Comparison of Measured and Evaluated Capture Widths  
(Widths are given in mV)

	Year	Ref.	$E_0$ (eV)	6.67	20.9	36.7	66.0	80.7	102.5	10.2
Harvey et al.	55	B1			25 <sub>+5</sub>	29 <sub>+9</sub>	17 <sub>+10</sub>			
Levin	56	B2	24 <sub>+2</sub>		30 <sub>+6</sub>	40 <sub>+20</sub>				
Lynn	56	B3	26.1 <sub>+1.5</sub>		28.8 <sub>+2.3</sub>	24.9 <sub>+4.2</sub>	18.6 <sub>+2.7</sub>		15.5 <sub>+5.4</sub>	
Fluharty	56	B4			25.9 <sub>+12</sub>	27.7 <sub>+24</sub>	39.1 <sub>+26</sub>		24 <sub>+26</sub>	
Bollinger	57	B5	26 <sub>+3</sub>		21.9 <sub>+2.3</sub>	29 <sub>+10</sub>	25.6 <sub>+9</sub>			
Radkevich	57	B6	21.15 <sub>+1.30</sub>		36 <sub>+3.5</sub>	34 <sub>+10</sub>	25.5 <sub>+12</sub>	21 <sub>+15</sub>		
Rosen	60	B7							21 <sub>+6</sub>	
Jackson	62	B8	27.2 <sub>+4</sub>							
Moxon	62	B9				21.2 <sub>+3.5</sub>	24.1 <sub>+2</sub>		24.1 <sub>+2</sub>	
Firk	63	B10				31.3 <sub>+2.2</sub>	25.1 <sub>+1.6</sub>		30.6 <sub>+3.3</sub>	
Michaudon	65	B12	23 <sub>+1</sub>		23 <sub>+1</sub>	23 <sub>+1</sub>				
Ashgar	66	B13	23.43 <sub>+10.12</sub>		33.83 <sub>+4</sub>	26.33 <sub>+3</sub>	26.07 <sub>+2</sub>	21.17 <sub>+10</sub>	25.95 <sub>+2</sub>	
Glass	68	B14				20.9 <sub>+6</sub>	17.35 <sub>+4</sub>		24.9 <sub>+5</sub>	
Rohr	68	B16					19.6 <sub>+3</sub>		26.1 <sub>+2.3</sub>	
Maletski	72	B19					25 <sub>+2</sub>		26 <sub>+2</sub>	
Rahn	72	B20			22 <sub>+3</sub>	23 <sub>+2</sub>	21 <sub>+2</sub>		28 <sub>+3</sub>	
Liou	77	B30	21.8 <sub>+1</sub>		23.5 <sub>+1.5</sub>	23.6 <sub>+2</sub>	22.2 <sub>+2</sub>	23.7 <sub>+2.5</sub>	24.3 <sub>+2.5</sub>	
Olsen	77	B31	23 <sub>+8</sub>		22.8 <sub>+8</sub>	22.9 <sub>+8</sub>	23.2 <sub>+8</sub>	24.3 <sub>+1.3</sub>	24.1 <sub>+9</sub>	22.2 <sub>+2</sub>
Poortmans	77	B32			23.2 <sub>+6</sub>	22.9 <sub>+3</sub>	24.0 <sub>+4</sub>		24.3 <sub>+4</sub>	
BNL-325	65	C2	26 <sub>+2</sub>		26 <sub>+4</sub>	26 <sub>+4</sub>	24 <sub>+2</sub>	21 <sub>+15</sub>	24 <sub>+3</sub>	
	73	C2	26 <sub>+2</sub>		25 <sub>+3</sub>	25 <sub>+2</sub>	22 <sub>+2</sub>		26 <sub>+2</sub>	
Moxon	74	C5	26.9 <sub>+37</sub>		25.7 <sub>+1</sub>	26.55 <sub>+1.2</sub>	23.56 <sub>+76</sub>	21.17 <sub>+8.9</sub>	25.78 <sub>+94</sub>	
ENDF/B-IV	75	C1	25.6		26.8	26.0	23.5	23.5	25.0	23.5
This Evaluation*	77		22.5 <sub>+6</sub>		23.1 <sub>+5</sub>	22.9 <sub>+3</sub>	23.7 <sub>+3</sub>	24.2 <sub>+1.2</sub>	24.4 <sub>+3</sub>	23.5

\*Error given here is statistical (uncorrelated) standard deviation also given in Table XXII.

For these seven levels, there is no significant systematic trend associated with a particular experiment. The radiation widths of Lynn and Pattenden<sup>B3</sup> are higher than average for the levels at 6.67 eV and 20.9 eV but the reverse is true for the levels at 66.0 and 102.5 eV. Inversely, the radiation widths of Rahn et al.<sup>B20</sup> are lower than average at 66.0 eV but higher at 102.5 eV.

The measurements reported since 1970 give consistent results but, for the first three s-wave levels, the values from these recent measurements are significantly different from the averages of the earlier measurements. The capture widths obtained in all of the recent measurements are at least 10% lower than that of all the older evaluations. For the levels at 20.9 eV and 36.7 eV the neutron widths obtained in the four most recent measurements<sup>B20, B30-32</sup> are very consistent but are approximately 10% higher than the corresponding widths reported in earlier experiments.<sup>C2</sup>

There are valid reasons to ignore, or at least down weight, the older measurements. Modern time-of-flight techniques provide much better energy resolutions and higher neutron intensities than were available a decade ago. Recent measurements were also done with a wide range of thicknesses and often with highly depleted uranium thus reducing corrections for <sup>235</sup>U contaminant. In Figs. 5 and 6 we compare the transmission data of Firk, Lynn, and Moxon<sup>B10</sup> with those of Olsen et al.<sup>B31</sup> in the vicinity of

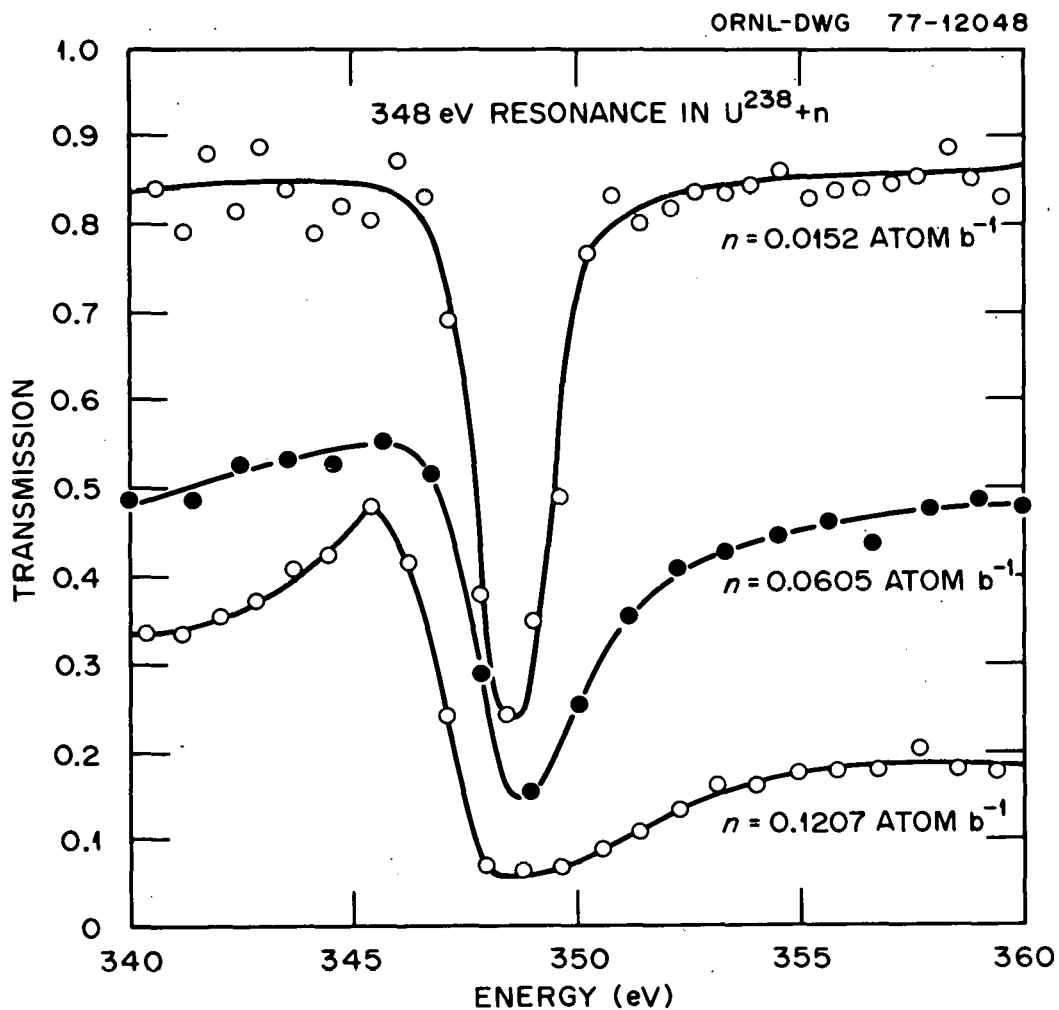


Fig. 5. Typical resonance transmission curves in the region of neutron energy 340 eV to 360 eV. This figure was published by Firk, Lynn, and Moxon in 1962. A comparison with Fig. 6 illustrates the improvement in statistical accuracy and in energy resolution obtained in the past 15 years.

ORNL-DWG 76-7862R

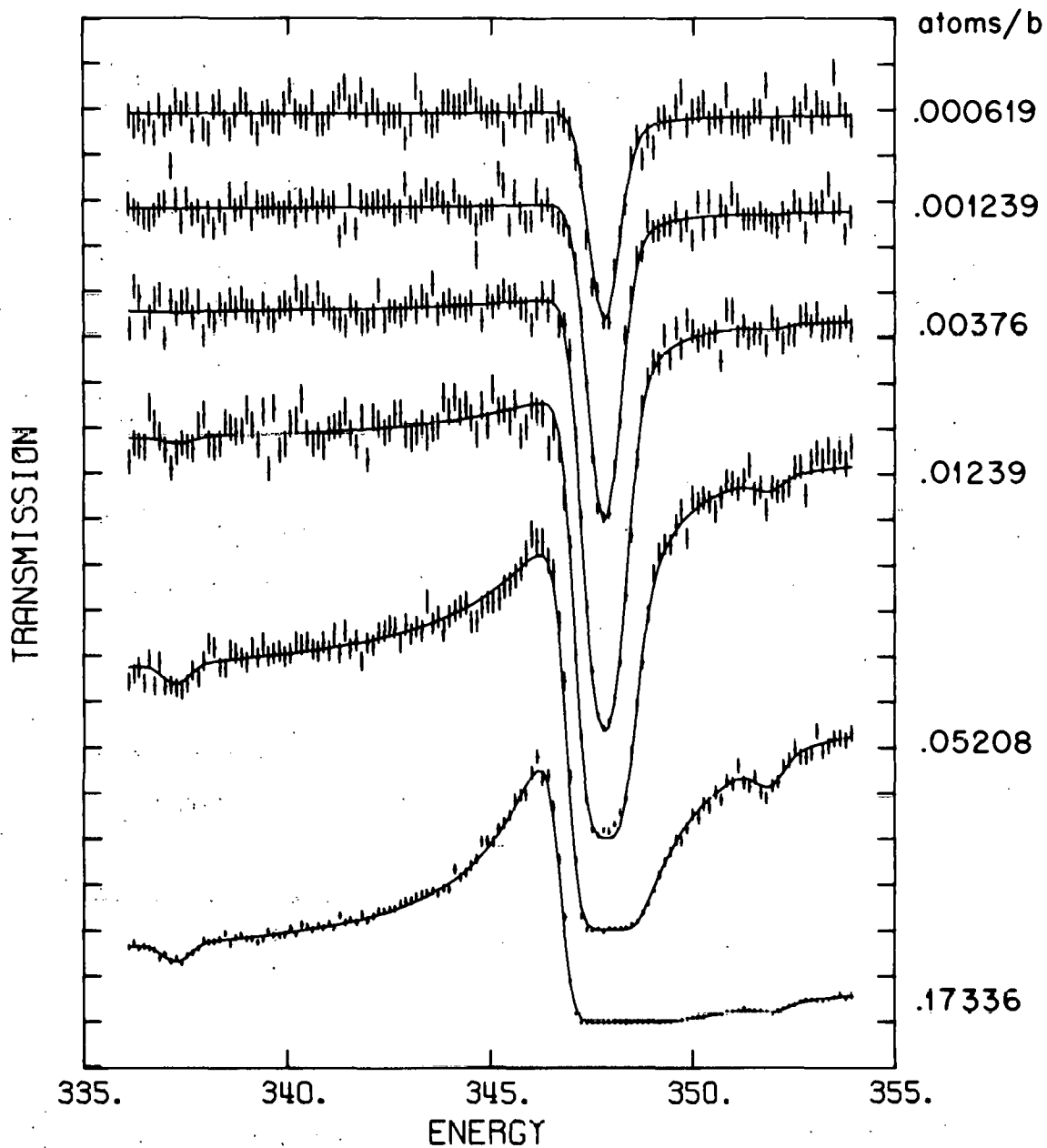


Fig. 6. Resonance transmission curves in the region of neutron energy 335 eV to 355 eV. This figure was recently published by Olsen et al. The solid lines represent a simultaneous least-square fit to the transmissions through seven sample thicknesses.

350 eV. The improvements in resolution, statistical accuracy and number of samples used are evident.

Many of the early values of the resonance parameters were obtained using scattering and capture measurements where multiple scattering corrections were ignored or roughly approximated, whereas the most recent values were derived primarily from precise transmission measurements which do not require multiple scattering corrections.

In Section 2 we have referred to the recent reexamination of the work of Lynn and Jackson.

#### H. Resonance Formalism and Scattering Radius

We have followed the structure<sup>D10</sup> of the ENDF/B-IV evaluation of  $^{238}\text{U};\text{C1}$  below 1 eV the cross sections are defined entirely by their File 3 contribution; above 1 eV the smooth cross section contributions of File 3 are added to a resonance contribution from File 2. The evaluation of the File 3 smooth cross sections will be discussed in the next section.

The resonance contributions should be computed by the Breit-Wigner multilevel formula. Olsen et al.,<sup>B31</sup> Liou and Chrien,<sup>B30</sup> and Finch<sup>D1</sup> have recently stressed the importance of using a multilevel formula to obtain an accurate representation of the transmission through thick samples of  $^{238}\text{U}$ . DeSaussure et al.<sup>D11</sup> have shown that for  $^{238}\text{U}$  the Breit-Wigner multilevel formula approximates very accurately the more exact multilevel formulae.

In order to improve the representation of the cross sections just above 1 eV and just below 4000 eV, two "outside" s-wave levels are included in File 2, in addition to the levels with energies between 1 and 4000 eV. The parameters for the level at 4040 eV were evaluated by the same methods as used for the levels between 1 and 4000 eV. The parameters of the bound level were adjusted to yield the measured cross sections at thermal energies, as will be discussed in the next section.

The value of the effective scattering radius was evaluated as  $.944 \times 10^{-12}$  cm. This value is somewhat higher than the value  $.9184 \times 10^{-12}$  cm evaluated by T. A. Pitterle for ENDF/B-II,<sup>C1</sup> but it is more consistent with the recent measurements of Rahn et al.<sup>B20</sup> and Olsen et al.<sup>B31</sup> In Table X are listed a few values reported for the effective scattering radius of <sup>238</sup>U.<sup>B5,B20,B31,D12-15</sup>

Table X. Measured and Evaluated Values of the <sup>238</sup>U Effective Scattering Radius  $\hat{a}$

Author*	Year	$\hat{a}$ in $10^{-12}$ cm
Hughes and Pilcher	1956	.93
Bollinger et al.	1957	.91
Hughes and Zimmerman	1959	.922 $\pm$ .020
Lynn	1963	.918 $\pm$ .013
Utlej	1964	.9184
Divadeenam	1968	.911
Rahn et al.	1972	.96 $\pm$ .03
Olsen et al.	1976	.944 $\pm$ .005
ENDF/B II, III, IV	1970	.9184
BNL-325	1973	.94 $\pm$ .03
This Evaluation	1977	.944 $\pm$ .025

\*References are given in the text.

#### 4. EVALUATION OF THE SMOOTH BACKGROUNDS (File 3)

As previously stated, we have followed the structure <sup>D10</sup> of the ENDF/B-IV evaluation of <sup>238</sup>U. <sup>C1</sup> Below 1 eV the cross sections are defined entirely by their File 3 contribution. Above 1 eV the smooth cross section contributions of File 3 are added to a resonance contribution from File 2.

In addition to the contribution of the levels of File 2 below 1 eV, File 3 represents the contribution of those levels which are not included in File 2, either because their resonance energy is outside the range 1 to 4000 eV (only two "outside levels" were included in File 2), or because those levels were not detected experimentally because they are very small or "overlapped" by large levels.

The contributions of the levels in the range from 4000 to 4500 eV were obtained by evaluating the resonance parameters of the main levels in this range, using the same methods that were used for the evaluation of the parameters in the range 1 to 4000 eV. The parameters of the main levels with energies in the range 4 to 4.5 keV are given in Table XI. The first of these levels was included in File 2. The contributions of the other levels given in Table XI to the cross sections below 4 keV were computed with the single level Breit-Wigner formula and included in File 3.

The contributions of the bound levels and of the levels above 4.5 keV were computed by assuming a bound level at -20 eV and a "picket fence" of uniform equidistant levels extending from  $-\infty$  to -20 eV and from 4.5 keV to  $+\infty$ . The cross sections due to such a

Table XI. Principal s-Wave Levels with Energies between 4 and 4.5 keV

$E_0$ (keV)	$\Gamma_n$ (mV)
4.041	64.1
4.064	19.6
4.090	95.3
4.125	41.5
4.132	16.8
4.169	192.3
4.179	32.2
4.210	40.4
4.258	32.7
4.300	143.9
4.307	115.8
4.325	87.4
4.371	158.3
4.376	139.6
4.398	176.4
4.436	103.0
4.512	608.1

All of the above levels are assumed to have a capture width of 23.5 mV.

picket fence of levels can be approximated analytically, as shown by deSaussure et al.<sup>D11</sup> The parameters of the assumed level at -20 eV and the "strengths" of the uniform picket fence were adjusted to yield the measured total and capture cross sections at .0253 eV.

The resonance parameters of the level assumed at -20 eV and the parameters used in computing the contribution of the picket fence of uniform levels are given in Table XII. The reduced neutron width of the level at -20 eV was chosen ten times smaller than the average s-wave reduced neutron width in the resolved region. Even so the contribution of the picket fence to the capture and scattering cross sections had to be reduced by the factors FGC and FGN defined in Table XII, to yield the measured values of the cross sections at .0253 eV. Leonard<sup>D16-17</sup> and Olsen et al.<sup>B31</sup> have already noted that the local strength-function of the bound levels near the binding energy is appreciably lower than the average s-wave strength function over the resonance region.

The various contributions to the computed capture and total cross sections at .0253 eV are listed in Tables XIII and XIV, where these computed cross sections are also compared to "measured" values obtained from the 1973 edition of BNL-325.<sup>C2</sup> These "measured" values were really evaluated from the existing direct measurements. The measurements of the thermal capture cross section are summarized in Table XV, taken from the article of Hunt, Robertson, and Ryves.<sup>D18</sup> The total cross section in the thermal group corresponds to a coherent scattering amplitude of  $(0.84 \pm 0.01) 10^{-12}$  cm, a value in agreement with

Table XII. Contributions to the Smooth Scattering and Capture Cross Sections

1. Picket fences of uniform levels extending from  $-\infty$  to  $E^- = -20$  eV and from  $E^+ = 4512$  eV to  $+\infty$ , with level spacing  $D = 24.8$  eV, reduced neutron width  $\Gamma_n^0 = 2.88$  mV and capture width  $\Gamma_\gamma = 23.5$  mV. The contributions to the scattering and capture cross sections are approximated as (see Ref. D11):

$$\sigma_n^\infty = \text{FGN} \cdot c_3 \cdot \left[ \Gamma_n^0 r_1 - 4 k_0 \hat{a} f_2 \right] \quad \sigma_\gamma^m = \text{FGC} \cdot \frac{c_5}{E^{1/2}} \Gamma_\gamma f_1$$

$$f_1 = \frac{E^+ - E^- + D}{(E^+ - E + \frac{1}{2}D)(E - E^- + \frac{1}{2}D)} \quad f_2 = \ln \left( \frac{E - E^- + .582D}{E^+ - E + .582D} \right)$$

where  $\text{FGN} = .557$  and  $\text{FGC} = .827$  are adjustment factors discussed in the text,  $k_0 = 2.1875 \cdot 10^9 \text{ cm}^{-1}$  is the neutron wave number at 1 eV,  $\hat{a} = .944 \times 10^{-12} \text{ cm}$  is the effective scattering radius, and  $c_5 = \frac{\pi \Gamma_n^0}{k_0^2 D} = 77.3$  barn.

2. Levels with energies between 4040 and 4512 eV, parameters given in Table XI.
3. Below 1 eV, levels of File 2, including an assumed bound level  $E_0 = -20$  eV,  $\Gamma_n^0 = .287$  mV,  $\Gamma_\gamma = 23.5$  mV; and an outside level at  $E_0 = 4040$  eV, first level given in Table XI.
4. Unresolved p-wave above 1 keV:  $1000, < E < 1340$  eV  $\sigma_\gamma^{\text{ur}} = (E - 1000) \cdot .3994 \text{ mb}$   
 $E > 1340$  eV  $\sigma_\gamma^{\text{ur}} = 3.71 E^{1/2} \text{ mb}$

Table XIII. Computed and Measured Cross Sections at .0253 eV

	$\sigma(n,\gamma)$ b.	$\sigma(n,n)$ b.	$\sigma_t$ b.
1. Picket Fences Contribution	.295	1.741	2.036
2. Resolved Levels of File 2 (includes potential scattering)	2.405	7.198	9.603
3. Levels with Energies Between 4040 and 4512 eV	0	-.038	-.038
Total	2.700	8.901	11.601
Evaluated from direct measurements (from Ref. C2 and Table XIV)	2.70 $\pm$ .02	8.90 $\pm$ .16	11.60 $\pm$ .16

Table XIV. Computed and Measured Scattering Length at .0253 eV

Computed Scattering Cross Section (see Table XIII)	8.901 b.
Corresponding Scattering Length: $a_{\text{coh}} = \left[ \frac{\sigma}{4\pi} \right]^{1/2}$	.842 x 10 <sup>-12</sup> cm
Direct Measurements: (in 10 <sup>-12</sup> cm)	
Atoji (1961)	.851 $\pm$ .022
Roof et al. (1962)	.84 $\pm$ .02
Willis (1963)	.850 $\pm$ .006

Table XV. Measurements of the  $^{238}\text{U}$  Thermal Capture Cross Section

Reference	$\sigma(n, \gamma)$ (barn)	Methods and Comments
Harris, Rose, and Schroeder (1954)	$2.71 \pm 0.05$	Reactivity measurements in CP3 using a sample of very low $^{238}\text{U}$ content. Cd ratio measurements by activation to correct for resonance absorption. Revised using $\sigma_A(\text{B}) = 757.7$ b at 2200 m/sec for the standard.
Egelstaff (1954)	$2.8 \pm 0.10$	Transmission measurements with a slow neutron chopper. Sample of very low $^{235}\text{U}$ content was used.
Crocker (1955)	$2.72 \pm 0.10$	Activation in a thermal spectrum with $\sigma_0[\text{Au}] = 98.8$ b. Corrected for fission activity by Ryves (1959).
Small (1955)	$2.72 \pm 0.06$	Local oscillator in well moderated spectrum. Measurements with natural and depleted uranium. Revised assuming $\sigma_A(\text{MnSO}_4) = 13.73$ b.
Cocking and Egelstaff (1955)	$2.69 \pm 0.04$	Transmission measurements using cold neutrons from a Bi filter extrapolated to 2200 m/sec. Sample was of a very low $^{235}\text{U}$ content.
Egelstaff and Hall (1955)	$2.69 \pm 0.04$	Transmission measurements at long wavelengths with slow neutron chopper. Sample was of very low $^{235}\text{U}$ content.
Palevsky (1955)	$2.73 \pm 0.07$	Transmission measurements at long wavelengths with slow neutron chopper. Sample was of natural uranium.
Bingham, Durham, and Ungrin (1968)	$2.721 \pm 0.016$	Relative to thermal fission cross section of $^{235}\text{U}$ .
Hunt et al. (1969)	$2.69 \pm 0.03$	Activation in a thermal spectrum $< 0.005\%$ $^{235}\text{U}$ .

the results of three neutron diffraction measurements.<sup>D19</sup> The potential scattering cross section corresponds to an effective scattering radius of  $.944 \times 10^{-12}$  cm as evaluated in the previous section.

The contribution to the cross sections of s-wave levels with energies between 1 and 4000 eV, which have not been observed experimentally, was estimated to be negligible. The contribution of missed p-wave levels to the capture cross section was estimated as follows: Figure 7 is a plot of the cumulative sums of the p-wave reduced neutron widths versus energy. The slope of the curve should be proportional to the p-wave strength-function, which should be roughly constant. Above 1.5 keV the slope decreases, probably because a number of p-wave levels are missed due to the poorer energy resolution of the measurements, causing an increased overlap of p-wave and s-wave levels and also because the measurements of Corvi, Rohr and Weigmann<sup>B25</sup> from which many of the evaluated p-wave levels were obtained, ends at 1550 eV. The strength of the missed p-wave levels was estimated by extrapolating the slope of the curve of Fig. 7 from the region below 1.3 keV to the region between 1.3 and 4 keV. The calculation of the contribution of these missed p-wave levels to the capture cross section is outlined in Table XVI. This contribution was included as a smooth capture cross section in File 3.

From 1 to 4000 eV the subthreshold fission cross section was evaluated to be the fission cross section computed from the parameters listed in File 2, so that the fission component of File 3 was set identically zero above 1 eV. Below 1 eV the fission cross section

ORNL-DWG 77-12052 R

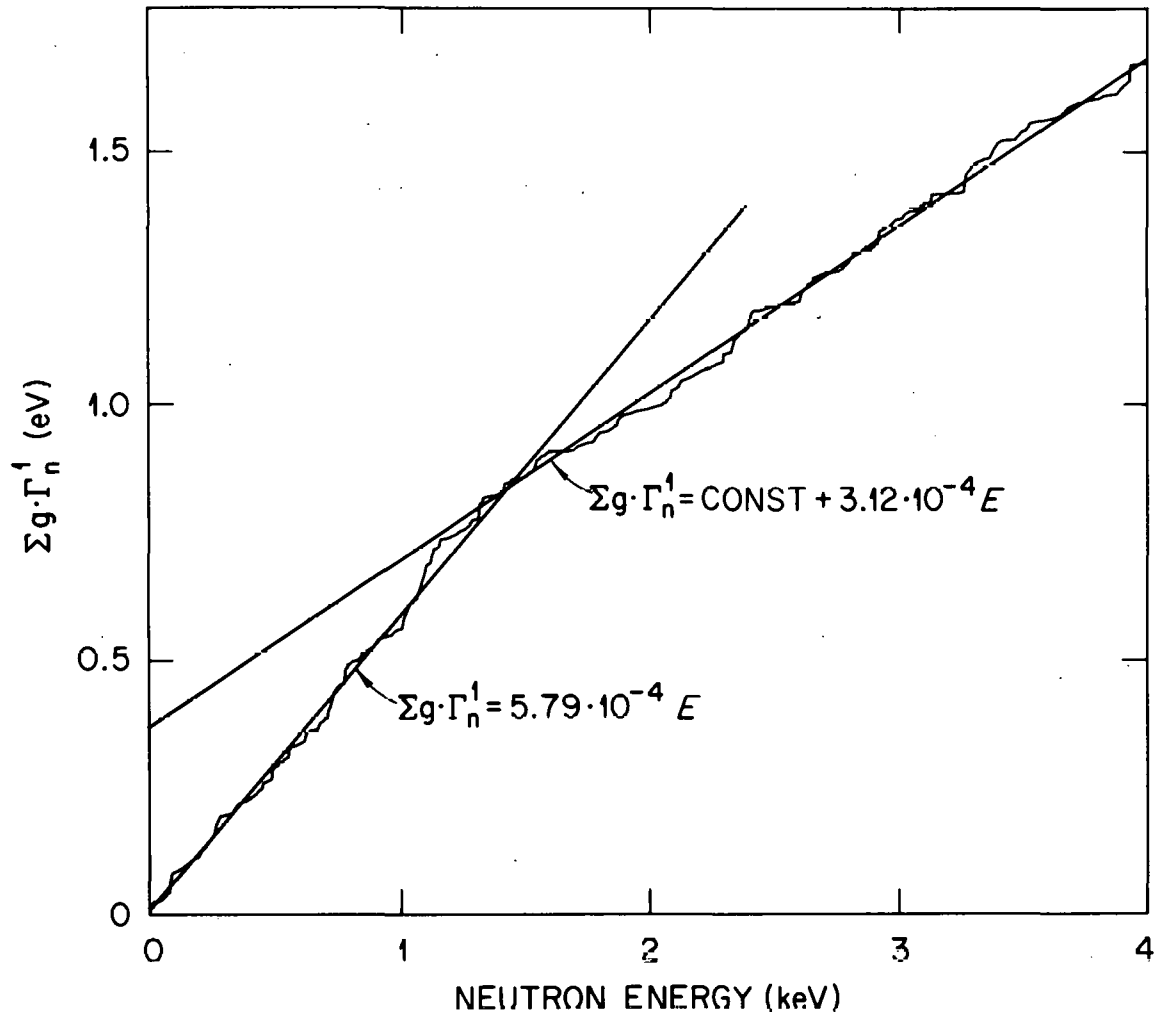


Fig. 7. Cumulative sum of the p-wave reduced widths vs neutron energy. The slope decreases near 1500 eV, probably because many small levels are missed, due to the increasingly poor resolution of the time-of-flight measurements.

Table XVI. Missed p-Wave Capture Above 1 keV

The average p-wave capture cross section is given by:

$$\langle \sigma_{n\gamma}(\ell=1) \rangle = \frac{2\pi^2}{k^2} \frac{1}{D^1} \cdot \left\langle \frac{g\Gamma_n \Gamma_\gamma}{\Gamma} \right\rangle_{\ell=1} \cong \frac{2\pi^2}{k^2} \cdot \left\langle \frac{g\Gamma_n}{D^1} \right\rangle_{\ell=1}$$

(since for p-wave  $\Gamma_n \ll \Gamma_\gamma$  and hence  $\Gamma \cong \Gamma_\gamma$ )

Using the definition of the p-wave strength function:

$$S^1 = \frac{\langle g\Gamma_n^1 \rangle}{3D^1} = \frac{(kR)^2}{1+(kR)^2} \cdot \frac{\langle g\Gamma_n \rangle_{\ell=1}}{3D^1} \cdot E^{1/2}$$

we obtain:

$$\langle \sigma_{n\gamma}(\ell=1) \rangle \cong 6\pi^2 R^2 S^1 E^{1/2}, \text{ since } (kR)^2 \ll 1$$

(where  $R = .84 \times 10^{-12}$  cm is the nuclear radius)

From Fig. 7 we see that below 1 keV  $S^1 \cong 1.93 \times 10^{-4}$ , above 1.34 keV  $S^1 \cong 1.04 \times 10^{-4}$ , so that the missed p-wave capture above 1.34 keV is:

$$6\pi^2 R^2 \times .89 \times 10^{-4} E^{1/2} = 3.71 E^{1/2} \text{ mb}$$

(where E is in eV)

was evaluated to be proportional to  $E^{-1/2}$ . The fission cross section at .0253 eV was evaluated as 1.5 times the contribution of the levels with energies between 1 and 4000 eV. The contribution of the bound levels was somewhat arbitrarily evaluated to be only 50% of that of the positive levels, since much of the contribution of the positive levels comes from the first few s-wave levels, and there are strong indications, as discussed above, that the local strength function of the bound levels near the binding energy is smaller than the strength function averaged over the resolved range. The contributions of the positive energy levels to the fission cross section at .0253 eV are given in Table XVII, where the result of this evaluation is also compared with other evaluations. B18,B29

Table XVII. The  $^{238}\text{U}$  Thermal Fission Cross Section

1. Contributions of levels with energies between 1 and 4000 eV			
$E_0(\text{eV})$	$\Gamma_n(\text{mV})$	$\Gamma_f(10^{-9}\text{eV})$	$\delta\sigma_f^{(a)}(\mu\text{b})$
6.672	1.510	10.33	0.5599
20.86	10.12	59.95	1.260
36.67	33.91	8.877	0.1526
66.01	24.61	51.48	0.1477
80.73	1.907	66.15	0.8892E-02
102.5	71.64	12.25	0.3405E-01
189.6	167.0	47.72	0.6645E-01
208.5	49.60	88.09	0.2873E-01
237.3	26.48	60.03	0.7564E-02
347.8	81.73	267.6	0.4002E-01
376.9	1.148	205.4	0.3529E-03
463.1	5.494	1474.	0.7243E-02
478.4	4.188	240.9	0.8319E-03
518.3	49.60	292.6	0.9795E-02
535.3	44.28	367.0	0.1012E-01
595.0	86.41	1099.	0.4539E-01
619.9	30.76	214.7	0.2849E-02
708.3	21.79	0.2564E 05	0.1727
721.6	1.720	0.1096E 07	0.5563
730.1	0.9341	0.9261E 05	0.2479E-01
765.1	7.767	5945.	0.1177E-01
851.0	62.91	1215.	0.1493E-01
856.1	86.17	1107.	0.1836E-01
1140.	233.1	1595.	0.3497E-01
1168.	87.71	0.1171E 05	0.9093E-01
1211.	9.193	0.2734E 06	0.2033
1257.	29.17	4282.	0.9023E-02

Total contribution of levels with energies between 1 and 4000 eV	3.52 $\mu\text{b}$
Estimated contribution of bound levels and levels above 4000 eV	1.76 $\mu\text{b}$
Total thermal fission cross section	5.28 $\mu\text{b}$
Silbert and Bergen	$3 \pm 5 \mu\text{b}$
Slovacek et al.*	$2.7 \pm .3 \mu\text{b}$

\*Contribution from positive energy levels only.

$$(a) \delta\sigma_f = 4127550 \cdot \frac{\Gamma_n \Gamma_f}{E_0^{5/2}} \text{ in barns}$$

## 5. FINE ADJUSTMENTS TO THE PARAMETERS AND SMOOTH BACKGROUNDS

In Sections 3 and 4 we have described the evaluation of the resonance parameters and of the background files. Some fine adjustments to these evaluations were then performed on the basis of a direct comparison of calculated and measured transmission through a thick sample of  $^{238}\text{U}$  and of high resolution capture data. The thick sample transmission experiments were done by Olsen et al.<sup>B31</sup> with a sample of .175 at/b, both on flight paths of 40 m and 150 m. The capture data were taken by deSaussure et al.<sup>D20</sup> on a 40-m flight path.

The fine adjustments consisted mostly in small changes in the scattering cross section background (File 3) near the boundaries of the resolved range, and in the removal or addition of very small levels. A few levels which had been reported by only one set of experimenters and which could not be observed--neither in the thick sample transmission measurement nor in the capture data--were removed from the file. A few levels which had not been reported previously but which could be observed clearly both in the transmission and capture data were added to the file. The neutron widths of these levels were estimated from the transmission dips and capture peaks.

## 6. CAPTURE CROSS SECTIONS

The infinitely dilute capture cross section was integrated over 100-eV-wide intervals below 1-keV- and over 1-keV-wide intervals above 1 keV. The contributions of the s-wave levels, p-wave levels, and "missed" p-wave levels are listed separately in Table XVIII where they are compared with direct measurements of the infinitely dilute capture.<sup>D20-22</sup> The computed values given in Table XVIII were obtained analytically using the relation:

$$\int \sigma_{\gamma j} dE \cong 2g \frac{\pi^2}{k_0^2} \frac{\Gamma_{\gamma j} \Gamma_{nj}}{E_{oj} \Gamma_j} \quad (8)$$

for the contribution of the  $j^{\text{th}}$  level to the capture cross section, where  $k_0 = 2.1875 \times 10^9 \text{ cm}^{-1}$  is the reduced wave number at 1 eV; the other symbols have their usual meaning. In the calculation, the entire contribution defined by equation (8) was assigned to the interval containing the resonance energy  $E_{oj}$ , this assumes that the effects of resonance tails across energy intervals cancel. The contribution of the missed p-waves were obtained analytically as indicated in Table XVI. This is the only appreciable contribution due to File 3.

Above 1 keV the capture cross section computed from this evaluation is consistent with that directly measured by Moxon,<sup>D22</sup> is about 8% lower than that measured by deSaussure et al.,<sup>D20</sup> and 13% higher than that obtained by Friesenhahn et al.<sup>D21</sup> Below 900 eV the computed cross section is generally lower than the direct measurements of Moxon and of deSaussure et al. The discrepancies between

Table XVIII. Computed and Measured Average Capture Cross Section\*

Energy Interval (eV)	Contributions of:			Total Computed Average Capture	Directly Measured Average Capture		
	s-wave	resolved p-wave	unresolved p-wave		Moxon	Friesenhahn et al.	deSaussure et al.
0 - 100	46.5	.07		46.6			
100 - 200	17.1	.05		17.2			18.72 $\pm$ .44
200 - 300	8.49	.17		8.67			9.77 $\pm$ .30
300 - 400	2.88	.08		2.96			3.40 $\pm$ .17
400 - 500	2.46	.19		2.65			3.12 $\pm$ .15
500 - 600	4.83	.13		4.96	4.97 $\pm$ .13		5.39 $\pm$ .17
600 - 700	3.43	.18		3.61	3.75 $\pm$ .11		4.02 $\pm$ .14
700 - 800	1.36	.39		1.75	2.105 $\pm$ .08		2.10 $\pm$ .12
800 - 900	2.83	.13		2.96	3.37 $\pm$ .10		3.29 $\pm$ .12
900 - 1000	4.10	.14		4.24	3.64 $\pm$ .11		4.54 $\pm$ .14
1000 - 2000	1.62	.20	.10	1.93	1.97 $\pm$ .08	1.70 $\pm$ .20	2.12 $\pm$ .09
2000 - 3000	1.07	.22	.19	1.47	1.48 $\pm$ .07	1.33 $\pm$ .13	1.56 $\pm$ .08
3000 - 4000	.865	.195	.219	1.28	1.23 $\pm$ .06	1.06 $\pm$ .08	1.31 $\pm$ .07

\*All values given in barns

measured and computed capture cross sections, particularly below 1 keV, exceed the quoted uncertainties on the measurements and the estimated uncertainties in the calculation and are not understood. In Figs. 8 to 11, the capture probability measured by deSaussure et al.<sup>D20</sup> is compared with a Monte-Carlo calculation based on this evaluation.

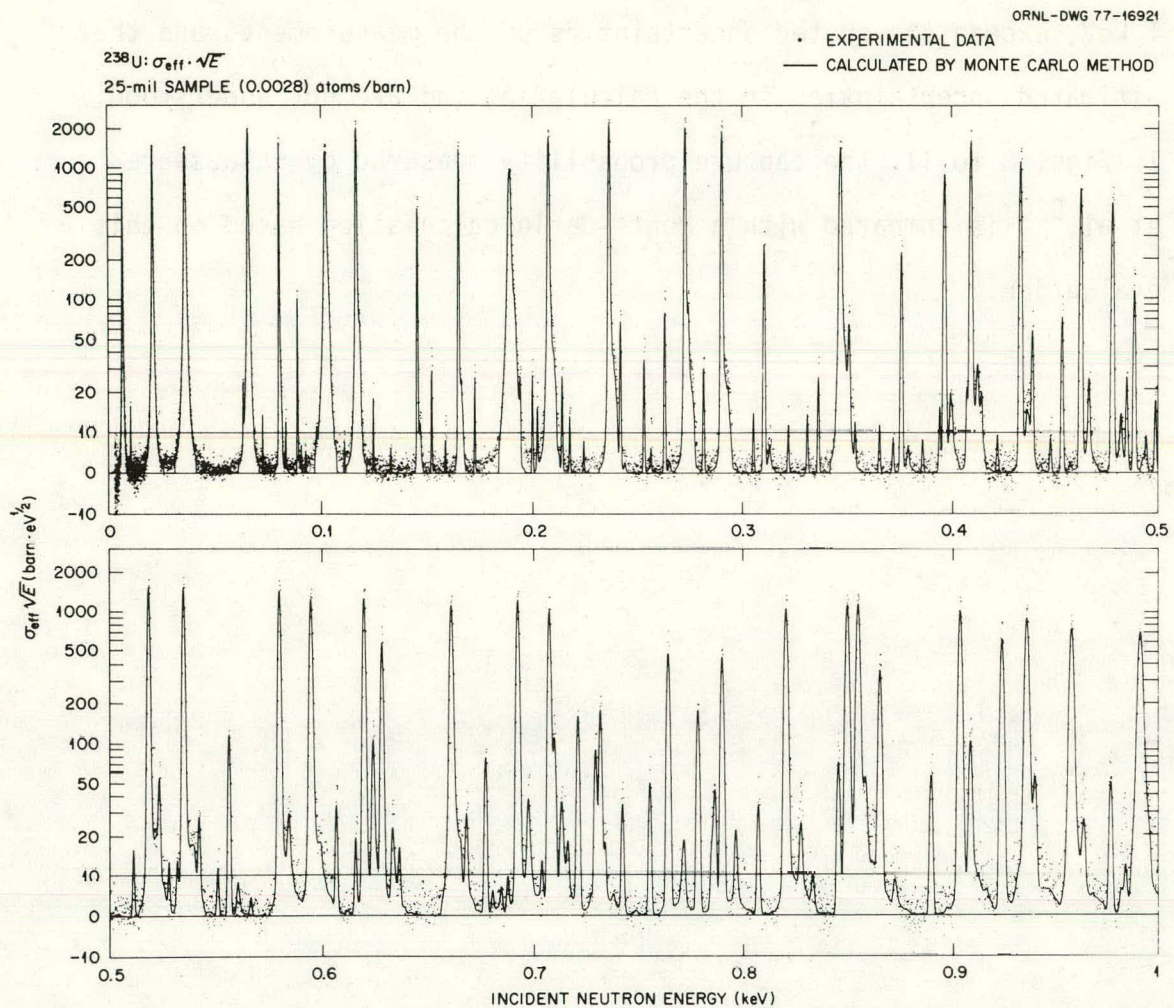


Fig. 8. Comparison of the measured and computed capture probabilities for a  $^{238}\text{U}$  sample of .0028 atoms/barn and for incident neutron energies up to 1.0 keV. The ordinate is the probability of capture multiplied by the square root of the energy and divided by the sample thickness in atoms/barn. The calculation was done with the Monte Carlo code MULTSCA using the resonance parameters of this evaluation. Note that the ordinate is linear from -10 to +10 barn  $\times$   $\text{eV}^{1/2}$  and logarithmic above 10 barn  $\times$   $\text{eV}^{1/2}$ .

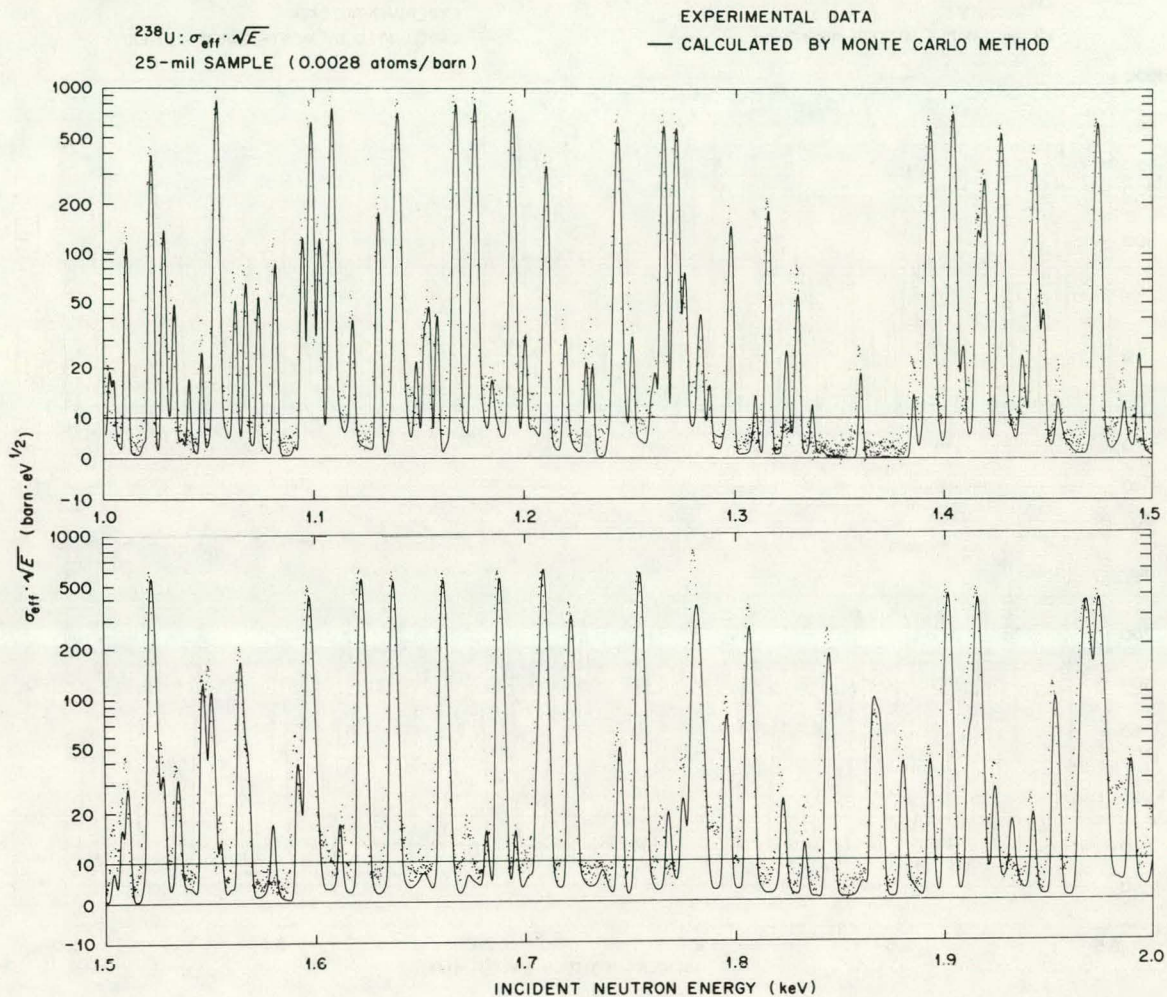


Fig. 9. Comparison of the measured and computed capture probabilities for a  $^{238}\text{U}$  sample of .0028 atoms/barn and for incident neutron energies from 1 to 2 keV. The ordinate is the probability of capture multiplied by the square root of the energy and divided by the sample thickness in atoms/barn. The calculation was done with the Monte Carlo code MULTSCA using the resonance parameters of this evaluation. Note that the ordinate is linear from -10 to +10 barn  $\times$   $\text{eV}^{1/2}$  and logarithmic above 10 barn  $\times$   $\text{eV}^{1/2}$ .

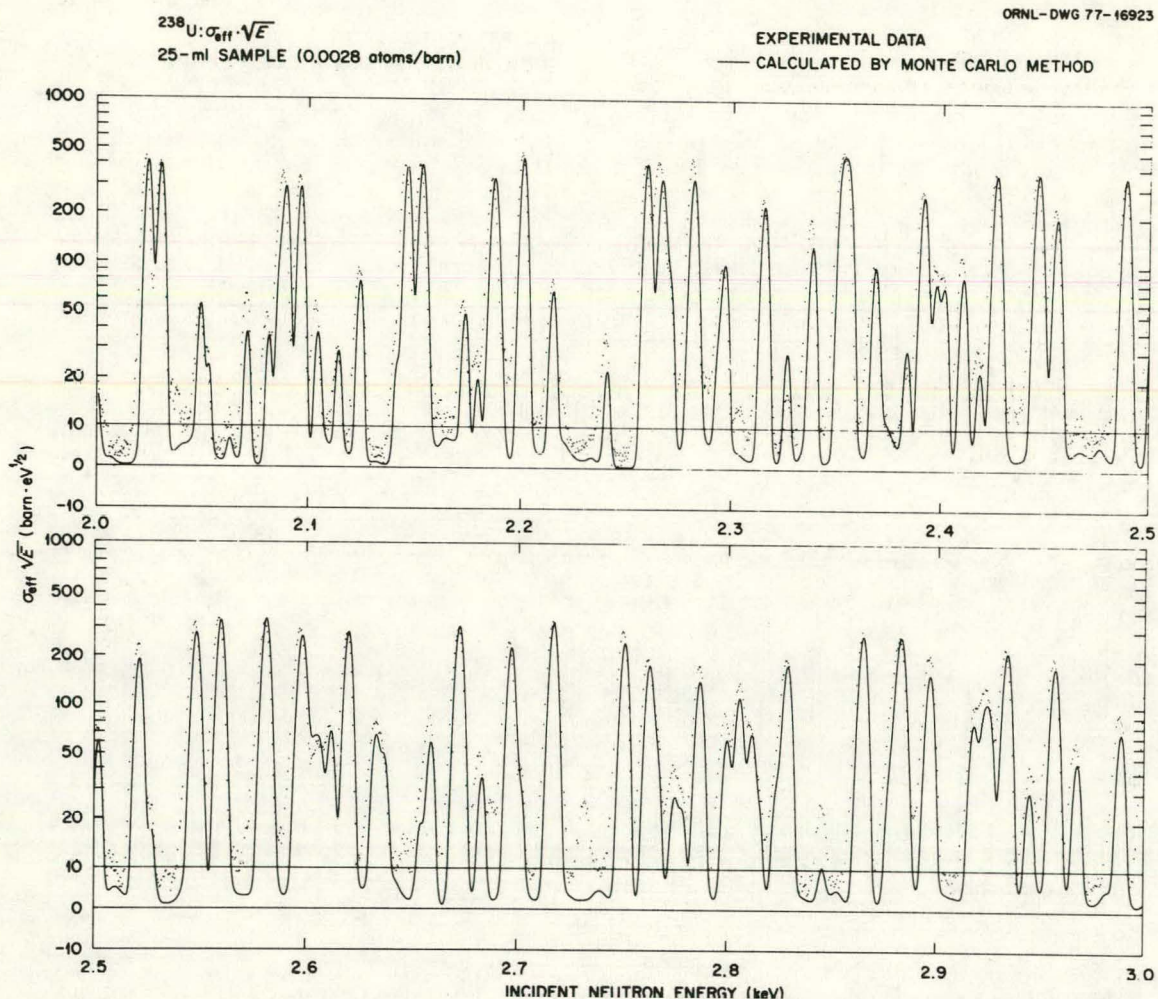


Fig. 10. Comparison of the measured and computed capture probabilities for a  $^{238}\text{U}$  sample of .0028 atoms/barn and for incident neutron energies from 2 to 3 keV. The ordinate is the probability of capture multiplied by the square root of the energy and divided by the sample thickness in atoms/barn. The calculation was done with the Monte Carlo code MULTSCA using the resonance parameters of this evaluation. Note that the ordinate is linear from -10 to +10 barn  $\times$   $\text{eV}^{1/2}$  and logarithmic above 10 barn  $\times$   $\text{eV}^{1/2}$ .

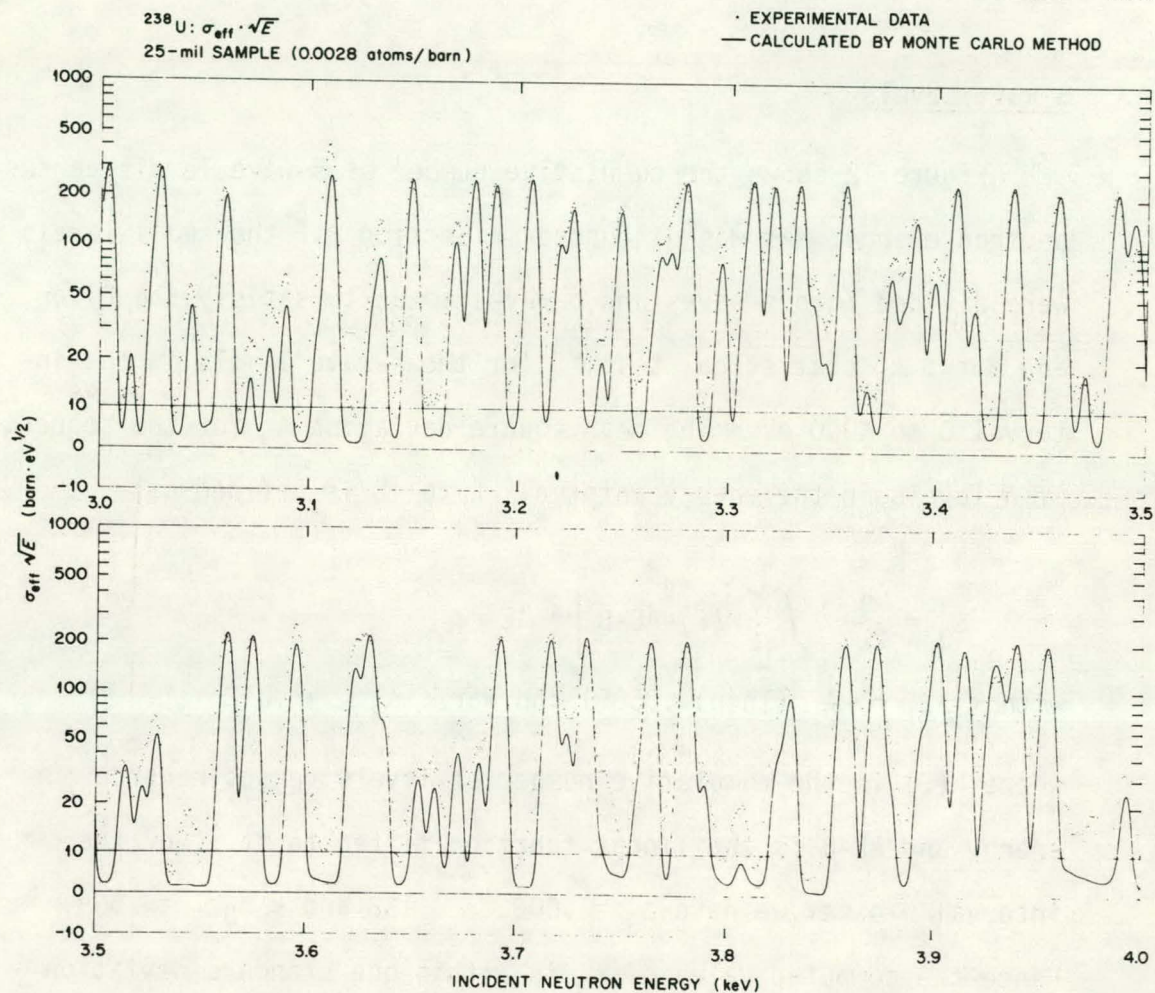


Fig. 11. Comparison of the measured and computed capture probabilities for a  $^{238}\text{U}$  sample of .0028 atoms/barn and for incident neutron energies from 3 to 4 keV. The ordinate is the probability of capture multiplied by the square root of the energy and divided by the sample thickness in atoms/barn. The calculation was done with the Monte Carlo code MULTSCA using the resonance parameters of this evaluation. Note that the ordinate is linear from -10 to +10 barn  $\times$   $\text{eV}^{1/2}$  and logarithmic above 10 barn  $\times$   $\text{eV}^{1/2}$ .

## 7. DISTRIBUTION OF THE RESONANCE PARAMETERS

A. S-wave Levels

Figure 12 shows the cumulative number of s-wave levels versus neutron energy. As was discussed in Section 3.F the small levels were divided into s-waves and p-waves so as to satisfy the Dyson and Metha  $\Delta_3$  statistical test,<sup>D8</sup> for the s-wave levels in the interval 0 to 4000 eV. The mean square deviation  $\Delta_3$  for the sequence of n levels in the energy interval -L to +L is defined as:

$$\Delta_3 = \frac{1}{2L} \int_{-L}^L [N(E) - AE - B]^2 \delta E \quad (9)$$

$$\text{with } \langle \Delta_3 \rangle = \frac{1}{\pi^2} (\ln(n) - .0686) \text{ and } \text{var } \langle \Delta_3 \rangle = .012$$

where  $N(E)$  is the cumulative number of levels versus neutron energy and  $AE - B$  is the linear function fitted to it. For the interval 0-4 keV we have  $\Delta_3 = .606$ ;  $n = 162$  and  $\langle \Delta_3 \rangle = .509$ . Hence the computed value of  $\Delta_3$  is within one standard deviation of the most probable value  $\langle \Delta_3 \rangle$ .

The average s-wave level spacing  $\overline{D^0}$  can best be obtained from the Dyson and Metha linear statistics  $W$ :<sup>D8</sup>

$$W = \sum_{j=1}^n \left[ 1 - \left( \frac{E_j}{L} \right)^2 \right]^{1/2} \text{ with } \langle W \rangle = \frac{\pi L}{2\overline{D^0}} \text{ and } \text{var } \langle W \rangle = 1/2 \quad (10)$$

which yields a value  $\overline{D^0} = 24.78 \pm .14$  eV. Of course, the error estimate is the "sampling error" associated with the statistics

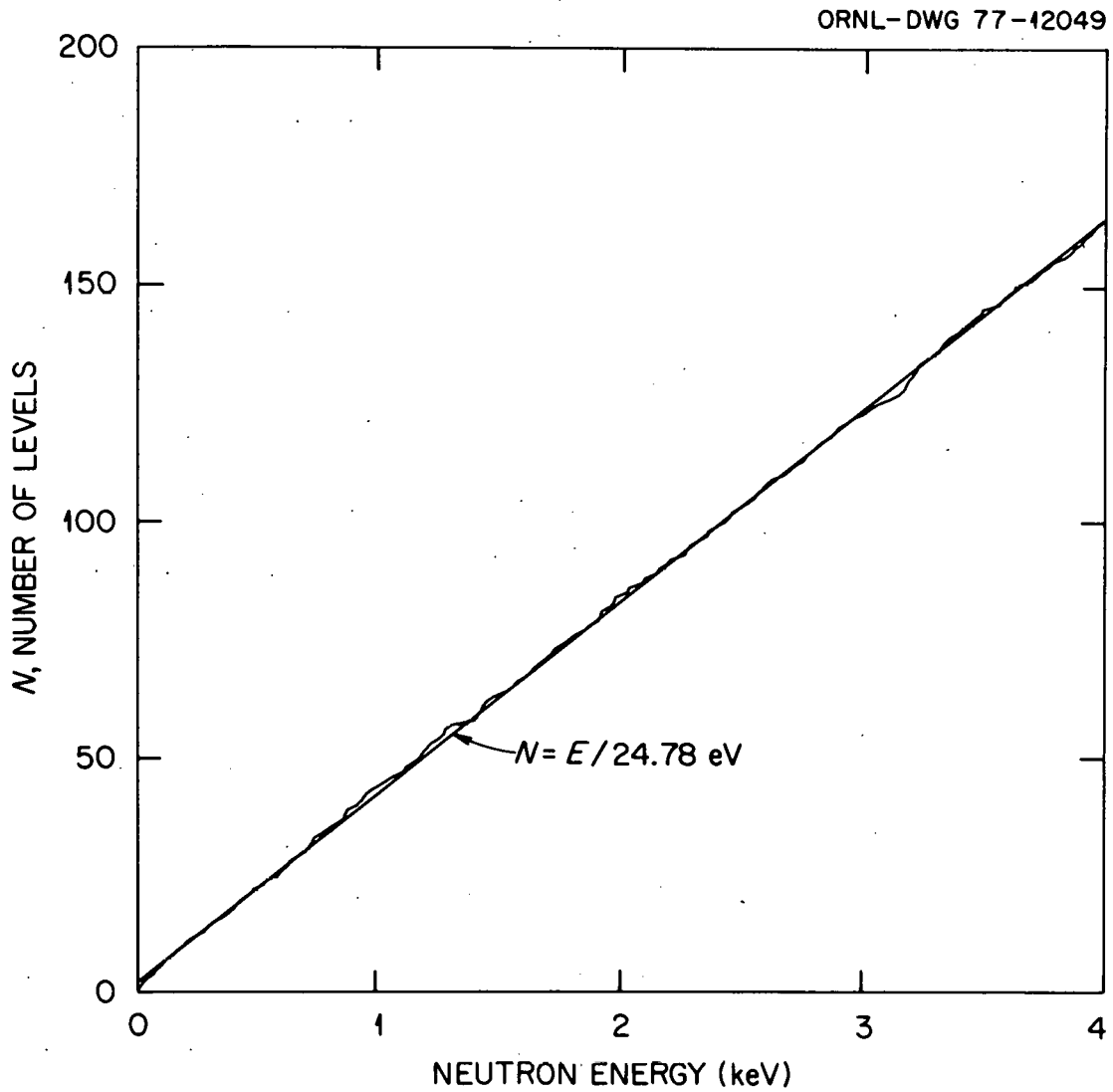


Fig. 12. Cumulative number of s-wave levels vs neutron energy. The solid line is a linear fit to  $N(E)$  and corresponds to an average spacing of 24.78 eV.

of the energy levels and does not include a possible error associated with an incorrect distribution of the small levels between s- and p-waves. This error is estimated to be  $\pm 2$  eV.

The value of  $\overline{D^0}$  obtained in this evaluation is larger than the 20.8 eV given by Rahn et al.<sup>B20</sup> and the 21.05 eV of ENDF/B-IV.<sup>C1</sup> The reason is that a number of small levels which had been assumed to be s-wave by Rahn et al., and by the evaluator of ENDF/B-IV have since been shown to be more likely p-wave, by the work of Corvi, Rohr and Weigmann.<sup>B25</sup> For the interval 1 to 2 keV the present evaluation yields a spacing of  $22.9 \pm 1.8$  eV in good agreement with the value  $22.4 \pm 1.0$  eV obtained by Corvi et al.

In Fig. 13 the observed distribution of s-wave nearest-neighbor spacings is compared with a Wigner distribution for one population.<sup>D23</sup>

$$P(x) = \frac{\pi}{2} x e^{-\frac{\pi}{4} x^2} \quad x = \frac{S}{\overline{D^0}} \quad (11)$$

where  $x$  is the ratio of the spacing  $S$  to the average spacing  $\overline{D^0}$ .

The agreement between the observed distribution and the Wigner distribution is good, except that one large spacing is observed with a value of  $x$  between 3.8 and 4.0. The probability to observe a spacing in this range, with 161 spacings, is only  $1.4 \times 10^{-3}$ .

The spacing is that between the s-wave levels at 1298.7 eV and 1393.8 eV. Eight small levels have been observed in this interval, but the most important levels at 1317 eV, 1331.5 eV, and 1386.1 eV have been shown to be likely p-waves by Corvi, Rohr, and Weigmann.<sup>B25</sup>

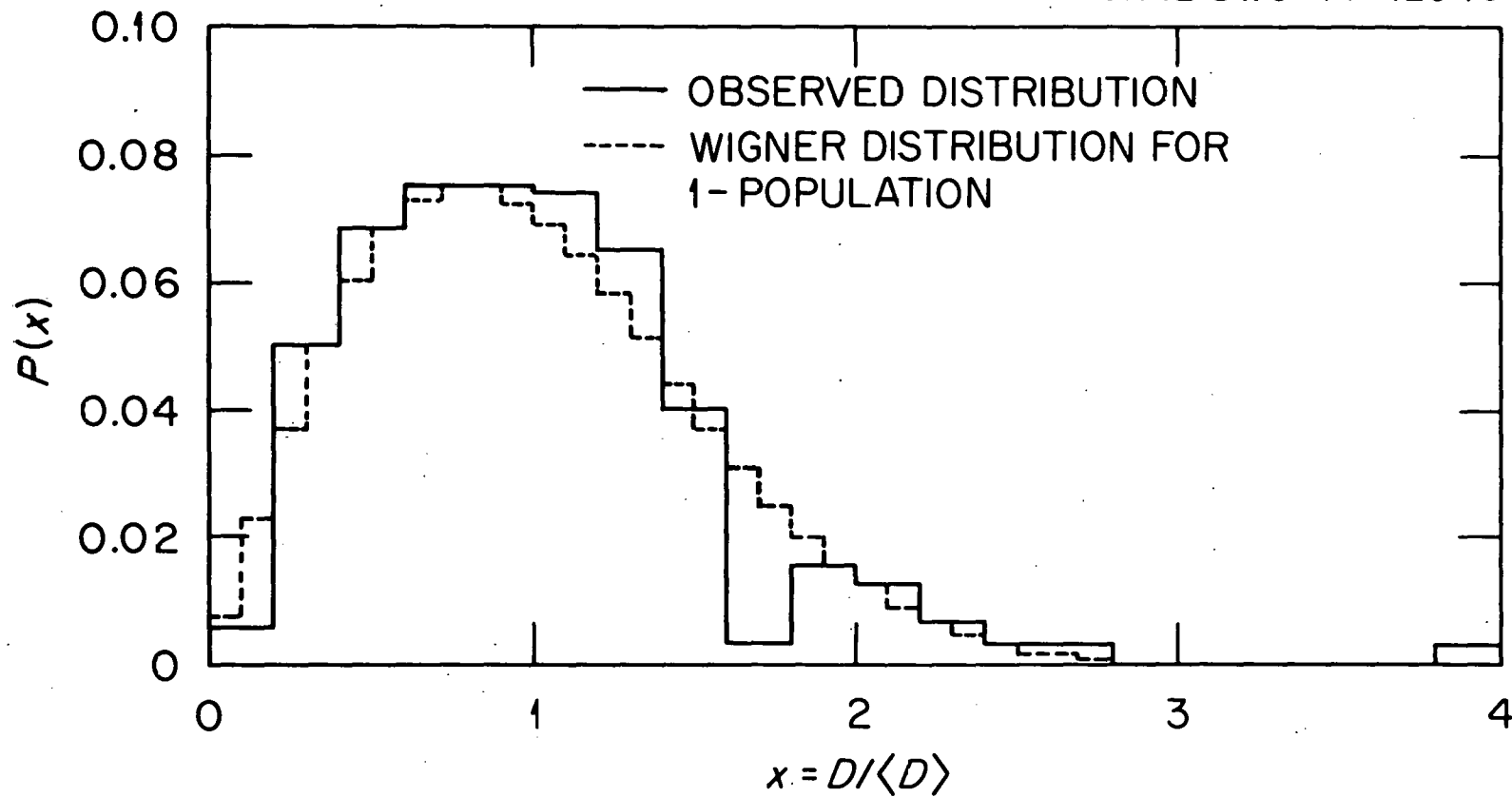


Fig. 13. Nearest neighbor spacing distribution of s-wave levels. The observed distribution (solid line) is compared with a Wigner distribution for one population (dashed line).

The remaining levels have neutron widths smaller than .6 mV hence are very unlikely to be s-wave levels.<sup>B15</sup> If a level had been added at 1360.7 eV, the computed value of  $\Delta_3$ , equation (9), would have become .650 for a most probable value  $\langle \Delta_3 \rangle = .509$  and a standard deviation of .1095.

Figure 14 shows the cumulative sum of the s-wave reduced neutron widths versus energy. The slope of the curve determines the s-wave strength function. The cumulative sum of reduced widths does not behave very linearly with respect to energy so that the "local strength function" varies considerably from one energy region to another. This variation of the local strength function with energy has already been observed by Carraro and Kolar,<sup>B17</sup> Rahn et al.<sup>B20</sup> and by McCrosson.<sup>C1</sup> In Table XIX we give a few recent determinations of the s-wave strength function,  $S^0$ . Above 1 keV the values obtained in this evaluation are approximately 10% higher than those of ENDF/B-IV because ENDF/B-IV is mostly based on the measurements of Rahn et al.<sup>B20</sup> whereas the more recent measurements of Nakajima et al.,<sup>B26</sup> Poortmans et al.<sup>B32</sup> and Olsen et al.<sup>B31</sup> all yield values of  $\Gamma_n$  somewhat larger, on the average, than those of Rahn et al. as indicated in Table VI.

In Fig. 15 the integral distribution of s-wave reduced neutron widths:

$$P(x) = \frac{1}{N_T} \int_x^{\infty} N(Z) dZ \quad \text{with} \quad N_T = \int_0^{\infty} N(Z) dZ \quad (12)$$

Table XIX. Comparison of s-Wave Strength Functions

Energy Interval (keV)	(All values are multiplied by $10^4$ )					ENDF/B-IV	This Evaluation
	Carraro <sup>(1)</sup> and Kolar	Rahn <sup>(1)</sup> et al.	Olsen <sup>(1)</sup> et al.	Poortmans <sup>(1)</sup> et al.			
0- .5	(1.02) <sup>(2)</sup>	1.065	1.001	.992	1.014	1.006	
.5-1	1.041	.996	1.009	.996	.997	1.004	
1-1.5	.924	.894	.932	.927	.861	.927	
1.5-2	1.586	1.452	1.597	1.617	1.452	1.566	
2-2.5	1.029	.912	1.024	1.019	.933	.988	
2.5-3	1.473	1.294	1.551	1.441	1.258	1.461	
3-3.5	1.176	.983	1.261	1.150	.895	1.172	
3.5-4	1.267	1.009	1.293	1.250	1.088	1.221	
0-4	1.190	1.075	1.208	1.175	1.062	1.168	

- (1) These values were obtained by adding the reduced neutron widths reported by the indicated authors for the levels assigned to s-wave in the present evaluation.
- (2) Carraro and Kolar do not report neutron widths for the first three s-wave levels. The values of this evaluation were used for these three levels in computing the strength function.

ORNL-DWG 77-12050

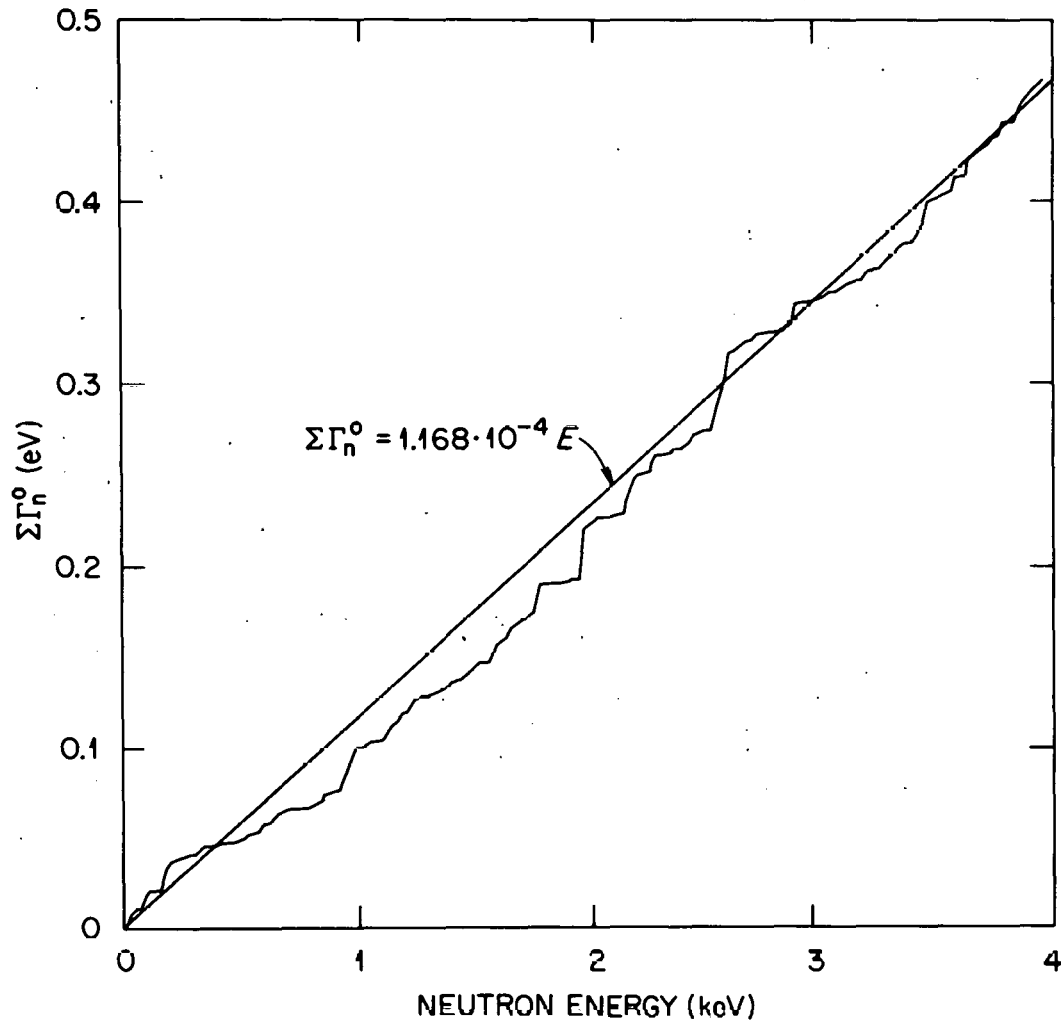


Fig. 14. Cumulative sum of the s-wave reduced neutron widths vs energy. The slope of the curve determines the s-wave strength function.

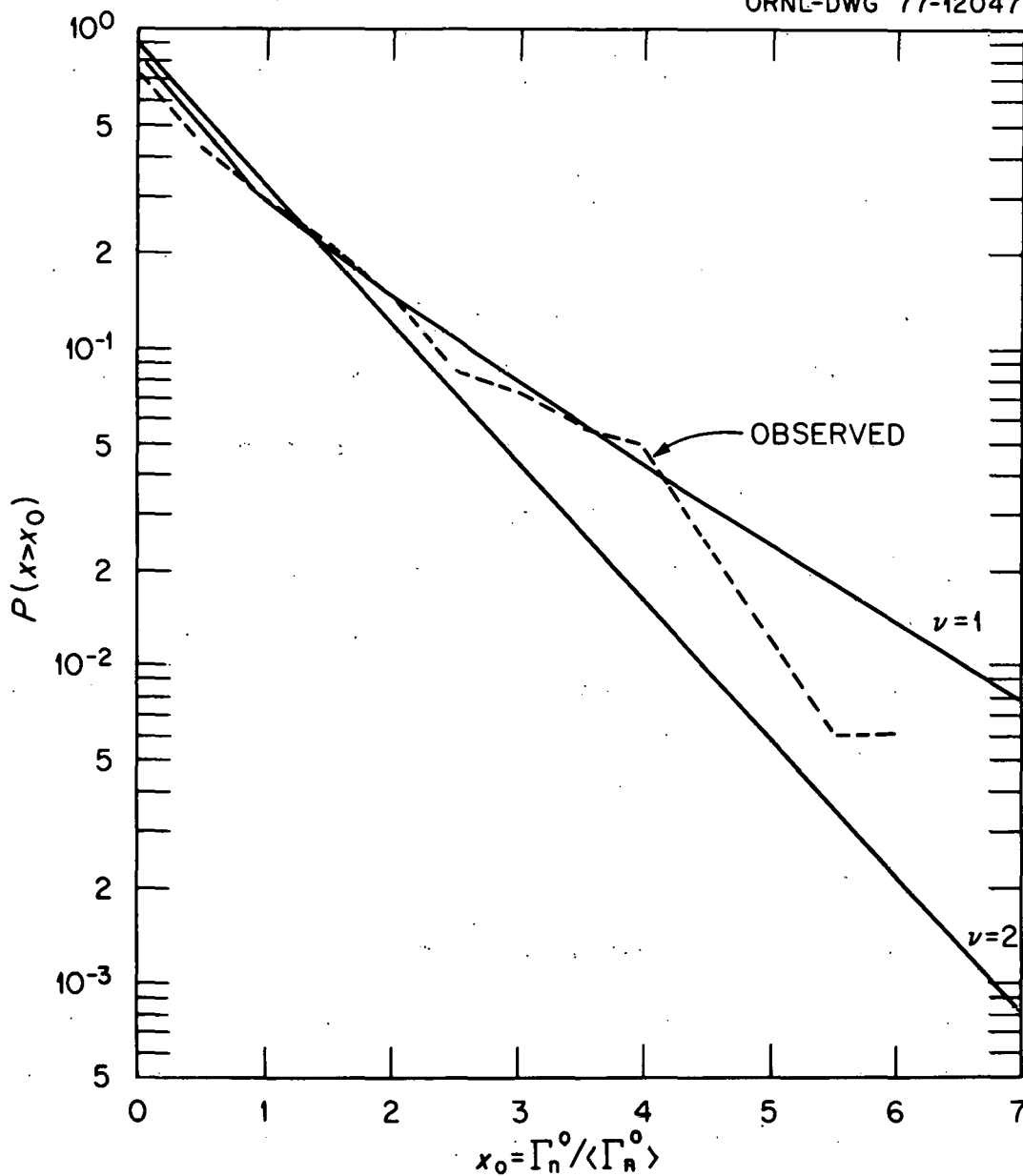


Fig. 15. Integral distribution of s-wave reduced neutron widths. The observed distribution is represented by the dashed line. The solid lines correspond to  $\chi^2$  distribution laws with 1 and 2 degrees of freedom respectively. The observed distribution seems to agree better with the  $\nu=1$  distribution law (Porter-Thomas Distribution).

where  $Z = \frac{\Gamma_{n0}}{\langle \Gamma_{n0} \rangle}$ , is compared to integral distributions corresponding to  $\chi^2$  distribution laws<sup>D24</sup> with  $\nu = 1$  and  $\nu = 2$

$$P_{\nu}(x) = \frac{\nu}{2\Gamma(\frac{\nu}{2})} \int_x^{\infty} \left(\frac{1}{2} Z\nu\right)^{\frac{1}{2}\nu-1} e^{-\frac{1}{2}Z\nu} dZ \quad (13)$$

The observed distribution seems in better agreement with the distribution corresponding to  $\nu = 1$  (Porter-Thomas distribution).

As was explained in Section 3.D the capture widths of most s-wave levels have not been measured, and a value of  $\Gamma_Y = 23.5$  mV was assigned to those levels. The average value of the capture width of those levels for which one or more measurements were reported was found to be 23.23 mV with a variance  $\langle \Gamma_Y^2 \rangle - \langle \Gamma_Y \rangle^2$  of 4.61 mV<sup>2</sup>.

## B. P-wave Levels

Figure 16 is a histogram of the cumulative number of p-wave levels versus neutron energy. Up to 800 eV the histogram increases approximately linearly with energy. Above 800 eV, the slope decreases with increasing energy, probably because an increasing fraction of small levels are not detected, since the energy resolution deteriorates with increasing energy.

The average p-wave level spacing was obtained over the interval 0 to 800 eV as  $\overline{D^1} = 8.91 \pm .1$  eV. The error is the sampling error

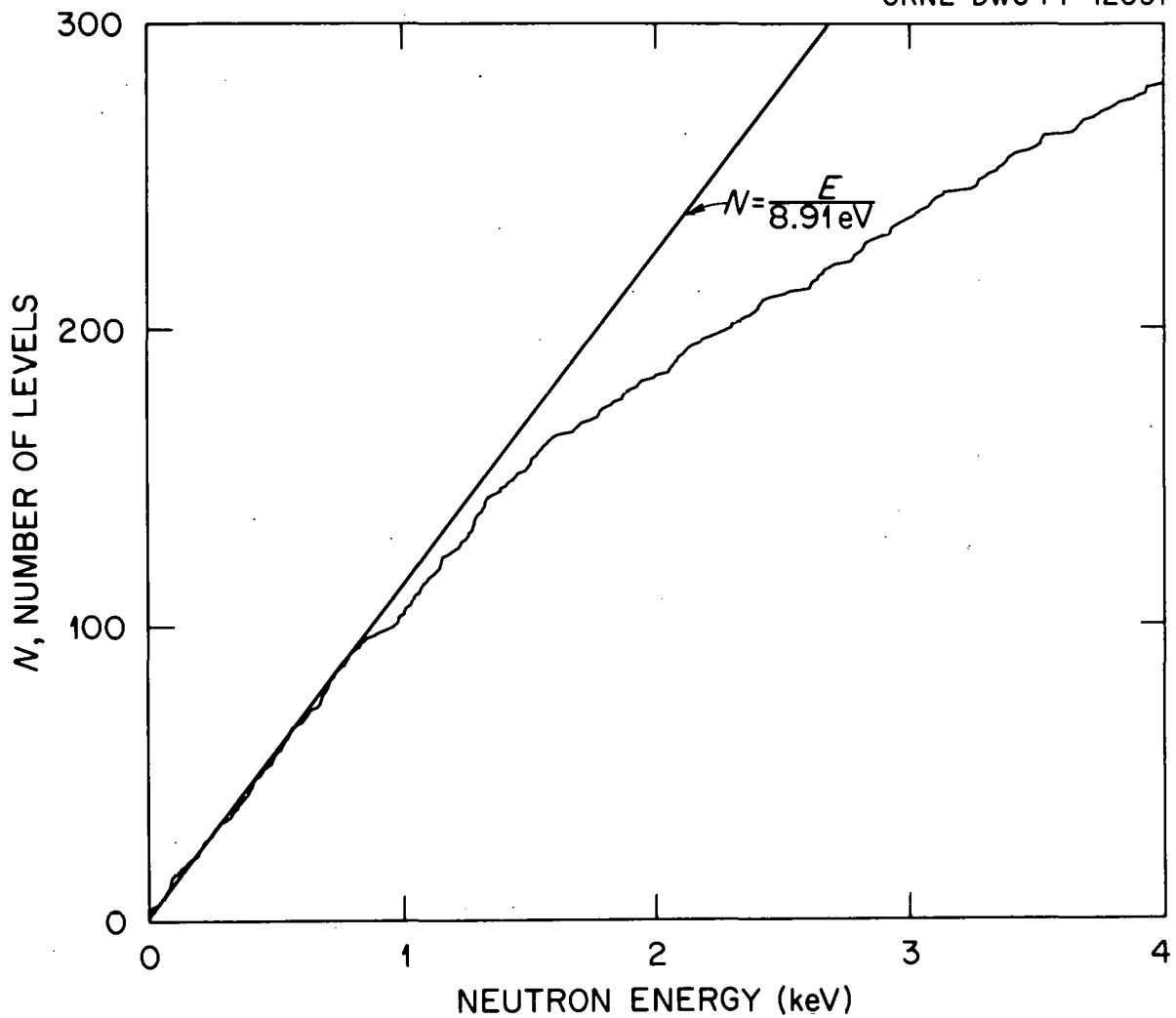


Fig. 16. Histogram of the cumulative number of p-wave levels vs neutron energy. Up to 800 eV, the histogram increases approximately linearly with energy. Above 800 eV, the slope decreases with increasing energy, probably because an increasing fraction of small levels are not detected, since the energy resolution deteriorates with increasing energy.

only. This value is not very different from the value  $\overline{D^0}/3 = 8.3$  eV which would be expected if the density of states were proportional to  $2J + 1$  and independent of parity where  $J$  is the spin of the state.<sup>B15</sup>

In Fig. 17 the nearest neighbor spacings distribution of p-wave levels below 800 eV is compared to a Wigner distribution for two populations with a ratio of level densities  $\rho = 2$ .

$$P(\rho, x) = P_s(r_1, r_2, x) + P_s(r_2, r_1, x) + \frac{2\rho}{(\rho+1)^2} e^{-\frac{\pi}{4} x^2} \frac{\rho^2+1}{(\rho+1)^2} \quad (14)$$

with:

$$P_s(r_1, r_2, x) = \frac{\pi}{2} r_1^3 x \left[ 1 - \operatorname{erf}\left(\sqrt{\frac{\pi}{2}} r_2 x\right) \right] e^{-\frac{\pi}{4} x^2} r_1^2 \quad (15)$$

$$\text{and } r_1 = \frac{\rho}{1+\rho}, \quad r_2 = \frac{1}{1+\rho}$$

The distribution law (14) has been discussed by Gurevitch and Pevzner<sup>D25</sup> and Harvey and Hughes.<sup>D26</sup> P-wave neutrons may form <sup>239</sup>U states with  $J = 1/2$  and  $J = 3/2$ ; if the density of states is proportional to  $2J + 1$ , the ratio  $\rho$  of the two populations is 2. The agreement between the observed and expected nearest neighbors distributions is considered reasonable.

The cumulative sum of the p-wave reduced neutron widths is shown in Fig. 7. If all the p-wave levels were detected experimentally, the p-wave strength function would be proportional to the "slope" of the histogram shown in Fig. 7. This slope is approximately constant up to 1500 eV. Above that energy it decreases

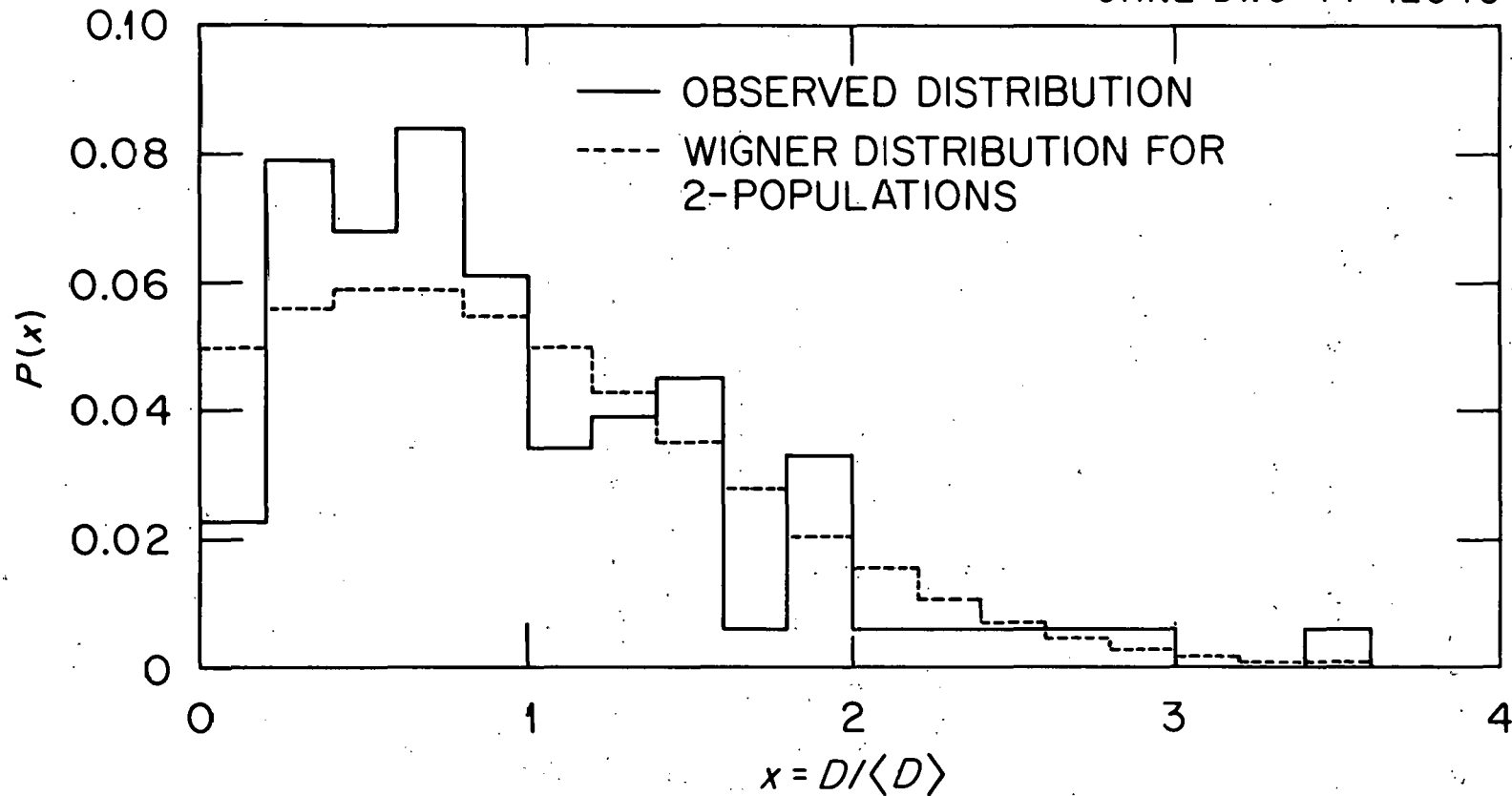


Fig. 17. Nearest neighbor spacing distribution of the p-wave levels below 800 eV. The solid line represents the observed distribution. The dashed line represents the expected distribution for two populations ( $J=1/2$  and  $J=3/2$ ).

sharply and this is interpreted as indicating that many p-wave levels are missed above 1500 eV, because of the increasingly poorer resolution of the time-of-flight measurements and because the measurements of Corvi, Rohr and Weigmann<sup>B25</sup> from which many of the evaluated p-wave levels were obtained, extends only to 1550 eV.

The p-wave strength function was evaluated from the slope of the histogram of Fig. 7 below 1500 eV as:

$$S^1 = \frac{1}{3} \left( \frac{N-1}{N} \right) \frac{1}{(k_0 R)^2} \frac{\sum_{n=1}^N g \frac{\Gamma_n}{E_0^{3/2}}}{E_0(N) - E_0(1)} = (1.93 \pm .5) \times 10^{-4} \quad (16)$$

where  $k_0$  is the reduced wave number at 1 eV, previously defined and where  $R = .84 \times 10^{-12}$  cm is the channel radius. The uncertainty in the strength function was estimated from the variations in the slope of the histogram of Fig. 7. The value of  $S^1$  obtained here is consistent with ENDF/B-IV below 500 eV ( $1.89 \times 10^{-4}$ ) and with the values given by Rahn et al.<sup>B20</sup> ( $1.4 \times 10^{-4}$ ) and by Corvi et al.<sup>B25</sup> ( $2.3 \pm .4 \times 10^{-4}$ ).

The average p-wave reduced neutron width can be obtained as:

$$\langle g\Gamma_n^1 \rangle = 3 D^1 S^1 = 5.2 \pm 1.4 \text{ mV} \quad (17)$$

this value is larger than that estimated by Rahn et al. (2.95 mV) but in very good agreement with that obtained by Corvi et al. ( $5.42 \pm 1.11$  mV). The value corresponds to an average p-wave reduced neutron width of 5.2 mV for the  $J = 1/2$  states and of 2.6 mV for the  $J = 3/2$  states.

In Fig. 18 the integral distribution of the variable  $Z = g\Gamma_n^1 / \langle g\Gamma_n^1 \rangle$  is compared to integral distributions corresponding to  $\chi^2$  distributions with  $\nu = 1$  and  $\nu = 2$  (equation 13). Only p-wave levels up to 800 eV were used in obtaining the observed distribution of Fig. 18. The observed distribution is consistent with a  $\nu = 1$  (Porter-Thomas) distribution for  $g\Gamma_n^1$ , as predicted by Bollinger and Thomas.<sup>B15</sup> In Table XX we summarize the values obtained for the s-wave and p-wave average resonance parameters.

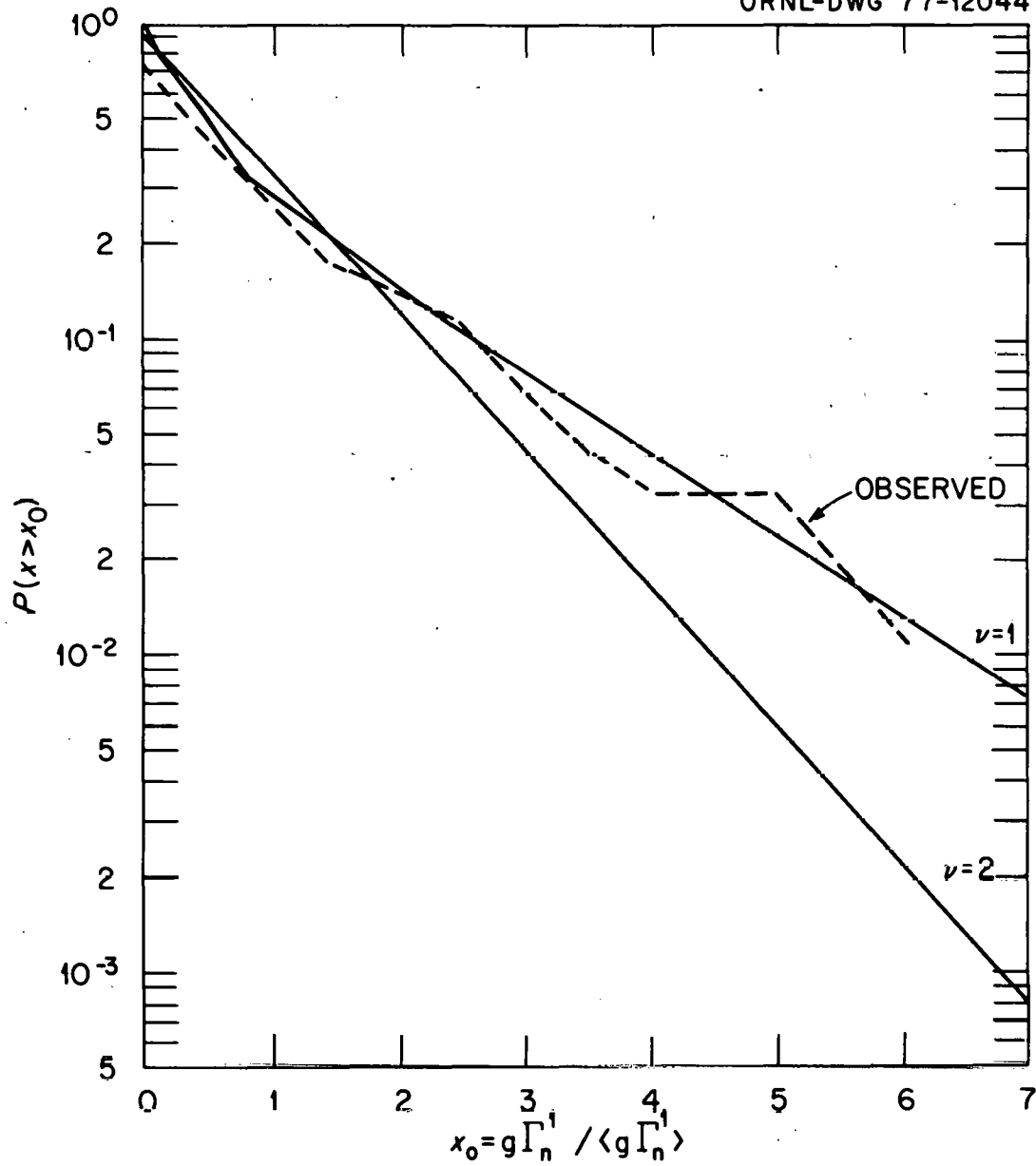


Fig. 18. Integral distribution of the p-wave reduced neutron widths below 800 eV. The solid lines correspond to  $\chi^2$  distribution laws with 1 and 2 degrees of freedom, respectively. The observed distribution agrees better with the  $\nu=1$  distribution law (Porter-Thomas distribution).

Table XX. Average Resonance Parameters

	ENDF/B-III	ENDF/B-IV	This Evaluation
<u>I. s-wave Levels</u>			
Number of levels below 4 keV	199	190	162
Average spacing $D^0$ (eV)	20.1	21.05	24.8 $\pm$ 2
Strength function $S^0$ ( $\times 10^4$ )	1.045	1.062	1.168 $\pm$ .02
Average neutron width $\langle \Gamma_n^0 \rangle$ (mV)	2.090	2.224	2.88 $\pm$ .24
<u>II. p-wave Levels</u>			
Number of levels below 4 keV	258	220	280
Average spacing $D^1$ at low energy (eV)			8.91 $\pm$ .1 (a)
Strength function $S^1$ at low energy ( $\times 10^4$ )		1.89 <sup>(b)</sup>	1.93 $\pm$ .5 (c)
Average neutron width $\langle g \Gamma_n^1 \rangle$ (mV)			5.2 $\pm$ 1.4 (a)
(a) below 800 eV			
(b) below 500 eV			
(c) below 1500 eV			

## 8. ESTIMATED UNCERTAINTIES

In principle the uncertainty associated with a particular measurement of a parameter can be obtained by a careful analysis of the possible sources of error in the measurement. This analysis is best done by the experimenter performing the measurement, and presumably this is the method used to obtain the errors reported. However, as we have already stated in Section 3, the method generally does not lead to a correct estimate of the uncertainties. This is evident from the fact that data from different experiments often differ by amounts far exceeding the estimated uncertainties as illustrated in Tables II, III, VIII and IX for example. In Table XXI we compare the neutron widths of the larger levels between 3500 and 4000 eV from Garg et al.<sup>B11</sup> and Carraro and Kolar.<sup>B17</sup> It is interesting to note that of the 13 levels given, the neutron widths as given by Garg et al. and by Carraro and Kolar are consistent within the errors given only in one case.

Since the "internal" error estimates given by the measurers can be shown to be often unreliable, it seems more appropriate to evaluate the errors "externally," that is from the dispersion between results from independent measurements.

The methods used to evaluate the errors parallels the methods described in Section 3 and used to evaluate the "best values." We distinguish between "statistical" errors which are uncorrelated from one resonance to the next, and "systematic" errors which are correlated over energy.

Table XXI. Comparison of Two Sets of Neutron Widths Between  
3.5 and 4.0 keV

E <sub>0</sub> (eV)	$\Gamma_n$ (mV)	
	Garg et al.	Carraro and Kolar
3561	143+48	256+20
3574	239+60	420+30
3595	15.6+3	47.5+7
3630	217+30	559+55
3693	243+61	415+20
3717	61+15	102+10
3734	153+61	225+10
3765	34+6	94+5
3782	277+62	466+25
3832	6.2+3.1	12.6+2.5
3858	342+62	560+30
3873	249+93	201+10
3902	225+3.75	327+30

The "statistical" error  $\delta_j$  of the  $j^{\text{th}}$  parameter was obtained from the relation

$$\frac{1}{\delta_j^2} = \sum_k \frac{1}{\delta_{jk}^2} \quad (18)$$

where the  $\delta_{jk}^*$  are defined in equation 5. The statistical errors obtained for the s-wave and p-wave levels are listed in Tables XXII and XXIII respectively. A number of capture widths have not been measured and have been assigned a value of 23.5 mV. For these parameters no statistical error can be obtained, but a reasonable uncorrelated uncertainty for these capture widths is estimated to be  $\pm 2.35$  mV. This corresponds to a  $\chi^2$  distribution with  $\nu=200$  for the capture widths.<sup>D24</sup>

The systematic relative error on the level energies is estimated to be:

$$\frac{\delta E}{E} = 2.5 \times 10^{-4} \quad (19)$$

and is, of course, fully correlated with respect to energy. As was stated in Section 3B the level energies were aligned on the scale given by Olsen et al.<sup>B31</sup> Below 4 keV the error in the energy scale of time-of-flight experiments is mostly due to the uncertainty in flight path length. This length uncertainty in the measurement of Olsen et al. is estimated to produce a relative energy uncertainty of  $2.0 \times 10^{-4}$ . However, a comparison of recently determined energy scales suggests that the relative energy uncertainty given above is more realistic. The recent work concerning neutron energy standards has been reviewed by G. D. James.<sup>D5</sup>

Table XXII-a. s-Wave Resonance Parameters and Their Uncorrelated Standard Deviations<sup>1</sup> (All values in eV.)

	$E_0$	$\delta E_0$	$\Gamma_n$	$\delta \Gamma_n$	$\Gamma_\gamma$	$\delta \Gamma_\gamma$
1	-2.000000E C1	0.0	1.284E-03	0.0	2.350E-02	0.0
2	6.672000E C1	2.04E-04	1.510E-03	1.50E-05	2.253E-02	6.25E-04
3	2.086400E C1	2.04E-04	1.012E-02	9.69E-05	2.307E-02	4.52E-04
4	3.667100E C1	2.04E-04	3.391E-02	4.12E-04	2.292E-02	2.76E-04
5	6.601500E C1	2.04E-04	2.461E-02	3.79E-04	2.369E-02	3.40E-04
6	8.072900E C1	2.04E-04	1.907E-03	4.19E-05	2.417E-02	1.15E-03
7	1.025300E C2	2.04E-03	7.164E-02	4.10E-04	2.441E-02	3.49E-04
8	1.166740E C2	2.04E-03	2.754E-02	3.01E-04	2.267E-02	4.41E-04
9	1.456300E C2	2.04E-03	9.119E-04	1.89E-05	2.220E-02	3.50E-03
10	1.652500E C2	2.04E-03	3.400E-03	7.38E-05	2.336E-02	2.01E-03
11	1.896360E C2	2.04E-03	1.670E-01	1.73E-03	2.305E-02	4.87E-04
12	2.084740E C2	2.04E-03	4.960E-02	7.85E-04	2.282E-02	4.09E-04
13	2.373420E C2	2.04E-03	2.648E-02	4.51E-04	2.475E-02	4.67E-04
14	2.736210E C2	2.04E-03	2.593E-02	4.14E-04	2.273E-02	5.00E-04
15	2.905610E C2	2.04E-03	1.647E-02	3.45E-04	2.265E-02	5.39E-04
16	3.112810E C2	2.04E-03	1.026E-03	3.00E-05	2.350E-02	2.35E 00
17	3.477510E C2	2.04E-03	8.173E-02	1.05E-03	2.275E-02	2.89E-04
18	3.765520E C2	2.04E-03	1.148E-03	2.40E-05	2.350E-02	2.35E 00
19	3.975830E C2	2.04E-03	6.258E-03	1.42E-04	2.383E-02	3.93E-03
20	4.102050E C2	2.04E-03	2.018E-02	3.02E-04	2.371E-02	5.27E-04
21	4.340360E C2	2.04E-03	9.817E-03	1.83E-04	2.329E-02	5.68E-04
22	4.631380E C2	2.04E-03	5.494E-03	1.48E-04	2.350E-02	1.20E-03
23	4.784000E C2	2.04E-03	4.188E-03	1.02E-04	2.350E-02	2.35E 00
24	5.183340E C2	2.04E-03	4.960E-02	7.50E-04	2.359E-02	5.02E-04
25	5.352760E C2	2.04E-03	4.428E-02	7.41E-04	2.382E-02	2.85E-04
26	5.800820E C2	2.04E-03	4.123E-02	7.92E-04	2.480E-02	4.50E-04
27	5.950140E C2	2.04E-03	8.641E-02	1.32E-03	2.314E-02	2.82E-04
28	6.195480E C2	2.04E-03	3.076E-02	5.10E-04	2.332E-02	3.78E-04
29	6.285290E C2	2.04E-03	6.249E-03	1.08E-04	2.350E-02	2.35E 00
30	6.611450E C2	2.04E-03	1.280E-01	2.03E-03	2.537E-02	9.73E-04
31	6.930500E C2	2.04E-03	4.222E-02	8.38E-04	2.350E-02	4.50E-04
32	7.082730E C2	2.04E-03	2.179E-02	5.89E-04	2.345E-02	5.52E-04
33	7.215860E C2	4.05E-03	1.720E-03	5.58E-05	2.350E-02	2.35E 00
34	7.301470E C2	6.12E-03	9.341E-04	4.76E-05	2.350E-02	2.35E 00
35	7.650550E C2	2.04E-03	7.767E-03	2.77E-04	1.700E-02	2.00E-03
36	7.908210E C2	4.05E-03	6.618E-03	1.23E-04	2.350E-02	2.35E 00
37	8.215590E C2	2.04E-03	6.549E-02	1.33E-03	2.272E-02	5.36E-04
38	8.505860E C2	2.04E-03	6.291E-02	1.46E-03	2.552E-02	7.56E-04
39	8.560770E C2	2.04E-03	8.617E-02	1.98E-03	2.355E-02	7.31E-04
40	8.664200E C2	4.05E-03	5.533E-03	2.00E-04	2.350E-02	2.35E 00
41	9.050310E C2	2.04E-03	5.457E-02	1.05E-03	2.461E-02	1.25E-03
42	9.251100E C2	4.05E-03	1.360E-02	4.60E-04	2.500E-02	4.00E-03
43	9.370200E C2	2.04E-03	1.493E-01	2.21E-03	2.366E-02	5.78E-04
44	9.585200E C2	2.04E-03	2.038E-01	3.21E-03	2.285E-02	7.16E-04
45	9.916300E C2	2.04E-03	3.773E-01	3.78E-03	2.989E-02	1.36E-03
46	1.022560E C3	6.13E-03	8.442E-03	3.35E-04	2.350E-02	2.35E 00
47	1.055440E C3	2.04E-03	9.393E-02	1.95E-03	2.311E-02	4.61E-04
48	1.098620E C3	4.05E-03	2.195E-02	6.83E-04	2.350E-02	2.12E-03
49	1.105060E C3	4.05E-03	3.361E-02	8.58E-04	2.400E-02	2.00E-03
50	1.140350E C3	2.04E-03	2.331E-01	3.20E-03	2.382E-02	7.21E-04
51	1.167630E C3	4.05E-03	8.771E-02	2.32E-03	2.410E-02	4.79E-04
52	1.177070E C3	4.05E-03	7.016E-02	1.84E-03	2.200E-02	1.66E-03
53	1.194810E C3	4.05E-03	9.486E-02	2.02E-03	2.040E-02	1.79E-03
54	1.211110E C3	6.13E-03	9.193E-03	2.80E-04	2.350E-02	2.35E 00
55	1.245060E C3	2.04E-03	2.521E-01	4.10E-03	2.271E-02	7.43E-04
56	1.267040E C3	4.05E-03	2.917E-02	7.02E-04	2.402E-02	1.09E-03
57	1.272970E C3	6.13E-03	2.847E-02	8.26E-04	2.288E-02	1.09E-03
58	1.295620E C3	1.22E-02	3.576E-03	2.84E-04	2.350E-02	2.35E 00
59	1.393810E C3	4.05E-03	2.075E-01	3.66E-03	2.427E-02	7.73E-04
60	1.405430E C3	4.09E-03	7.198E-02	1.82E-03	2.552E-02	7.43E-04
61	1.415760E C3	6.16E-03	9.361E-03	4.43E-04	2.350E-02	2.35E 00
62	1.426010E C3	4.09E-03	2.856E-02	8.98E-04	2.555E-02	9.49E-04
63	1.444050E C3	6.13E-03	1.626E-02	6.90E-04	2.200E-02	3.00E-03
64	1.473820E C3	4.05E-03	1.223E-01	2.67E-03	2.387E-02	5.88E-04
65	1.522700E C3	4.05E-03	2.452E-01	4.24E-03	2.388E-02	1.47E-03
66	1.550590E C3	1.22E-02	3.372E-03	2.73E-04	2.350E-02	2.35E 00
67	1.565450E C3	1.02E-02	5.519E-03	3.20E-04	2.350E-02	2.35E 00
68	1.597890E C3	4.05E-03	3.747E-01	6.56E-03	2.223E-02	6.90E-04
69	1.622670E C3	4.05E-03	1.019E-01	2.65E-03	2.232E-02	6.82E-04
70	1.636070E C3	4.05E-03	5.183E-02	1.56E-03	2.298E-02	6.82E-04
71	1.662450E C3	4.05E-03	2.211E-01	4.58E-03	2.419E-02	7.84E-04
72	1.686780E C3	4.09E-03	1.053E-01	2.57E-03	2.355E-02	6.82E-04
73	1.705850E C3	4.05E-03	9.031E-02	2.61E-03	2.800E-02	5.00E-03
74	1.722890E C3	6.13E-03	1.727E-02	7.71E-04	2.210E-02	2.00E-03
75	1.755890E C3	4.09E-03	1.365E-01	2.98E-03	2.700E-02	4.00E-03
76	1.782690E C3	4.05E-03	6.532E-01	9.45E-03	2.350E-02	2.35E 00
77	1.808400E C3	6.17E-03	1.843E-02	9.15E-04	1.700E-02	5.00E-03
78	1.846100E C3	6.17E-03	1.060E-02	5.55E-04	1.500E-02	5.00E-03
79	1.867600E C3	6.35E-02	8.807E-04	4.41E-04	2.350E-02	2.35E 00
80	1.902830E C3	4.05E-03	4.438E-02	1.41E-03	2.465E-02	9.70E-04
81	1.913270E C3	1.43E-02	2.221E-03	3.07E-04	2.350E-02	2.35E 00
82	1.917160E C3	4.05E-03	3.975E-02	1.56E-03	2.313E-02	1.44E-03

<sup>1</sup> For the fission widths, see Table XXII-b.

Table XXII-a. (Continued)

	$E_0$	$\delta E_0$	$\Gamma_n$	$\delta \Gamma_n$	$\Gamma_\gamma$	$\delta \Gamma_\gamma$
83	1.95378E C3	1.43E-02	4.192E-03	1.68E-04	2.350E-02	2.35E 00
84	1.96298E C3	4.09E-03	8.094E-01	8.79E-03	3.000E-02	1.00E-02
85	1.97491E C3	4.09E-03	4.293E-01	5.49E-03	2.350E-02	2.35E 00
86	2.02368E C3	4.09E-03	2.211E-01	5.74E-03	2.348E-02	9.70E-04
87	2.03049E C3	6.17E-03	4.757E-02	2.32E-03	2.471E-02	1.17E-03
88	2.08662E C3	6.17E-03	2.485E-02	1.22E-03	2.200E-02	4.00E-03
89	2.09629E C3	6.17E-03	2.454E-02	1.25E-03	2.350E-02	2.35E 00
90	2.14566E C3	4.09E-03	7.436E-02	2.24E-03	2.378E-02	1.07E-03
91	2.15276E C3	4.09E-03	2.881E-01	5.28E-03	2.438E-02	7.96E-04
92	2.16588E C3	4.09E-03	5.784E-01	8.59E-03	2.420E-02	9.90E-04
93	2.20126E C3	6.13E-03	1.064E-01	3.61E-03	2.600E-02	5.00E-03
94	2.25670E C3	1.22E-02	1.081E-01	3.93E-03	2.540E-02	1.00E-03
95	2.26654E C3	6.17E-03	2.321E-01	6.89E-03	2.000E-02	5.00E-03
96	2.28192E C3	6.17E-03	1.844E-01	5.08E-03	1.800E-02	5.00E-03
97	2.31594E C3	1.43E-02	1.937E-02	1.21E-03	2.350E-02	2.35E 00
98	2.35274E C3	6.17E-03	5.346E-02	2.80E-03	2.800E-02	5.00E-03
99	2.35573E C3	1.02E-02	7.131E-02	3.26E-03	2.400E-02	5.00E-03
100	2.39198E C3	1.02E-02	2.977E-02	1.06E-03	2.350E-02	2.35E 00
101	2.42689E C3	6.13E-03	1.533E-01	4.71E-03	2.350E-02	2.35E 00
102	2.44670E C3	6.13E-03	2.165E-01	5.55E-03	2.350E-02	1.20E-03
103	2.45575E C3	1.63E-02	1.729E-02	9.55E-04	2.350E-02	2.35E 00
104	2.48518E C3	6.13E-03	1.032E-01	3.02E-03	2.450E-02	1.30E-03
105	2.52145E C3	1.02E-02	1.718E-02	1.03E-03	2.350E-02	2.35E 00
106	2.54159E C3	4.09E-03	7.150E-01	1.04E-02	2.350E-02	2.35E 00
107	2.54595E C3	4.09E-03	2.645E-01	6.27E-03	2.350E-02	2.35E 00
108	2.58211E C3	4.09E-03	4.270E-01	7.24E-03	2.350E-02	2.35E 00
109	2.59761E C3	4.09E-03	7.477E-01	1.39E-02	2.250E-02	1.10E-03
110	2.62005E C3	1.22E-02	4.868E-02	2.20E-03	2.350E-02	2.35E 00
111	2.67222E C3	6.13E-03	2.801E-01	6.26E-03	2.400E-02	1.40E-03
112	2.69550E C3	1.23E-02	2.952E-02	1.50E-03	2.350E-02	2.35E 00
113	2.71733E C3	6.13E-03	1.702E-01	4.98E-03	2.350E-02	2.35E 00
114	2.75074E C3	1.23E-02	4.030E-02	1.71E-03	2.350E-02	2.35E 00
115	2.76266E C3	1.84E-02	1.863E-02	1.07E-03	2.350E-02	2.35E 00
116	2.78742E C3	1.84E-02	1.310E-02	1.15E-03	2.350E-02	2.35E 00
117	2.80638E C3	2.22E-02	9.444E-03	1.16E-03	2.350E-02	2.35E 00
118	2.82532E C3	1.43E-02	1.991E-02	1.27E-03	2.350E-02	2.35E 00
119	2.86539E C3	1.23E-02	2.016E-01	8.91E-03	2.200E-02	1.40E-03
120	2.88278E C3	6.18E-03	5.951E-01	1.53E-02	2.460E-02	1.40E-03
121	2.89722E C3	2.83E-02	1.714E-02	1.55E-03	2.350E-02	2.35E 00
122	2.93365E C3	1.23E-02	3.673E-02	1.88E-03	2.360E-02	1.50E-03
123	2.95693E C3	1.63E-02	2.179E-02	1.79E-03	2.350E-02	2.35E 00
124	3.00362E C3	6.18E-03	1.216E-01	4.19E-03	2.490E-02	1.50E-03
125	3.02661E C3	6.18E-03	1.358E-01	4.22E-03	2.350E-02	2.35E 00
126	3.05665E C3	1.43E-02	3.064E-02	1.78E-03	2.400E-02	3.00E-03
127	3.10591E C3	6.13E-03	2.314E-01	6.42E-03	2.350E-02	2.35E 00
128	3.14503E C3	6.18E-03	1.066E-01	3.48E-03	2.320E-02	1.40E-03
129	3.16875E C3	2.65E-02	1.079E-02	1.08E-03	2.350E-02	2.35E 00
130	3.17883E C3	6.18E-03	9.341E-02	3.13E-03	2.350E-02	2.35E 00
131	3.18591E C3	6.18E-03	1.091E-01	3.54E-03	2.150E-02	2.00E-03
132	3.20681E C3	6.18E-03	9.569E-02	3.19E-03	2.350E-02	2.35E 00
133	3.21570E C3	4.09E-02	1.010E-02	1.01E-03	2.350E-02	2.35E 00
134	3.22435E C3	1.84E-02	2.533E-02	2.30E-03	2.350E-02	2.35E 00
135	3.24886E C3	1.43E-02	2.531E-02	1.42E-03	2.250E-02	2.50E-03
136	3.27551E C3	6.13E-03	2.740E-01	7.95E-03	2.350E-02	2.35E 00
137	3.31218E C3	6.18E-03	1.626E-01	5.04E-03	2.350E-02	2.35E 00
138	3.32164E C3	6.18E-03	1.335E-01	4.98E-03	2.230E-02	2.00E-03
139	3.33366E C3	1.02E-02	1.026E-01	4.23E-03	2.390E-02	1.80E-03
140	3.35681E C3	1.02E-02	1.242E-01	4.49E-03	2.360E-02	1.50E-03
141	3.38575E C3	1.43E-02	2.235E-02	1.44E-03	2.350E-02	2.35E 00
142	3.40677E C3	6.13E-03	2.306E-01	6.20E-03	2.350E-02	2.35E 00
143	3.43645E C3	6.13E-03	3.966E-01	8.13E-03	2.390E-02	1.50E-03
144	3.45814E C3	6.13E-03	6.967E-01	1.25E-02	2.480E-02	2.00E-03
145	3.48580E C3	1.02E-02	9.598E-02	3.53E-03	2.350E-02	2.35E 00
146	3.49259E C3	1.31E 00	1.444E-02	2.74E-03	2.350E-02	2.35E 00
147	3.56159E C3	6.13E-03	2.574E-01	6.65E-03	2.350E-02	2.35E 00
148	3.57404E C3	6.13E-03	4.166E-01	8.59E-03	2.350E-02	2.35E 00
149	3.59502E C3	1.23E-02	5.311E-02	2.72E-03	2.350E-02	2.35E 00
150	3.62324E C3	1.23E-02	2.084E-02	2.01E-03	2.360E-02	2.35E 00
151	3.62580E C3	6.13E-03	5.153E-01	1.40E-02	2.350E-02	2.35E 00
152	3.69319E C3	6.13E-03	4.044E-01	8.64E-03	2.360E-02	2.35E 00
153	3.71680E C3	1.02E-02	1.102E-01	4.21E-03	2.350E-02	2.35E 00
154	3.73421E C3	6.18E-03	2.155E-01	5.32E-03	2.350E-02	2.35E 00
155	3.76511E C3	1.02E-02	9.719E-02	2.98E-03	2.350E-02	2.35E 00
156	3.78156E C3	6.13E-03	4.565E-01	9.59E-03	2.400E-02	2.20E-03
157	3.83159E C3	3.47E-02	1.339E-02	1.05E-03	2.350E-02	2.35E 00
158	3.85775E C3	6.13E-03	5.651E-01	1.22E-02	2.350E-02	2.35E 00
159	3.87310E C3	2.25E-02	1.708E-01	1.07E-02	2.350E-02	2.35E 00
160	3.90222E C3	6.13E-03	2.884E-01	9.35E-03	2.430E-02	2.50E-03
161	3.91503E C3	1.23E-02	1.049E-01	4.03E-03	2.240E-02	2.50E-03
162	3.94006E C3	1.02E-02	1.834E-01	5.90E-03	2.390E-02	2.50E-03
163	3.95494E C3	1.23E-02	1.278E-01	3.91E-03	2.350E-02	2.35E 00
164	4.04103E C3	4.94E-01	6.501E-02	3.55E-03	2.350E-02	2.35E 00

Table XXII-b. s-Wave Resonance Parameters and Their Uncorrelated Standard Deviations  
(All values in eV)

	$E_0$	$\delta E_0$	$\Gamma_f$	$\delta \Gamma_f$
1	-2.00000E C1	0.0		
2	6.67200E C0	2.04E-04	1.033E-08	1.03E-09
3	2.08640E C1	2.04E-04	5.995E-08	6.00E-09
4	3.66710E C1	2.04E-04	8.877E-09	8.88E-10
5	6.60150E C1	2.04E-04	5.146E-08	5.15E-09
6	8.07250E C1	2.04E-04	6.615E-08	6.61E-09
7	1.02530E C2	2.04E-03	1.225E-08	1.22E-09
8	1.16674E C2	2.04E-03		
9	1.45630E C2	2.04E-03		
10	1.68825E C2	2.04E-03		
11	1.89636E C2	2.04E-03	4.772E-06	4.77E-09
12	2.08474E C2	2.04E-03	8.809E-08	8.81E-09
13	2.37342E C2	2.04E-03	6.003E-08	6.00E-09
14	2.73621E C2	2.04E-03		
15	2.90561E C2	2.04E-03		
16	3.11281E C2	2.04E-03		
17	3.47751E C2	2.04E-03	2.676E-07	2.68E-08
18	3.76652E C2	2.04E-03	2.054E-07	2.05E-08
19	3.97683E C2	2.04E-03		
20	4.10205E C2	2.04E-03		
21	4.34036E C2	2.04E-03		
22	4.63138E C2	2.04E-03	1.474E-06	1.47E-07
23	4.78400E C2	2.04E-03	2.405E-07	2.41E-08
24	5.18334E C2	2.04E-03	2.926E-07	2.93E-08
25	5.35276E C2	2.04E-03	3.670E-07	3.67E-08
26	5.80082E C2	2.04E-03		
27	5.95014E C2	2.04E-03	1.095E-06	1.10E-07
28	6.19548E C2	2.04E-03	2.147E-07	2.15E-08
29	6.28525E C2	2.04E-03		
30	6.61145E C2	2.04E-03		
31	6.93000E C2	2.04E-03		
32	7.08273E C2	2.04E-03	2.564E-05	2.56E-06
33	7.21586E C2	4.00E-03	1.056E-03	1.10E-04
34	7.30147E C2	6.12E-03	9.261E-05	9.26E-06
35	7.65055E C2	2.04E-03	5.945E-06	5.95E-07
36	7.90821E C2	4.05E-03		
37	8.21559E C2	2.04E-03		
38	8.50686E C2	2.04E-03	1.215E-06	1.21E-07
39	8.56077E C2	2.04E-03	1.107E-06	1.11E-07
40	8.66420E C2	4.00E-03		
41	9.05031E C2	2.04E-03		
42	9.25110E C2	4.00E-03		
43	9.37020E C2	2.04E-03		
44	9.58520E C2	2.04E-03		
45	9.51630E C2	2.04E-03		
46	1.02256E C3	6.13E-03		
47	1.05445E C3	2.04E-03		
48	1.09822E C3	4.00E-03		
49	1.10906E C3	4.00E-03		
50	1.14035E C3	2.04E-03	1.595E-06	1.60E-07
51	1.16763E C3	4.00E-03	1.171E-05	1.17E-06
52	1.17707E C3	4.00E-03		
53	1.19481E C3	4.00E-03		
54	1.21111E C3	6.13E-03	2.734E-04	2.73E-05
55	1.24506E C3	2.04E-03		
56	1.26704E C3	4.00E-03	4.282E-06	4.28E-07

Table XXIII. p-Wave Resonance Parameters and Their Uncorrelated Standard Deviation

(All values in eV)

	$E_0$	$\delta E_0$	$\Gamma_n$	$\delta \Gamma_n$	$\Gamma_\gamma$	$\delta \Gamma_\gamma$
1	4.4040CE	CC	2.04E-04	1.121E-07	1.47E-08	2.350E-02
2	1.0236CE	C1	2.04E-04	1.674E-06	3.55E-08	2.350E-02
3	1.1305CE	C1	4.09E-04	4.002E-07	2.73E-08	2.350E-02
4	1.62512E	C1	1.63E-01	4.966E-08	1.06E-08	2.350E-02
5	1.9523CE	C1	4.09E-04	1.393E-06	7.38E-08	2.350E-02
6	4.5166CE	O1	4.09E-04	1.963E-06	3.84E-07	2.350E-02
7	4.9626CE	C1	6.13E-03	9.691E-07	3.55E-07	2.350E-02
8	6.3505CE	C1	8.17E-04	1.031E-05	5.31E-07	2.350E-02
9	7.2760CE	C1	7.28E-01	1.000E-05	1.000E-05	2.350E-02
10	7.43601E	C1	7.44E-01	2.700E-06	2.000E-06	2.350E-02
11	8.36836E	C1	1.83E-03	1.081E-05	6.96E-07	2.350E-02
12	8.59764E	C1	1.47E-02	9.489E-03	2.63E-06	2.350E-02
13	9.10577E	C1	5.1CE-01	6.000E-06	1.20E-05	2.350E-02
14	9.11746E	C1	4.09E-03	5.932E-06	6.04E-07	2.350E-02
15	11.1205E	C2	5.82E-01	4.800E-06	2.00E-06	2.350E-02
16	11.8457CE	C2	6.18E-03	8.399E-06	1.47E-06	2.350E-02
17	11.8457CE	C2	6.01E-03	2.268E-06	1.07E-06	2.350E-02
18	11.33252E	C2	1.02E-02	8.651E-06	2.76E-06	2.350E-02
19	11.52419E	C2	4.09E-03	5.075E-05	3.16E-06	2.350E-02
20	11.58944E	C2	6.12E-03	1.533E-05	2.80E-06	2.350E-02
21	11.73167E	C2	4.09E-03	4.677E-05	3.71E-06	2.350E-02
22	11.54779E	C2	1.55E-00	4.965E-05	1.06E-05	2.350E-02
23	2.00711E	C2	5.99E-03	5.846E-05	5.12E-06	2.350E-02
24	2.03108E	C2	5.98E-03	3.584E-05	4.15E-06	2.350E-02
25	2.14850E	C2	7.03E-03	6.214E-05	6.19E-06	2.350E-02
26	2.18323E	C2	1.27E-02	3.136E-05	5.25E-06	2.350E-02
27	2.24567E	C2	2.0CE-00	1.986E-05	1.06E-05	2.350E-02
28	4.2711E	C2	4.02E-03	1.871E-04	7.67E-06	2.350E-02
29	2.53691E	C2	4.04E-03	1.082E-04	8.11E-06	2.350E-02
30	2.57239E	C2	1.81E-02	1.723E-05	4.47E-06	2.350E-02
31	2.63531E	C2	4.02E-03	2.580E-04	1.05E-05	2.350E-02
32	2.75113E	C2	6.09E-03	1.825E-04	1.40E-05	2.350E-02
33	2.82431E	C2	6.06E-03	1.043E-04	8.52E-06	2.350E-02
34	3.06242E	C2	2.0CE-00	5.000E-05	4.00E-05	2.350E-02
35	3.22E61E	C2	1.64E-02	4.326E-05	5.87E-06	2.350E-02
36	3.21571E	C2	1.23E-02	5.342E-05	8.54E-06	2.350E-02
37	3.7251E	C2	2.0CE-03	1.049E-04	9.56E-06	2.350E-02
38	3.51562E	C2	6.09E-03	2.224E-04	1.52E-05	2.350E-02
39	3.54762E	C2	1.63E-01	3.596E-05	2.11E-05	2.350E-02
40	3.66333E	C2	2.0CE-00	5.000E-05	4.00E-05	2.350E-02
41	3.72642E	C2	6.03E-03	3.906E-05	1.53E-05	2.350E-02
42	3.87133E	C2	2.0CE-00	4.000E-05	4.00E-05	2.350E-02
43	3.95264E	C2	2.0CE-00	7.070E-05	1.45E-05	2.350E-02
44	4.00432E	C2	2.0CE-00	4.000E-05	4.00E-05	2.350E-02
45	4.08212E	C2	1.22E-02	8.312E-05	1.51E-05	2.350E-02
46	4.13431E	C2	2.0CE-00	5.000E-06	1.00E-05	2.350E-02
47	4.15431E	C2	2.0CE-00	5.000E-05	4.00E-05	2.350E-02
48	4.22531E	C2	2.0CE-00	5.000E-05	1.00E-04	2.350E-02
49	4.39736E	C2	6.09E-03	2.896E-04	1.52E-05	2.350E-02
50	4.48357E	C2	2.68E-02	4.815E-05	1.30E-05	2.350E-02
51	4.54046E	C2	4.09E-03	4.264E-04	1.67E-05	2.350E-02
52	4.67149E	C2	2.45E-02	6.419E-05	1.82E-05	2.350E-02
53	4.65280E	C2	1.23E-02	1.464E-04	1.91E-05	2.350E-02
54	4.68680E	C2	4.08E-03	7.623E-04	3.35E-05	2.350E-02
55	4.54526E	C2	2.0CE-00	5.000E-05	2.00E-05	2.350E-02
56	4.58675E	C2	1.55E-02	1.087E-04	1.67E-05	2.350E-02
57	5.11025E	C2	2.0CE-00	1.000E-04	4.00E-05	2.350E-02
58	5.23334E	C2	8.0CE-03	2.768E-04	2.14E-05	2.350E-02
59	5.28124E	C2	2.0CE-00	7.000E-05	6.00E-05	2.350E-02
60	5.32124E	C2	2.0CE-00	6.404E-05	2.01E-05	2.350E-02
61	5.42433E	C2	1.5CE-02	1.532E-04	1.85E-05	2.350E-02
62	5.50580E	C2	2.96E-02	7.937E-05	2.00E-05	2.350E-02
63	5.55624E	C2	1.53E-02	6.709E-04	4.25E-05	2.350E-02
64	5.60123E	C2	2.0CE-00	4.500E-05	2.00E-05	2.350E-02
65	5.66423E	C2	2.0CE-00	3.300E-05	2.00E-05	2.350E-02
66	5.64463E	C2	4.09E-02	9.775E-05	2.98E-05	2.350E-02
67	6.08713E	C2	1.43E-02	2.700E-04	3.14E-05	2.350E-02
68	6.15746E	C2	1.8CE-02	1.461E-04	2.62E-05	2.350E-02
69	6.24197E	C2	6.0CE-03	7.980E-04	3.99E-05	2.350E-02
70	6.33290E	C2	3.07E-02	1.261E-04	3.58E-05	2.350E-02
71	6.36421E	C2	2.0CE-00	1.200E-04	6.00E-05	2.350E-02
72	6.68410E	C2	2.16E-02	2.045E-04	3.58E-05	2.350E-02
73	6.77744E	C2	6.06E-03	7.264E-04	4.92E-05	2.350E-02
74	6.81021E	C2	2.0CE-00	5.190E-05	2.81E-05	2.350E-02
75	6.85121E	C2	2.0CE-00	6.000E-05	6.00E-05	2.350E-02
76	6.88121E	C2	2.0CE-00	8.000E-05	6.00E-05	2.350E-02
77	6.98078E	C2	2.71E-02	2.936E-04	4.69E-05	2.350E-02
78	7.04721E	C2	2.0CE-00	1.000E-04	6.00E-05	2.350E-02
79	7.10589E	C2	5.37E-02	1.048E-03	6.67E-05	2.350E-02
80	7.13774E	C2	2.51E-02	2.219E-04	3.64E-05	2.350E-02
81	7.16821E	C2	2.0CE-00	1.000E-04	1.00E-04	2.350E-02
82	7.22469E	C2	4.08E-03	1.954E-03	6.21E-05	2.350E-02
83	7.34721E	C2	2.0CE-00	1.625E-04	3.46E-05	2.350E-02
84	7.43140E	C2	1.42E-02	3.537E-04	3.73E-05	2.350E-02
85	7.56243E	C2	1.02E-02	5.358E-04	3.99E-05	2.350E-02
86	7.72652E	C2	2.0CE-00	1.390E-04	7.41E-05	2.350E-02
87	7.79305E	C2	4.08E-03	2.129E-03	7.76E-05	2.350E-02
88	7.85520E	C2	5.11E-02	1.365E-04	3.98E-05	2.350E-02
89	7.97322E	C2	3.45E-02	4.605E-04	2.98E-05	2.350E-02
90	7.97322E	C2	2.0CE-00	1.300E-04	2.60E-04	2.350E-02
91	8.08160E	C2	1.43E-02	3.826E-04	4.60E-05	2.350E-02
92	8.28749E	C2	2.68E-02	1.780E-04	2.68E-05	2.350E-02
93	8.34447E	C2	2.0CE-00	8.833E-05	3.99E-05	2.350E-02

Table XXIII. (Continued)

	$E_0$	$\delta E_0$	$\Gamma_n$	$\delta \Gamma_n$	$\Gamma_\gamma$	$\Gamma_\gamma$	
94	8.46656E	C2	8.16E-03	8.725E-04	6.30E-05	2.350E-02	2.35E 00
95	8.59521E	C2	2.0CE-00	4.116E-04	4.19E-05	2.350E-02	2.35E 00
96	8.91228E	C2	1.62E-02	7.670E-04	7.07E-05	2.350E-02	2.35E 00
97	9.10016E	C2	1.22E-02	1.360E-03	7.09E-05	2.350E-02	2.35E 00
98	9.40536E	C2	3.39E-02	6.227E-04	8.83E-05	2.350E-02	2.35E 00
99	9.74446E	C2	4.84E-02	2.883E-04	5.35E-05	2.350E-02	2.35E 00
100	9.77363E	C2	1.59E-02	7.656E-04	6.66E-05	2.350E-02	2.35E 00
101	9.82423E	C2	2.0CE-00	8.932E-05	5.29E-05	2.350E-02	2.35E 00
102	9.84483E	C2	2.0CE-00	1.620E-04	5.12E-05	2.350E-02	2.35E 00
103	1.00337E	C3	2.0CE-00	2.100E-04	8.00E-05	2.350E-02	2.35E 00
104	1.00500E	C3	1.64E-01	1.995E-04	2.94E-04	2.350E-02	2.35E 00
105	1.01145E	C3	1.62E-02	1.867E-03	9.98E-05	2.350E-02	2.35E 00
106	1.02912E	C3	1.21E-02	2.308E-03	1.09E-04	2.350E-02	2.35E 00
107	1.03382E	C3	3.02E-02	7.426E-04	7.54E-05	2.350E-02	2.35E 00
108	1.04103E	C3	2.0CE-00	2.500E-04	2.00E-04	2.350E-02	2.35E 00
109	1.04731E	C3	3.67E-02	3.933E-04	6.00E-05	2.350E-02	2.35E 00
110	1.06268E	C3	2.62E-02	7.661E-04	6.97E-05	2.350E-02	2.35E 00
111	1.06768E	C3	2.16E-02	1.069E-03	8.42E-05	2.350E-02	2.35E 00
112	1.07407E	C3	2.20E-02	9.082E-04	9.16E-05	2.350E-02	2.35E 00
113	1.08172E	C3	1.59E-02	1.519E-03	1.05E-04	2.350E-02	2.35E 00
114	1.09519E	C3	1.1E-02	2.276E-03	1.24E-04	2.350E-02	2.35E 00
115	1.10290E	C3	1.40E-02	2.221E-03	1.10E-04	2.350E-02	2.35E 00
116	1.11897E	C3	4.50E-02	5.169E-04	8.92E-05	2.350E-02	2.35E 00
117	1.13137E	C3	6.07E-03	3.641E-03	1.81E-04	2.350E-02	2.35E 00
118	1.14544E	C3	2.0CE-00	9.923E-06	5.29E-06	2.350E-02	2.35E 00
119	1.14864E	C3	2.0CE-00	2.977E-04	1.06E-04	2.350E-02	2.35E 00
120	1.15268E	C3	5.55E-02	5.721E-04	1.30E-04	2.350E-02	2.35E 00
121	1.15509E	C3	3.75E-02	8.023E-04	8.25E-05	2.350E-02	2.35E 00
122	1.15939E	C3	3.66E-02	7.368E-04	8.92E-05	2.350E-02	2.35E 00
123	1.16475E	C3	2.0CE-00	2.000E-04	2.00E-04	2.350E-02	2.35E 00
124	1.20135E	C3	7.67E-02	5.435E-04	8.14E-05	2.350E-02	2.35E 00
125	1.21588E	C3	7.59E-02	5.549E-04	1.51E-04	2.350E-02	2.35E 00
126	1.22000E	C3	5.76E-02	3.976E-04	1.51E-04	2.350E-02	2.35E 00
127	1.22309E	C3	6.34E-02	4.043E-04	1.14E-04	2.350E-02	2.35E 00
128	1.22155E	C3	7.07E-02	5.738E-04	1.32E-04	2.350E-02	2.35E 00
129	1.22092E	C3	2.0CE-00	1.985E-04	1.06E-04	2.350E-02	2.35E 00
130	1.22966E	C3	2.0CE-00	3.000E-04	4.00E-04	2.350E-02	2.35E 00
131	1.27660E	C3	4.33E-02	7.194E-04	2.57E-04	2.350E-02	2.35E 00
132	1.27702E	C3	2.0CE-00	6.946E-04	3.71E-04	2.350E-02	2.35E 00
133	1.28362E	C3	2.0CE-00	3.969E-04	2.12E-04	2.350E-02	2.35E 00
134	1.28548E	C3	1.21E-01	4.211E-04	1.30E-04	2.350E-02	2.35E 00
135	1.28932E	C3	2.0CE-00	2.426E-04	9.36E-05	2.350E-02	2.35E 00
136	1.29622E	C3	2.0CE-00	9.922E-05	6.35E-05	2.350E-02	2.35E 00
137	1.21099E	C3	1.66E-01	2.338E-04	2.37E-04	2.350E-02	2.35E 00
138	1.31701E	C3	1.01E-02	4.793E-03	2.54E-04	2.350E-02	2.35E 00
139	1.32485E	C3	1.72E-01	1.981E-04	2.94E-04	2.350E-02	2.35E 00
140	1.32566E	C3	2.0CE-00	4.000E-04	2.00E-04	2.350E-02	2.35E 00
141	1.33147E	C3	2.16E-02	1.282E-03	1.00E-04	2.350E-02	2.35E 00
142	1.33797E	C3	2.0CE-00	2.400E-04	2.00E-04	2.350E-02	2.35E 00
143	1.36066E	C3	6.13E-02	4.304E-04	1.72E-04	2.350E-02	2.35E 00
144	1.38432E	C3	7.51E-02	2.674E-04	9.14E-05	2.350E-02	2.35E 00
145	1.38710E	C3	2.0CE-00	8.906E-05	5.21E-05	2.350E-02	2.35E 00
146	1.40598E	C3	3.52E-01	5.044E-04	3.99E-04	2.350E-02	2.35E 00
147	1.41892E	C3	1.42E-02	3.479E-03	1.92E-04	2.350E-02	2.35E 00
148	1.43605E	C3	2.0CE-00	4.372E-04	1.05E-04	2.350E-02	2.35E 00
149	1.44768E	C3	3.59E-02	1.099E-03	1.97E-04	2.350E-02	2.35E 00
150	1.45476E	C3	2.0CE-00	1.953E-04	8.60E-05	2.350E-02	2.35E 00
151	1.46677E	C3	5.41E-03	1.902E-04	9.07E-05	2.350E-02	2.35E 00
152	1.45445E	C3	2.0CE-00	6.000E-04	4.00E-04	2.350E-02	2.35E 00
153	1.50427E	C3	7.77E-02	1.902E-04	9.07E-05	2.350E-02	2.35E 00
154	1.50810E	C3	7.77E-02	3.946E-04	2.94E-04	2.350E-02	2.35E 00
155	1.51057E	C3	3.74E-02	7.578E-04	1.32E-04	2.350E-02	2.35E 00
156	1.52775E	C3	6.59E-02	7.726E-04	1.51E-04	2.350E-02	2.35E 00
157	1.53485E	C3	4.79E-02	7.869E-04	1.78E-04	2.350E-02	2.35E 00
158	1.55721E	C3	1.62E-02	3.898E-03	1.85E-04	2.350E-02	2.35E 00
159	1.55527E	C3	1.43E-01	3.389E-04	8.92E-05	2.350E-02	2.35E 00
160	1.56621E	C3	3.27E-02	1.249E-03	2.15E-04	2.350E-02	2.35E 00
161	1.57960E	C3	2.0CE-00	4.000E-04	2.00E-04	2.350E-02	2.35E 00
162	1.59152E	C3	3.07E-02	1.144E-03	1.92E-04	2.350E-02	2.35E 00
163	1.61161E	C3	2.0CE-00	4.000E-04	2.00E-04	2.350E-02	2.35E 00
164	1.67270E	C3	2.39E-01	9.303E-05	3.13E-05	2.350E-02	2.35E 00
165	1.68232E	C3	2.0CE-00	4.000E-04	4.00E-04	2.350E-02	2.35E 00
166	1.69595E	C3	1.55E-01	4.072E-04	2.96E-04	2.350E-02	2.35E 00
167	1.70670E	C3	3.27E-02	1.375E-03	4.41E-04	2.350E-02	2.35E 00
168	1.74567E	C3	3.04E-02	1.687E-03	1.87E-04	2.350E-02	2.35E 00
169	1.76664E	C3	2.0CE-00	5.000E-04	4.00E-04	2.350E-02	2.35E 00
170	1.77641E	C3	4.06E-02	6.894E-04	1.91E-04	2.350E-02	2.35E 00
171	1.78134E	C3	1.53E-01	1.177E-03	1.03E-03	2.350E-02	2.35E 00
172	1.79747E	C3	3.67E-02	2.788E-03	2.95E-04	2.350E-02	2.35E 00
173	1.82360E	C3	7.47E-02	7.158E-04	1.49E-04	2.350E-02	2.35E 00
174	1.83410E	C3	2.62E-01	4.163E-04	1.82E-04	2.350E-02	2.35E 00
175	1.86566E	C3	2.0CE-00	2.900E-03	1.00E-03	2.350E-02	2.35E 00
176	1.86953E	C3	3.84E-02	2.610E-03	2.78E-04	2.350E-02	2.35E 00
177	1.88105E	C3	4.09E-02	1.435E-03	1.87E-04	2.350E-02	2.35E 00
178	1.88385E	C3	3.89E-02	1.558E-03	1.87E-04	2.350E-02	2.35E 00
179	1.92542E	C3	6.75E-02	9.447E-04	2.50E-04	2.350E-02	2.35E 00
180	1.93337E	C3	2.0CE-00	4.000E-04	4.00E-04	2.350E-02	2.35E 00
181	1.94275E	C3	5.0CE-02	6.688E-04	1.72E-04	2.350E-02	2.35E 00
182	1.99000E	C3	1.45E-01	1.437E-03	3.51E-04	2.350E-02	2.35E 00
183	2.00067E	C3	3.19E-01	4.886E-04	1.89E-04	2.350E-02	2.35E 00
184	2.04901E	C3	5.11E-02	2.248E-03	3.67E-04	2.350E-02	2.35E 00
185	2.05275E	C3	1.47E-01	8.683E-04	1.99E-04	2.350E-02	2.35E 00
186	2.06334E	C3	2.0CE-00	2.479E-04	1.59E-04	2.350E-02	2.35E 00

Table XXIII. (Continued)

	$E_0$	$\delta E_0$	$\Gamma_n$	$\delta \Gamma_n$	$\Gamma_\gamma$	$\Gamma_\gamma$	
187	2.07139E	C3	3.66E-02	1.664E-03	1.52E-04	2.350E-02	2.35E 00
188	2.08076E	C3	5.32E-02	1.595E-03	1.99E-04	2.350E-02	2.35E 00
189	2.08605E	C3	2.25E-02	4.352E-03	5.51E-04	2.350E-02	2.35E 00
190	2.10413E	C3	5.52E-02	1.406E-03	1.53E-04	2.350E-02	2.35E 00
191	2.11402E	C3	1.55E-01	9.536E-04	3.39E-04	2.350E-02	2.35E 00
192	2.12416E	C3	2.85E-02	3.893E-03	3.37E-04	2.350E-02	2.35E 00
193	2.14063E	C3	2.00E 00	9.917E-04	5.29E-04	2.350E-02	2.35E 00
194	2.17272E	C3	4.62E-02	2.220E-03	1.99E-04	2.350E-02	2.35E 00
195	2.17503E	C3	2.00E 00	7.933E-04	4.24E-04	2.350E-02	2.35E 00
196	2.21543E	C3	4.50E-02	3.418E-03	2.99E-04	2.350E-02	2.35E 00
197	2.24144E	C3	2.07E-01	1.080E-03	2.91E-04	2.350E-02	2.35E 00
198	2.27143E	C3	2.00E 00	3.768E-03	3.18E-04	2.350E-02	2.35E 00
199	2.29395E	C3	1.47E-01	1.260E-03	1.17E-03	2.350E-02	2.35E 00
200	2.29652E	C3	5.89E-02	5.734E-03	3.15E-04	2.350E-02	2.35E 00
201	2.32691E	C3	3.13E-01	1.461E-03	2.81E-04	2.350E-02	2.35E 00
202	2.33656E	C3	2.03E-02	8.839E-03	8.82E-04	2.350E-02	2.35E 00
203	2.36875E	C3	3.84E-02	6.117E-03	6.43E-04	2.350E-02	2.35E 00
204	2.38442E	C3	1.42E-01	1.494E-03	4.74E-04	2.350E-02	2.35E 00
205	2.39776E	C3	3.87E-01	4.670E-03	2.74E-04	2.350E-02	2.35E 00
206	2.40119E	C3	3.87E-02	4.709E-03	6.97E-04	2.350E-02	2.35E 00
207	2.41122E	C3	2.64E-02	5.144E-03	3.62E-04	2.350E-02	2.35E 00
208	2.41867E	C3	2.00E 00	1.038E-03	3.67E-04	2.350E-02	2.35E 00
209	2.44742E	C3	2.00E 00	3.900E-04	2.12E 01	2.350E-02	2.35E 00
210	2.50223E	C3	3.66E-02	3.855E-03	3.82E-04	2.350E-02	2.35E 00
211	2.52706E	C3	1.25E-01	8.677E-04	5.87E-04	2.350E-02	2.35E 00
212	2.60420E	C3	6.44E-01	3.094E-03	1.18E-02	2.350E-02	2.35E 00
213	2.60555E	C3	1.15E-01	3.194E-03	4.12E-04	2.350E-02	2.35E 00
214	2.61205E	C3	7.77E-02	4.865E-03	5.17E-04	2.350E-02	2.35E 00
215	2.63270E	C3	7.03E-02	4.313E-03	4.67E-04	2.350E-02	2.35E 00
216	2.63681E	C3	9.21E-02	2.882E-03	4.92E-04	2.350E-02	2.35E 00
217	2.65403E	C3	2.00E 00	9.913E-04	3.18E-04	2.350E-02	2.35E 00
218	2.68868E	C3	4.65E-02	4.254E-03	8.63E-04	2.350E-02	2.35E 00
219	2.68276E	C3	1.43E-01	2.360E-03	5.83E-04	2.350E-02	2.35E 00
220	2.70195E	C3	6.59E-02	1.767E-03	7.87E-04	2.350E-02	2.35E 00
221	2.76665E	C3	5.11E-02	3.084E-03	4.07E-04	2.350E-02	2.35E 00
222	2.77483E	C3	1.23E-01	1.500E-03	5.40E-04	2.350E-02	2.35E 00
223	2.77873E	C3	2.00E 00	1.289E-03	4.24E-04	2.350E-02	2.35E 00
224	2.79554E	C3	4.04E-02	4.968E-03	4.53E-04	2.350E-02	2.35E 00
225	2.81163E	C3	5.11E-02	5.162E-03	4.83E-04	2.350E-02	2.35E 00
226	2.81620E	C3	1.53E-01	1.371E-03	6.01E-04	2.350E-02	2.35E 00
227	2.82353E	C3	2.00E 00	1.982E-03	1.06E-03	2.350E-02	2.35E 00
228	2.84554E	C3	9.85E-01	5.965E-04	3.18E-04	2.350E-02	2.35E 00
229	2.87760E	C3	4.50E-02	2.150E-03	2.99E-04	2.350E-02	2.35E 00
230	2.91837E	C3	5.11E-02	7.041E-03	7.50E-04	2.350E-02	2.35E 00
231	2.92267E	C3	7.45E-02	6.757E-03	6.48E-04	2.350E-02	2.35E 00
232	2.92556E	C3	5.73E-02	6.701E-03	1.64E-03	2.350E-02	2.35E 00
233	2.94531E	C3	7.30E-02	2.138E-03	7.87E-04	2.350E-02	2.35E 00
234	2.96756E	C3	6.01E-02	3.766E-03	4.63E-04	2.350E-02	2.35E 00
235	2.98860E	C3	4.05E-02	6.642E-03	6.06E-04	2.350E-02	2.35E 00
236	3.01517E	C3	1.95E-01	1.459E-03	8.93E-04	2.350E-02	2.35E 00
237	3.02470E	C3	4.25E-02	4.194E-03	1.17E-03	2.350E-02	2.35E 00
238	3.04380E	C3	5.49E-02	3.327E-03	5.29E-04	2.350E-02	2.35E 00
239	3.07222E	C3	1.91E-01	1.027E-03	3.07E-04	2.350E-02	2.35E 00
240	3.08113E	C3	1.20E-01	1.709E-03	3.98E-04	2.350E-02	2.35E 00
241	3.08671E	C3	7.36E-02	3.552E-03	7.87E-04	2.350E-02	2.35E 00
242	3.10356E	C3	1.15E-01	2.158E-03	9.45E-04	2.350E-02	2.35E 00
243	3.13041E	C3	6.38E-02	3.081E-03	1.12E-03	2.350E-02	2.35E 00
244	3.13388E	C3	3.05E-02	8.312E-03	6.08E-04	2.350E-02	2.35E 00
245	3.24045E	C3	3.00E-01	1.528E-03	4.83E-04	2.350E-02	2.35E 00
246	3.26402E	C3	1.80E-01	1.831E-03	1.03E-03	2.350E-02	2.35E 00
247	3.26753E	C3	3.46E-02	9.866E-03	1.13E-03	2.350E-02	2.35E 00
248	3.27329E	C3	1.64E-02	1.086E-02	1.42E-03	2.350E-02	2.35E 00
249	3.29748E	C3	3.47E-02	9.629E-03	9.21E-04	2.350E-02	2.35E 00
250	3.30781E	C3	4.25E-02	4.735E-03	1.32E-03	2.350E-02	2.35E 00
251	3.34120E	C3	7.77E-02	4.072E-03	6.03E-04	2.350E-02	2.35E 00
252	3.34682E	C3	2.07E-01	1.419E-03	1.47E-03	2.350E-02	2.35E 00
253	3.36657E	C3	2.00E 00	8.917E-04	5.29E-04	2.350E-02	2.35E 00
254	3.37829E	C3	3.46E-02	3.775E-03	1.17E-03	2.350E-02	2.35E 00
255	3.38376E	C3	4.78E-02	3.562E-03	7.87E-04	2.350E-02	2.35E 00
256	3.39527E	C3	3.47E-02	7.729E-03	9.61E-04	2.350E-02	2.35E 00
257	3.41780E	C3	1.03E-01	4.080E-03	5.75E-04	2.350E-02	2.35E 00
258	3.44705E	C3	1.31E 00	1.513E-03	5.47E-03	2.350E-02	2.35E 00
259	3.49571E	C3	4.47E-02	1.055E-02	1.07E-03	2.350E-02	2.35E 00
260	3.51346E	C3	1.52E-01	1.898E-03	4.96E-04	2.350E-02	2.35E 00
261	3.51485E	C3	2.00E 00	1.388E-03	5.29E-04	2.350E-02	2.35E 00
262	3.52226E	C3	1.27E-01	2.068E-03	4.98E-04	2.350E-02	2.35E 00
263	3.52653E	C3	5.09E-02	6.317E-03	8.61E-04	2.350E-02	2.35E 00
264	3.63653E	C3	1.15E-01	7.947E-03	8.27E-04	2.350E-02	2.35E 00
265	3.65422E	C3	1.78E-01	2.707E-03	9.08E-04	2.350E-02	2.35E 00
266	3.66240E	C3	2.27E-01	2.603E-03	5.91E-04	2.350E-02	2.35E 00
267	3.67334E	C3	6.71E-02	5.117E-03	5.88E-04	2.350E-02	2.35E 00
268	3.68324E	C3	6.65E-02	4.376E-03	8.59E-04	2.350E-02	2.35E 00
269	3.72469E	C3	6.55E-02	7.258E-03	9.26E-04	2.350E-02	2.35E 00
270	3.74155E	C3	2.25E-01	8.365E-04	4.15E-04	2.350E-02	2.35E 00
271	3.75851E	C3	2.00E 00	1.981E-03	4.24E-04	2.350E-02	2.35E 00
272	3.79112E	C3	2.00E 00	2.872E-03	6.35E-04	2.350E-02	2.35E 00
273	3.80522E	C3	2.00E 00	6.438E-04	5.29E-04	2.350E-02	2.35E 00
274	3.82665E	C3	7.67E-02	4.462E-03	6.91E-04	2.350E-02	2.35E 00
275	3.88037E	C3	1.57E-01	2.904E-03	6.18E-04	2.350E-02	2.35E 00
276	3.89476E	C3	5.62E-02	8.524E-03	1.80E-03	2.350E-02	2.35E 00
277	3.92760E	C3	5.73E-02	1.240E-02	1.65E-03	2.350E-02	2.35E 00
278	3.93033E	C3	2.00E 00	1.387E-02	3.18E-03	2.350E-02	2.35E 00
279	3.93336E	C3	4.05E-02	1.209E-02	2.10E-03	2.350E-02	2.35E 00
280	3.99254E	C3	2.00E 00	2.971E-03	1.59E-03	2.350E-02	2.35E 00

The systematic relative error on the neutron widths appears to increase linearly with energy and is approximately 4% at low energy and 20% near the upper limit of the resolved range. On that basis we estimate the systematic error to be:

$$\frac{\delta\Gamma_{nj}}{\Gamma_{nj}} = .03 + .04 E_j, \text{ with } E_j \text{ in keV} \quad (20)$$

This error is taken to be fully correlated over energy and among s- and p-wave levels.

There is reasonable agreement among recent determinations of the average capture width for s-wave, hence we estimate the systematic uncertainty on the capture width of s-wave levels to be .5 mV. This corresponds to an accuracy of approximately 2% for the average s-wave capture width. There is essentially no direct information concerning the p-wave average capture width. In fact the only p-wave capture width for which experimental values are available is that of the level at 10.24 eV. Some argument can be made for a parity dependence of the average capture width.<sup>D27</sup> Hence, the uncertainty in the average value of the capture widths is larger than that for s-wave levels and is somewhat arbitrarily estimated to be  $\pm 5$  mV.

There are difficult normalization problems arising in the determination of the subthreshold fission areas, hence it is not surprising to find systematic differences among the data from independent experiments. From the scatter of those data the systematic relative error in the fission widths is estimated to be 20%.

We have already noted in Section 3 that no significant external

correlations are observed among the partial widths of a level reported by different authors, in spite of the fact that most measurements will yield strongly correlated values for these partial widths. This was attributed to the fact that most determinations of the partial widths are based on a number of experiments which have different internal correlations, and also the statistical uncertainties on the capture and fission widths are sufficiently large as to obscure possible correlations. We conclude that the correlations between the evaluated values of different partial widths are not significant.

The uncertainty in the scattering radius was estimated at  $\pm .025 \times 10^{-12}$  cm from the scatter of the values reported in Table X.

The uncertainties in the smooth backgrounds (File 3) were estimated from the various approximations used in the computation of these backgrounds. The scattering background is estimated to have an uncertainty of  $\pm 0.2$  b. correlated over all energies. The capture background is estimated to have an uncertainty of  $\pm .02$  b correlated over all energies, and a second uncertainty of  $\pm (.0016E^{1/2})$  b, where  $E$  is the neutron energy in eV, also correlated over all energies but not correlated to the first uncertainty. The second uncertainty arises from the possibility of missing small levels or overcompensating for missed levels. The uncertainty in the subthreshold fission background below 1. eV is estimated to be  $\pm 60\%$ . The estimated systematic errors are summarized in Table XXIV.

Table XXIV. Systematic Uncertainties in the Evaluated Parameters

The following systematic uncertainties are correlated over the range 0 to 4 keV. Uncorrelated (statistical) uncertainties are given in Tables XXII and XXIII. See text for details.

1. Energy Scale:  $\frac{\delta E_0}{E_0} = 0.00025$
2. Neutron Widths:  $\frac{\delta \Gamma_n}{\Gamma_n} = 0.03 + 0.0004 E_0$  (for s- and p-waves)
3. Capture Widths:  $\frac{\delta \Gamma_\gamma}{\Gamma_\gamma} = \begin{cases} 0.05 & \text{for s-wave levels} \\ 0.2 & \text{for p-wave levels} \end{cases}$
4. Fission Widths:  $\frac{\delta \Gamma_f}{\Gamma_f} = 0.2$
5. Smooth Scattering Background:  $\delta \sigma_n = \pm 0.2b$
6. Smooth Capture Background:  $\delta \sigma_\gamma^{(1)} = \pm 0.02b$
7. Capture due to Unresolved Levels:  $\delta \sigma_\gamma^{(2)} = \pm .0016E^{1/2}$  in b.
8. Effective Scattering Radius:  $\delta \hat{a} = \pm .025 \times 10^{-12}$  cm

(in these expressions, the energy is assumed to be in eV)

## 9. CONCLUSIONS

The present evaluation differs significantly in many respects from ENDF/B-IV. These differences result mostly from new measurements and new analyses of older measurements.

The most significant changes, for computing performance parameters of thermal reactors, are surely the reduction of the capture widths of the first three s-wave levels, by about 15%, and the increased neutron widths of the levels at 20.9 eV and 36.8 eV, by about 10%.

Above 1.5 keV the  $\Gamma_n$ 's obtained in this evaluation are on the average 10 to 20% larger than those of ENDF/B-IV. This is because the ENDF/B-IV values were mostly based on the measurements of Rahn et al.<sup>B20</sup> whereas the new measurements of Nakajima et al.,<sup>B26</sup> Poortmans et al.,<sup>B32</sup> and Olsen et al.,<sup>B31</sup> as well as the older measurement of Carraro and Kolar<sup>B17</sup> all yield values of  $\Gamma_n$  larger than those given by Rahn et al. This is illustrated in Fig. 19 where the local s-wave strength function over successive intervals of 500 eV from different measurements are compared.

A number of small levels considered s-wave levels in ENDF/B-IV are here considered as p-wave levels, and vice versa. The ENDF/B-IV angular momentum assignments essentially followed that of Rahn et al.<sup>B20</sup> The different assignments in this evaluation mostly result from the work of Corvi, Rohr and Weigmann<sup>B25</sup> and from a systematic application of the  $\Delta_3$  statistic. The present evaluation has 162 s-wave and 258 p-wave levels in the interval 0-4 keV, whereas ENDF/B-IV had 190 s-wave and 220 p-wave levels in the same interval.

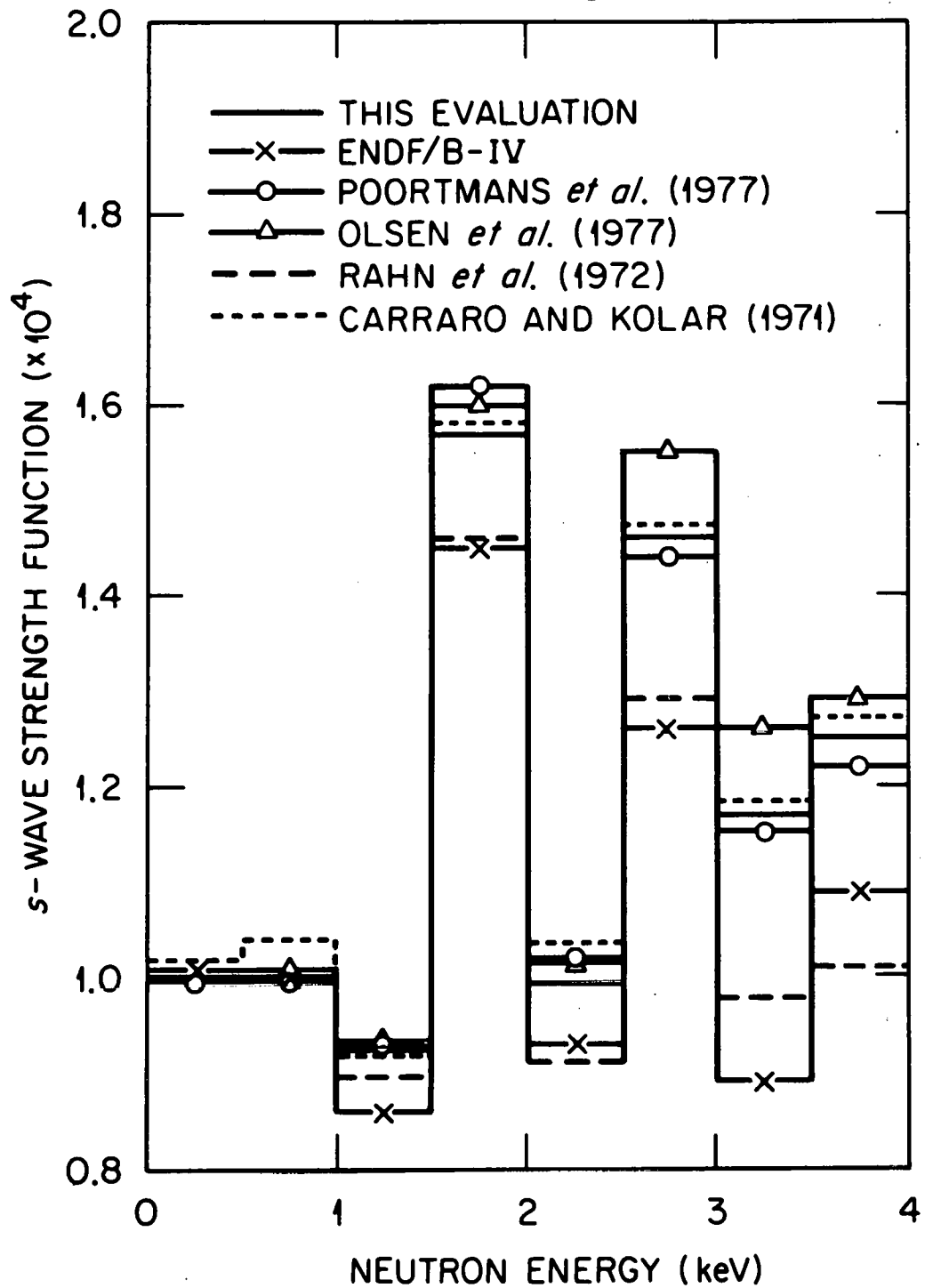


Fig. 19. Comparison of local s-wave strength functions. The values were obtained by adding the reduced neutron widths reported by the author indicated for the levels assigned to s-waves in the present evaluation.

The more precise calculation of the scattering background and the use of a multilevel formula for the calculation of the s-wave contribution will avoid "negative cross sections" and the systematic discrepancies between levels which were present in ENDF/B-IV.<sup>D11</sup>

Finally the recent measurements of Slovacek et al.<sup>B29</sup> and Difilippo et al.<sup>B33</sup> allow a much better definition of the subthreshold fission than what was included in ENDF/B-IV.

A number of problems have been encountered in this evaluation which point to the desirability of further work.

There are systematic discrepancies, often of the order of 20%, among the various values reported for  $\Gamma_n$ , particularly above 1.5 keV. These discrepancies are present even among the most recent measurements. In our opinion the discrepancies result from inadequate methods of analyzing transmission measurements, particularly at high energy where backgrounds are difficult to estimate and where resolution broadening is important and often asymmetric. The work of Derrien<sup>D3</sup> and Ribon<sup>D2</sup> illustrates some of the problems.

The most recent measurements (after 1972) of the capture and neutron widths of the important first few s-wave levels are very consistent but it is somewhat surprising that those recent measurements yield values so much different than the average of older measurements.

As illustrated in Table XVIII there are fairly large discrepancies between the direct measurements of the capture cross section and calculations based on the evaluated resonance parameters. Since there

are large discrepancies also among the various direct measurements of capture, we believe the computed values to be more reliable.

Finally, careful measurements of the capture and total cross sections below 1 eV appear very desirable. This energy region is of course very important for thermal reactor calculations. The "thermal cross sections" are well determined by a number of independent measurements, but it is difficult to reconcile these thermal values with any reasonable assumption concerning the bound levels near the binding energy. It is not unlikely that much of the thermal capture is due to a small p-wave level near zero energy. If this were so the capture cross section might not be inversely proportional to the velocity in the thermal region, as is usually assumed.

An attempt was made to evaluate statistical and systematic uncertainties for all the parameters of this evaluation. The evaluation of those uncertainties is based only on differential data. It would be desirable to test the evaluation against integral data such as performance parameters from thermal benchmarks. In Table XXV the infinitely dilute capture resonance integral computed from ENDF/B-IV and from this evaluation are compared with the value reported by BNL-325<sup>C2</sup> and based on direct experimental measurements.<sup>D28</sup> Both evaluated values agree well with the measurements.

An early version of this evaluation was used in a sensitivity analysis of the TRX-2 lattice parameters.<sup>D9</sup> The study indicated that the proposed modifications of the partial widths of the first few s-wave levels improved the agreement between calculated and measured

values of the ratio of epithermal-to-thermal  $^{238}\text{U}$  captures in TRX-2. This is consistent with the result of similar calculations<sup>A7</sup> based on a reduction of the capture width of the level at 6.67 eV.

Table XXV. Infinite Dilution Capture Resonance Integral

---

1. Computation with present evaluation:		
1/v part of cross section	1.215	b
Resolved s-wave levels	275.18	b
Resolved p-wave levels	.81	b
Cross section above 4 keV (estimated)	2.19	b
Total	279.4	b
2. Computed with ENDF/B-IV		
	278.4	b
3. Experimental value (BNL-325)		
	275 $\pm$ 5	b

---

## REFERENCES

- A. Proceedings of the following conferences contain a number of papers which have been used in this evaluation:
- A1. Conference on Neutron Cross Sections and Technology, March 4-7, 1968, Washington, D. C.; see NBS Special Publication 299 (September 1968), also identified as USAEC TIC publication CONF-6860083; hereinafter referred as "CONF-6860083."
  - A2. Conference on Nuclear Data for Reactors, June 15-19, 1970, Helsinki; see IAEA publication STI/PuB/259, Vienna, 1970; hereinafter referred as "Helsinki-1970."
  - A3. Conference on Neutron Cross Sections and Technology, March 15-17, 1971, Knoxville, TN; see USAEC DTIE publication CONF-710301; hereinafter referred as "CONF-710301."
  - A4. National Topical Meeting on New Developments in Reactor Physics and Shielding, September 12-15, 1972, Kiamesha Lake, NY; see USAEC TIC publication CONF-720901; hereinafter referred as "CONF-720901."
  - A5. Specialists Meeting on Resonance Parameters of Fertile Nuclei and  $^{239}\text{Pu}$ , May 20-22, 1974, Saclay; see NEANDC(E) publication 1634, January, 1975; hereinafter referred as "Specialist Meeting - 1974."
  - A6. Conference on Nuclear Cross Section Technology, March 3-7, 1975, Washington, D. C.; see NBS special publication 425 (October 1975), also identified as USERDA publication CONF-75619216; hereinafter referred as "CONF-75619216."
  - A7. Seminar on  $^{238}\text{U}$  Resonance Capture, March 18-20, 1975, Brookhaven National Laboratory; see BNL publication NCS -50451, ENDF-217 edited by S. Pearlstein (August 1975); hereinafter referred as "ENDF-217-1975."
  - A8. International Conference on the Interaction of Neutrons and Nuclei, July 6-9, 1976, Lowell, Massachusetts; see USERDA publication TIC CONF-760715; hereinafter referred as "CONF-760715."
- B. Measurements of the  $^{238}\text{U}$  resonance parameters were obtained from the following references:
- B1. J. A. Harvey, D. J. Hughes, R. S. Carter, and V. E. Pilcher, Phys. Rev. 99, 10 (1955); also private communication from J. A. Harvey (1976).

- B2. J. S. Levin and D. J. Hughes, Phys. Rev. 101, 1328 (1956).
- B3. J. E. Lynn and N. J. Pattenden, Proc. International Conf. on Peaceful Uses of Atomic Energy 4, 210 (1956).
- B4. R. G. Fluharty, F. B. Simpson, and O. D. Simpson, Phys. Rev. 103, 1778 (1956).
- B5. L. M. Bollinger, R. E. Coté, D. A. Dahlberg, and G. E. Thomas, Phys. Rev. 105, 661 (1957).
- B6. I. A. Radkevich, V. V. Vladimirov, and V. V. Sokolovskiy, J. Nuc. Energy 5, 92 (1967).
- B7. J. L. Rosen, J. S. Desjardins, J. Rainwater, and W. W. Havens, Phys. Rev. 118, 687 (1960).
- B8. H. E. Jackson and J. E. Lynn, Phys. Rev. 127, 461 (1962).
- B9. M. C. Moxon and C. M. Mycock (1962); given as private communication (1962) in BNL-325 (1965) (see ref. C2).
- B10. F. W. K. Firk, J. E. Lynn, and M. C. Moxon, Nucl. Phys. 41, 614 (1963).
- B11. J. B. Garg, J. Rainwater, J. S. Peterson, and W. W. Havens, Phys. Rev. 134, B985 (1964).
- B12. A. Michaudon, H. Derrien, P. Ribon, and M. Sanche-Cauvin, Nucl. Phys. 69, 545 (1965).
- B13. M. Asghar, C. M. Chaffey, and M. C. Moxon, Nucl. Phys. 85, 305 (1966).
- B14. N. W. Glass, A. D. Schelberg, L. D. Tatro, and J. W. Warren, "U-238 Neutron Capture Results from Bomb Source Neutrons," CONF-6860083 Vol. 1, p. 573 (1968) (see ref. A1).
- B15. L. M. Bollinger and G. E. Thomas, Phys. Rev. 171, 1293 (1968).
- B16. G. Rohr, W. Weigmann, and J. Winter, Helsinki - 1970, 1, 413, (see ref. A2).
- B17. G. Carraro and W. Kolar, Helsinki - 1970, 1, 403 (see ref. A2) and CONF-710301 2, 701 (1971) (see ref. A3).
- B18. M. G. Silbert and D. W. Bergen, Phys. Rev. C, 4, 220 (1971).
- B19. K. L. Maletski, L. B. Pikel'ner, I. M. Salamatin, and E. I. Sharapov. Sovt. J. At. Energy 32, 45 (1972).

- B20. F. Rahn, H. S. Camarda, G. Hacken, W. W. Havens, Jr., H. I. Liou, J. Rainwater, M. Slagowitz, and S. Wynchank, Phys. Rev. C, 6, 1854 (1972).
- B21. R. C. Block, R. W. Hockenbury, R. E. Slovacek, E. B. Bean, and D. S. Cramer, Phys. Lett. 31, 247 (1973).
- B22. H. Ceulemans, "Resonance Scattering Cross Section of  $^{238}\text{U}$  below 220 eV," Specialists Meeting - 1974, p. 145 (see ref. A5).
- B23. F. Poortmans, L. Mewissen, G. Rohr, H. Weigmann, and G. Vanpraet, "Neutron Scattering Cross Section Measurements on  $^{238}\text{U}$  in the Resolved Energy Range," Specialists Meeting - 1974, p.149 (see ref. A5).
- B24. J. A. Wartena, H. Weigmann and E. Migneco, CONF-75619216 2, 597 (see ref. A6).
- B25. F. Corvi, G. Rohr and H. Weigmann, CONF-75619216 2, 733 (see ref. A6).
- B26. Y. Nakajima, A. Asami, M. Mizumoto, T. Fuketa, and H. Takekoshi, CONF-75619216 2, 738 (see ref. A6).
- B27. R. C. Block, R. W. Hockenbury, R. E. Slovacek, Series II, Bull. Am. Phys. Soc. 20, 138 (1975); and R. E. Slovacek, D. S. Cramer, E. B. Bean, R. W. Hockenbury, J. R. Valentine, and R. C. Block, Series II, Bull. Am. Phys. Soc. 20, 581 (1975).
- B28. J. Blons, C. Mazur and D. Paya, CONF-75619216 2, 642 (see ref. A6).
- B29. R. E. Slovacek, D. S. Cramer, E. B. Bean, J. R. Valentine, R. W. Hockenbury, R. C. Block, Nucl. Sci. Eng. 62, 455 (1977).
- B30. H. I. Liou, R. E. Chrien, Nucl. Sci. Eng. 62, 463 (1977); and R. E. Chrien, H. I. Liou and J. Kopecky, CONF-760715, p. 1298 (see ref. A8); also private communication from the authors (1976).
- B31. D. K. Olsen, G. deSaussure, R. B. Perez, E. G. Silver, F. C. Difilippo, R. W. Ingle, and H. Weaver, Nucl. Sci. Eng. 62, 479 (1977); and D. K. Olsen, G. deSaussure, R. B. Perez, F. C. Difilippo and R. W. Ingle, "Note on  $^{238}\text{U} + n$  Resolved Resonance Energies" submitted for publication in Nucl. Sci. Eng. (1977).
- B32. F. Poortmans, E. Cornelis, L. Mewissen, G. Rohr, R. Shelley, T. Van der Veen, G. Vanpraet, and H. Weigmann, "Cross Sections and Neutron Resonance Parameters for  $^{238}\text{U}$  below 4 keV," p. 1246 CONF-760715 (see ref. A8); also private communication from F. Poortmans (April 1977).

- B33. F. C. Difilippo, R. B. Perez, G. deSaussure, D. K. Olsen, and R. W. Ingle, "Measurement of the  $^{238}\text{U}$  Subthreshold Fission Cross Section for Incident Neutron Energies between 0.6 and 100 keV," Nucl. Sci. Eng. 63, 153 (1977); also CONF-760715, p. 1401 (see ref. A8) and unpublished work (1977).
- B34. R. C. Block, D. R. Harris, and K. Kobayashi, "Recent  $^{238}\text{U}$  Self-indication Measurements at RPI," private communication from R. C. Block (January 1977).
- C. The following evaluations of the  $^{238}\text{U}$  cross sections and resonance parameters are very extensive:
- C1. ENDF/B  $^{238}\text{U}$
- Version I, Mat 1047
- W. A. Wittkopf, D. H. Roy, and A. Z. Livolsi, " $^{238}\text{U}$  Neutron Cross Section Data for ENDF/B," ENDF-103 (BAW-316) (May 1967).
- Version II, Mat 1107
- T. A. Pitterle, "Evaluation of  $^{238}\text{U}$  Neutron Cross Sections for ENDF/B Version II File," WARD-4181-1 (March 1971); "Evaluation of  $^{238}\text{U}$  Neutron Cross Sections for the ENDF/B File," Helsinki - 1970, p. 687 (see ref. A2).
- Version III, Mat 1158
- T. A. Pitterle, N. C. Paik, and C. Durston, "Evaluation and Integral Testing of Modifications to ENDF/B Version II Data," WARD-4210T4-1 (December 1971); and C. Durston and T. A. Pitterle, "Evaluation of  $^{238}\text{U}$  Neutron Cross Sections for ENDF/B Version III File," WARD-3045T4B2 (April 30, 1972).
- Version IV, Mat 1262
- F. J. McCrosson, "Evaluation of  $^{238}\text{U}$  Cross Sections for ENDF/B-IV" ENDF-217-1975, p. 122 (see ref. A7).
- C2. J. R. Stehn, M. D. Goldberg, R. Wiener Chasman, S. F. Mughabghab, B. A. Magurno, and V. M. May, "Neutron Cross Sections" Vol. III, BNL-325, Second Edition (1965); and S. F. Mughabghab and D. I. Garber, "Neutron Cross Sections, Vol. I, Resonance Parameters," BNL-325, Third Edition (1973).
- C3. J. J. Schmidt, "Neutron Cross Sections for Reactor Materials," KFK-120, Part I, (1966).
- C4. J. Ravier, "Evaluation des Section Efficaces de l'  $^{238}\text{U}$ ," Cadarache Report PNR/SETR R. .025, Cadarache, France (February 1968).

- C5. M. Moxon, "Evaluation of  $^{238}\text{U}$  Resonance Parameters" Specialists Meeting - 1974, p. 45 (see ref. A5).
- C6. J. R. Askew, "The Current U.K. Position on  $^{238}\text{U}$  Resonance Capture" ENDF-217-1975, p. 45, (see ref. A7).
- D. Other references are listed below:
- D1. D. R. Finch, private communication, October 6, 1976.
- D2. H. Derrien and P. Ribon, "On the Shape Analysis of Various  $^{232}\text{Th}$  and  $^{238}\text{U}$  Transmission Data," Specialists Meeting - 1974, p. 63 (see ref. A5).
- D3. H. Derrien, "Comments on  $^{238}\text{U}$  Neutron Width Evaluations," ENDF-217-1975, p. 156 (see ref. A7).
- D4. Experimental Neutron Resonance Spectroscopy, Edited by J. A. Harvey, Academic Press, New York and London, 1970.
- D5. G. D. James, "Neutron Energy Standards," paper presented at "International Specialists Symposium on Neutron Standards and Applications," March 28-31, 1977, NBS (proceedings to be published).
- D6. G. deSaussure, R. Gwin, L. W. Weston, R. W. Ingle, R. R. Fullwood, and R. W. Hockenbury, "Simultaneous Measurements of the Neutron Fission and Capture Cross Sections for  $^{235}\text{U}$  for Incident Neutron Energies from 0.4 to 3 keV," ORNL-TM-1804 (1967).
- D7. F. Rahn and W. W. Havens, Jr., "A Review of the Total Radiation Widths of Neutron Resonances of  $^{238}\text{U}$ ," EANDC(US)-179/U, European American Nuclear Data Committee.
- D8. F. G. Dyson and M. L. Metha, *J. Math. Phys.* 4, 701 (1963).
- D9. E. T. Tomlinson, G. deSaussure and C. R. Weisbin, "Sensitivity Analysis for TRX-2 Lattice Parameters with Emphasis on Epithermal  $^{238}\text{U}$  Capture," ERPI NP-346 (1977); and *Trans. ANS*, June 12-17, 1977.
- D10. ENDF/B formats are defined in ENDF-102, "Data Formats and Procedures for the Evaluated Nuclear Data File, ENDF," Revised by D. Garber, C. Dunford, and S. Pearlstein, BNL-NCS-50496 (October 1975 and June 1976).
- D11. G. deSaussure, D. K. Olsen, and R. B. Perez, *Nucl. Sci. and Eng.* 61, 496 (1976).

- D12. D. J. Hughes and R. L. Zimmerman, Nuclear Reactions, P. M. Endt and M. Demeur, Eds, Vol. 1, pp. 384-390, North Holland Publishers, Amsterdam (1959); and K. K. Seth, D. J. Hughes, R. L. Zimmerman, and R. C. Garth, Phy. Rev. 110, 692 (1958).
- D13. J. E. Lynn, Proc. Phys. Soc. 82, 903 (1963).
- D14. M. Divadeenam, unpublished Ph.D. Thesis, Duke University 1968.
- D15. C. A. Uttley, Proc. International Conf. on Nucl. Phys., Paris p. 700 (1964); C. A. Uttley, "Total Neutron Cross Section Measurements in Nuclear Data for Reactor," Program at AERE for Period 1, July 1963 - December 31, 1963, EANDC-(UK), 35L, p. 2 (1964).
- D16. B. R. Leonard, Jr., "Energy Dependent Cross Sections in the Thermal Regions," CONF-720901, p. 81 (see ref. A4).
- D17. B. R. Leonard, Jr., "Thermal Cross Sections of the Fissile and Fertile Nuclei for ENDF/B-II," BNWL-1586 (June 1971).
- D18. J. B. Hunt, J. C. Robertson, and T. B. Ryves, Nucl. Energy 23, 705 (1969).
- S. P. Harris, D. Rose, and H. D. Schroeder, ANL-LAT-109 (1954).
- P. A. Egelstaff, J. Nucl. Energy 1, 92 (1954).
- V. S. Crocker, J. Nucl. Energy 1, 234 (1955).
- V. G. Small, J. Nucl. Energy 1, 319 (1955).
- S. J. Cocking and P. A. Egelstaff, NRDC-84, part 2 (1955).
- P. A. Egelstaff and J. W. Hall, NRDC-84, part 2 (1955).
- H. Palevsky, unpublished, quoted in Proc. Geneva Conf. 4, 147 (1955).
- C. B. Bingham, R. W. Durham, and J. Ungrin, EANDC(Can) 34, (1968).
- D19. R. B. Roof, G. P. Arnold, and K. A. Gschneider, Acta. Cryst. 15, 351 (1962).
- M. Atoji, J. Chem. Phys. 35, 1950 (1961).
- B. T. M. Willis, Proc. Roy. Soc. London A, 274, 122 (1963).
- D.20 G. deSaussure, E. G. Silver, R. B. Perez, R. Ingle, and H. Weaver, "Measurement of the  $^{238}\text{U}$  Capture for Incident Neutron Energies up to 100 keV," (ORNL-TM-4059 (February 1973); also Nucl. Sci. Eng. 51, 385-404 (1973) and subsequent unpublished work (1975).

- D21. M. P. Fricke, W. M. Lopez, S. J. Friesenhahn, A. D. Carlson, and D. G. Costello, "Measurements of Cross Sections for the Radioactive Capture of 1 keV to 1 MeV Neutrons by Mo, Rh, Gd, Ta, W, Re, Au, and  $^{238}\text{U}$ ," Helsinki - 1750, Vol. II, p. 265 (see ref. A2).
- D22. M. C. Moxon, "The Neutron Capture Cross Section of  $^{238}\text{U}$  in the Energy Region 0.5 to 100 keV," AERE-R-6074 (1969) (see ref. C1 or D20 for 1971 update).
- D23. E. P. Wigner, "Proc. Conf. on Neutron Physics by Time-of-Flight, Gatlinburg, TN, 1956," ORNL-2309, 59 (1957).
- D24. C. E. Porter and R. G. Thomas, Phys. Rev. 104, 483 (1957).
- D25. J. J. Gurevitch and H. S. Pevzner, Soviet Phys. JETP4, 278 (1957).
- D26. J. A. Harvey and D. J. Hughes, Phys. Rev. 109, 471 (1958).
- D27. See for instance: H. Derrien, "Evaluation of  $^{232}\text{Th}$  Resonance Parameters," Specialists Meeting - 1974, p. 73 (see ref. A5); an argument somewhat similar to that made by Derrien for  $^{232}\text{Th}$  could be made for  $^{238}\text{U}$ .
- D28. J. Hardy, Jr., Nucl. Sci. Eng. 27, 131 (1967).

THIS PAGE  
WAS INTENTIONALLY  
LEFT BLANK

ORNL/TM-6152  
 ENDF-257  
 Dist. Category UC-79d

## INTERNAL DISTRIBUTION

1.	L. S. Abbott	74.	R. W. Roussin
2.	M. A. Bjerke	75.	E. G. Silver
3.	G. T. Chapman	76.	R. R. Spencer
4-28.	G. de Saussure	77.	M. L. Tobias
29.	J. K. Dickens	78.	E. T. Tomlinson
30.	F. C. Difilippo	79.	J. H. Todd
31.	J. D. Drischler	80.	H. Weaver
32.	G. F. Flanagan	81.	J. E. White
33.	C. Y. Fu	82.	C. R. Weisbin
34.	H. Goldstein (Consultant)	83.	L. W. Weston
35.	R. Gwin	84.	R. Q. Wright
36.	R. W. Ingle	85.	A. Zucker
37.	D. C. Larson	86.	P. Greebler (Consultant)
38.	R. L. Macklin	87.	W. W. Havens (Consultant)
39.	F. C. Maienschein	88.	A. F. Henry (Consultant)
40.	J. H. Marable	89.	R. E. Uhrig (Consultant)
41.	G. L. Morgan	90-91.	Central Research Library
42-56.	D. K. Olsen	92.	ORNL Y-12 Technical Library Document Reference Section
57.	R. W. Peele	93-94.	Laboratory Records Department
58.	F. G. Perey	95.	ORNL Patent Office
59-73.	R. B. Perez	96.	Laboratory Records (RC)

## EXTERNAL DISTRIBUTION

97. DOE Oak Ridge Operations, Research and Technical Support  
 Division, P. O. Box E, Oak Ridge, Tennessee 37830: Director

98. DOE Oak Ridge Operations, Reactor Division, P. O. Box E,  
 Oak Ridge, Tennessee 37830: Director

99-100. DOE Division of Reactor Research and Development, Washington,  
 DC 20545: Director

101-389. For distribution as shown in TID-4500 Distribution Category  
 UC-79d, Liquid Metal Fast Breeder Reactor Physics - Base  
 (62 copies - ENDF distribution)